



67 kDa metastasis-associated laminin binding protein : substrate recognition, catalytic activity and homology modeling  
by Dmitri Alexandrovich Kazmin

A dissertation submitted in partial fulfillment of the requirements for the degree of Doctor of Philosophy in Biochemistry  
Montana State University  
© Copyright by Dmitri Alexandrovich Kazmin (2002)

**Abstract:**

The 67 kDa laminin binding protein (LBP) is a multifunctional molecule that is expressed in most human tissues. It functions as part of the translational machinery within the cell, as well as on the cell surface as a laminin receptor and is also secreted to the extracellular space. The upregulation of expression of this protein in tumors is a hallmark of malignant disease and a negative prognostic factor.

In order to elucidate the molecular mechanisms of laminin binding by this protein I conducted the phage display peptide library screening of the epitopes of LBP that are involved in interactions with laminin through both peptide 11 and associated heparan sulfate moieties. Three epitopes were mapped, the central palindrome sequence of the previously characterized peptide G (LMWWML), the LBP205'229 peptide and D/EWS repeats located in the CAterminal part of the protein. The LBP205'229 peptide was shown to bind both peptide 11 and heparan sulfate in in vitro ELISA plate assays. The synthetic peptide containing consensus D/EWS repeat sequence was found to partially inhibit LBP-mediated adhesion of cancer cells to laminin. These findings allowed the building of a comprehensive model of the complex interactions between LBP and laminin.

I have also demonstrated the enzymatic activity of LBP. I have shown that this protein displays a sulfhydryl oxidase activity in vitro, which, at least in part, is not dependent on cysteine residues. This makes LBP distinct from most other known similar enzymes and opens the possibility of elucidating the role of LBP shedding by cancer cells.

Homology modeling of the N-terminal domain of LBP allowed me to predict the tertiary structure of the part of the protein involved in ribosome function. An analysis of the possible involvement of LBP in protein-protein and protein-RNA interactions within the eukaryotic ribosome is provided.

67 kDa metastasis-associated Laminin Binding Protein: Substrate  
recognition, catalytic activity and homology modeling

by

Dmitri Alexandrovich Kazmin

A dissertation submitted in partial fulfillment  
of the requirements for the degree

of

Doctor of Philosophy

in

Biochemistry

MONTANA STATE UNIVERSITY-BOZEMAN  
Bozeman, Montana

March 2002

D378  
K1895

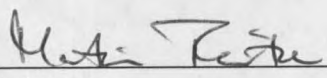
## APPROVAL

Of a dissertation submitted by

Dmitri Aleksandrovich Kazmin

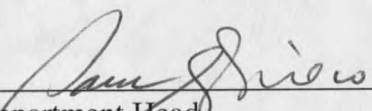
This dissertation has been read by each member of the dissertation committee and has been found to be satisfactory regarding content, English usage, format, citations, bibliographic style, and consistency, and is ready for submission to the College of Graduate Studies.

Dr. Martin Teintze

  
Chairperson3/11/02  
Date

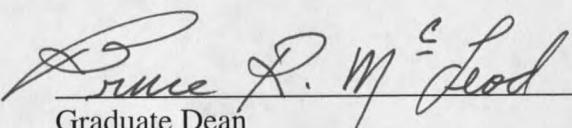
Approved for the Department of Chemistry and Biochemistry

Dr. Paul Grieco

  
Department Head3/11/02  
Date

Approved for the College of Graduate Studies

Dr. Bruce McLeod

  
Graduate Dean3-20-02  
Date

## STATEMENT OF PERMISSION TO USE

In presenting this dissertation in partial fulfillment of the requirements for a doctoral degree at Montana State University, I agree that the library shall make it available to borrowers under rules of the Library. I further agree that copying of this paper is allowable only for scholarly purposes, consistent with "fair use" as prescribed in the U.S. Copyright Law. Requests for extensive copying or reproduction of this dissertation should be referred to Bell & Howell Information and Learning, 300 North Zeeb Road, Ann Arbor, Michigan 48106, to whom I granted "the exclusive right to reproduce and distribute my dissertation in and from microform along with the non-exclusive right to reproduce and distribute my abstract in any format in whole or in part."

Signature

Date

D. Wolf  
3/11/02

## ACKNOWLEDGMENTS

I thank my thesis advisor, Dr. Jean Starkey, and committee members Drs. Martin Teintze, Valerie Copie, Clifford Bond and Patrick Callis for their support, enthusiasm and interest in my project. I also would like to thank people who shared their expertise, listened and gave valuable advises when I needed help: Drs. Seth Pincus, Edward Dratz, Jim Burritt, Heini Mittenen, Pati Glee and Mary Bateson. I am also thankful to late Joan Strange of University of Montana for help with DNA sequencing. Special thanks to fellow graduate students and coauthors of my papers – Lara Taubner and Eric Larson for valuable discussions, support, and Eric’s critical reading of this dissertation, and also to Deb Berglund for being fun to work with. Multiple alignment discussed in chapter 4 was built with Eric’s help. Also thanks to Dr. Y. Chinenov, University of Michigan, for building and validating the homology model presented in chapter 4.

Special thanks to my wife and daughter for constant support, understanding, help with all my projects (Anastasia mostly), and not smashing my computer and not painting on my papers (this goes mostly to Dasha).

This work was supported in part by the Doctoral Dissertation Award from the Susan G. Komen Breast Cancer Foundation.

## TABLE OF CONTENTS

1. INTRODUCTION.....	1
THE MODEL OF CARCINOGENESIS .....	2
FACTORS AFFECTING TUMOR'S BEHAVIOR.....	5
67 kDA LAMININ BINDING PROTEIN IN CANCER PROGRESSION.....	6
THE STORY OF DISCOVERY.....	8
67 kDA LBP AND CANCER PATHOLOGY .....	13
Gut carcinoma.....	13
Lung cancer .....	15
Breast cancer.....	16
Other cancers: thyroid, ovarian, cervical, gastric, nervous and lymphoid tissue .....	18
PHYLOGENETIC RELATIONSHIPS OF THE LBP.....	19
TRANSLATIONAL REGULATION .....	21
DIMERIZATION AND CELL SURFACE EXPRESSION.....	21
LBP AND VLA-6 INTEGRINS.....	24
INTERACTION WITH LAMININ .....	25
RIBOSOMAL FUNCTION.....	31
LBP AS VIRAL AND PRP RECEPTOR .....	31
GENE ORGANIZATION.....	33
STATEMENT OF THESIS .....	35
REFERENCES CITED.....	37
2. PHAGE DISPLAY MAPPING FOR PEPTIDE 11 SENSITIVE SEQUENCES	
BINDING TO LAMININ-1.....	62
INTRODUCTION .....	63
MATERIALS AND METHODS .....	67
Cell lines and tissue culture conditions.....	67
The 9-mer random sequence phage display library .....	68
Reagents used in the biopanning and ELISA assays .....	69
Screening of the phage display peptide library .....	70
ELISA assay for direct binding of phage to laminin-1 .....	71
Direct binding and crosslinking of the photoactivatable peptide 11 analog to LBP <sup>205-229</sup> peptide.....	73
Heparan sulfate binding assay .....	74
Cell adhesion inhibition assay .....	75
Computer-based modeling of a potential 3D structure for the LBP <sup>205-229</sup> peptide .....	76
RESULTS.....	77

Phage clones which bound to laminin-1 via peptide 11 sensitive mechanisms were obtained, but heparan sulfate binding phage clones could not be eliminated from the selected population .....	77
Sequence analysis of specifically eluted phage reveals inserts with similarities for three regions of the 67 kDa LBP .....	79
BLAST searches for similarities to phage LBP mimotope and putative heparin - binding sequences support specific relationships to the LBP sequence .....	82
Phage clones carrying LBP mimotopes re-bind directly to laminin-1 .....	83
Peptide 11 binds and crosslinks the LBP <sup>205-229</sup> peptide in a dose-dependent manner ..	84
Modeling of the LBP <sup>205-229</sup> peptide sequence reveals potential heparin binding characteristics .....	86
Synthetic LBP <sup>205-229</sup> peptide binds to isolated heparan sulfate .....	89
Synthetic QPATEDWSA peptide inhibits cell adhesion to laminin-1 .....	91
DISCUSSION .....	93
REFERENCES CITED .....	100

### 3. EVIDENCE FOR SULFHYDRYLOXIDASE ACTIVITY OF LBP..... 109

INTRODUCTION .....	109
Basic mechanism of PDI function .....	110
Role of active site cysteins .....	110
Mechanism of catalysis .....	113
Structural organization of the catalytic domain.....	114
Substrate recognition.....	116
Chaperone and antichaperone activities of PDI.....	118
Other functions of PDI-related proteins.....	120
Modulation of cell-ECM interactions .....	120
Shedding of surface-expressed proteins.....	121
Nitrositol transfer .....	121
Transcription and replication control.....	122
Other members of the family. FAD-containing proteins .....	124
Dithiol-disulfide oxidoreductases that lack the CXXC motif .....	125
MATERIALS AND METHODS.....	126
RNase refolding assays .....	126
Insulin reduction assays .....	127
LBP cloning and expression.....	128
Purification of recombinant LBP.....	129
Purification of shed LBP .....	131
Site-directed mutagenesis.....	132
Laminin binding assays.....	133
RESULTS .....	134
Expression and purification of rLBP and sLBP .....	134
Sulphydryl oxidase activity of sLBP.....	136
Shed LBP and rLBPs in insulin reduction.....	142

Laminin binding by rLBP and C → A mutants .....	147
DISCUSSION .....	147
REFERENCES CITED .....	157
4. HOMOLOGY MODELING OF THE N-TERMINAL DOMAIN OF THE 32 kDa LAMININ BINDING PROTEIN PRECURSOR .....	170
INTRODUCTION .....	170
METHODS .....	176
Alignment .....	176
Modeling .....	176
RESULTS .....	177
Multiple alignment reveals universally conserved residues .....	177
Description of the model .....	181
DISCUSSION .....	189
Protein-protein interactions .....	189
Protein-rRNA interactions .....	196
REFERENCES CITED .....	203
5. DISCUSSION .....	214
Conclusions .....	231
REFERENCES CITED .....	233
APPENDIX A: SEQUENCE ALIGNMENT OF S2P FAMILY MEMBERS .....	237

## LIST OF TABLES

Table	Page
2.1. Comparison of the numbers of phage specifically eluted from laminin-1 .....	78
2.2. Putative mimotopes and heparin binding sequences obtained from phage specifically eluted from laminin-1 by heparan sulfate or peptide 11 .....	80
3.1. Buffers used for rLBP purification .....	131
4.1. Summary of the protein-protein interactions with the involvement of S2p and LBP/p40 .....	195

## LIST OF FIGURES

Figure	Page
1.1. Schematics of laminin-1 molecule .....	26
2.1. ELISA assays showing the ability of specifically eluted phage clones to bind to laminin-1 .....	84
2.2. ELISA plate assay showing binding and crosslinking of the peptide-11 - based photo-activatable analogue to synthetic LBP 205-229 peptide.....	86
2.3. Helical wheel plot for LBP 205-229 .....	88
2.4. Computer-generated model of the LBP 205-229 domain .....	89
2.5. ELISA plate assay showing binding of synthetic LBP 205-229 to heparan sulfate .....	90
2.6. Cell adhesion assay .....	92
3.1. Thioredoxin fold.....	115
3.2. Mixed disulfide intermediate between thioredoxin single cysteine mutant and a substrate peptide.....	117
3.3. Time course of expression of rLNP in CD-41(DE3) .....	135
3.4. Purification of rLBP .....	135
3.5. Removal of polyhistidine tag from rLBP .....	135
3.6. Affinity-purified sLBP .....	135
3.7. Comparison of activity of native RNaseA with reduced and denatured RNaseA.....	137
3.8. Recovery of RNaseA activity .....	137
3.9. Kinetics of recovery of RNaseA activity.....	138
3.10. Kinetics of recovery of RNaseA activity after prolonged renaturation.....	140
3.11. PDI activity of rLBP purified under more stringent conditions .....	142
3.12. Catalysis of insulin reduction in the presence of DTT by BSA.....	143

3.13. Activity of bovine liver PDI in insulin reduction assay .....	144
3.14. Activity of shed LBP in insulin reduction assay.....	145
3.15. Activity of rLBP and three of its mutants in insulin reduction assay .....	146
3.16. Laminin binding by rLBP and C→A mutants .....	147
3.17. Change of electrophoretic mobility by shed LBP upon reduction by BME .....	152
3.18. BME-labile aggergation by wt and cysteine-less rLBPs.....	152
4.1. Representative alignment of the members of the S2p ribosomal protein family.....	179
4.2. Comparison of the LBP model and S2p of <i>T. thermophilus</i> used as the template.....	183
4.3. Overlap of the LBP model and S2p of <i>T. thermophilus</i> used as a template.....	184
4.4. Positions of cysteine residues on the modeled LBP.....	185
4.5. Positions of the preferred cleavage sites on rLBP as mapped on the LBP model .....	187
4.6. Sequence and structural alignment of S8p/S15Ae proteins.....	190
4.7. Position of the S2p on the ribosome of <i>T. thermophilus</i> .....	197
4.8. Electrostatic potentials of S2p of <i>T. thermophilus</i> and modeled LBP .....	198
4.9. Position of the putative transmembrane domain on the modeled LBP .....	200
5.1. The proposed interactions between laminin-1 and LBP.....	217

## LIST OF ABBREVIATIONS

aa, aminoacid;  
ATP, adenosine triphosphate  
AMP, cAMP, adenosine monophosphate, cyclic AMP  
BME,  $\beta$ -mercaptoethanol;  
bp, base-pairs;  
kbp, kilobase-pairs;  
BSA, bovine serum albumin;  
CD, circular dichroism  
CHO, Chinese hamster ovary;  
CMP, cCMP, cytosine monophosphate, cyclic CMP  
CT, cholera toxin;  
DNA, deoxyribonucleic acid;  
DTT, dithiotreitol;  
ECM, extracellular matrix;  
EGF, epidermal growth factor  
EHS, Engelbreth-Holm-Swarm (tumor);  
ELISA, enzyme-linked immunosorbent assay;  
ER, endoplasmic reticulum;  
ERE, estrogen response element;  
EsR, estrogen receptor;  
FACS, fluorescence-activated cell sorting;  
FAD, flavine adenosine diphosphate  
GTP, GDP, guanosine tri(di)phosphate  
GRE, glucocorticoid response element;  
GSH, reduced glutathione;  
GSSG, oxidized glutathione;  
HUVEC, human umbilical vein endothelial cell;  
HS, heparan sulfate;  
LBP, laminin binding protein;  
sLBP, shed laminin binding protein;  
rLBP, recombinant laminin binding protein;  
MDR, multiple drug resistance  
NAD(P)(H), nicotinamide dinucleotide (phosphate), (reduced form)  
NAC, N-acetyl L-cysteine;  
NMR, nuclear magnetic resonance  
ORF, open reading frame  
PBS, phosphate buffered saline (Cheryls);  
dPBS, Dulbecco phosphate buffered saline;  
PAGE, polyacrylamide gel electrophoresis  
PDI, protein disulfide isomerase;  
PDPL, phage display peptide library;

## LIST OF ABBREVIATIONS, CONTINUED

PGK, phosphoglycerate kinase;  
PgR, progesterone receptor;  
PrP, prion protein;  
RNA, ribonucleic acid;  
RNase, rdRNase, ribonuclease, reduced and denatured RNase;  
RNP, ribonucleoprotein;  
SAGE, serial analysis of gene expression;  
SV40, simian virus - 40;  
SOX, sulfhydryl oxidase;  
TIL, tumor-infiltrating lymphocyte;  
Wt, wild-type.

Standard one- and three-letter abbreviations of names of common aminoacids and nucleotides are used throughout the manuscript.

## ABSTRACT

The 67 kDa laminin binding protein (LBP) is a multifunctional molecule that is expressed in most human tissues. It functions as part of the translational machinery within the cell, as well as on the cell surface as a laminin receptor and is also secreted to the extracellular space. The upregulation of expression of this protein in tumors is a hallmark of malignant disease and a negative prognostic factor.

In order to elucidate the molecular mechanisms of laminin binding by this protein I conducted the phage display peptide library screening of the epitopes of LBP that are involved in interactions with laminin through both peptide 11 and associated heparan sulfate moieties. Three epitopes were mapped, the central palindrome sequence of the previously characterized peptide G (LMWWML), the LBP<sup>205-229</sup> peptide and D/EWS repeats located in the C-terminal part of the protein. The LBP<sup>205-229</sup> peptide was shown to bind both peptide 11 and heparan sulfate in *in vitro* ELISA plate assays. The synthetic peptide containing consensus D/EWS repeat sequence was found to partially inhibit LBP-mediated adhesion of cancer cells to laminin. These findings allowed the building of a comprehensive model of the complex interactions between LBP and laminin.

I have also demonstrated the enzymatic activity of LBP. I have shown that this protein displays a sulfhydryl oxidase activity *in vitro*, which, at least in part, is not dependent on cysteine residues. This makes LBP distinct from most other known similar enzymes and opens the possibility of elucidating the role of LBP shedding by cancer cells.

Homology modeling of the N-terminal domain of LBP allowed me to predict the tertiary structure of the part of the protein involved in ribosome function. An analysis of the possible involvement of LBP in protein-protein and protein-RNA interactions within the eukaryotic ribosome is provided.

## CHAPTER 1

## INTRODUCTION

Cancer is the second leading cause of death in the United States following cardiovascular insufficiency. According to the American Cancer Society about half of all men and one third of all women will develop cancer in their lifetime. Every year, over 500,000 people in the US alone die as a result of various forms of cancer. This amounts to almost a quarter of all deaths in the country, according to the National Center for Health Statistics. In 1995, for example, 1.25 million people were newly diagnosed with cancer, excluding non-melanoma skin cancers (more than a million cases a year), and 0.55 million patients died. A lot of scientific effort has gone into researching the molecular mechanisms of malignancy, or, speaking in lay terms, elucidating what allows a normal cell to become cancerous and what are the changes in its physiology that accompany such a transition. This change, called malignant transformation, involves all aspects of cell biochemistry, from the maintenance of genome integrity to the interactions with other cells and extracellular matrix. Because of the large number of factors involved in malignant transformation, each research group focuses on a small facet of the problem, which by itself may not advance our understanding of cancer, but when taken together with all the current knowledge, provides the big picture of fundamental mechanisms of cell function. In this dissertation, I present the results of my research of one of the many

factors that are known to be involved in progression of metastatic disease, the 67 kDa metastasis-associated laminin binding protein.

### The model of carcinogenesis

Cancer (malignancy) is a genetic disease, yet it is rarely inherited. It is a direct result of genome instability, an inherent ability of all cells to mutate. Development of a cancerous tumor results from accumulation of a large number of mutations and phenotypic expression of these mutations. A tumor is comprised of the progeny of a single progenitor cell that has acquired a sufficient number of mutations to alter the normal functioning of the genome, which lead to the loss of control of cell cycle progression. In the case of single-celled organisms such mutations might give an ultimate selective advantage, but for multi-cellular organisms such behavior of a cell within a body spells doom. It can be said that the risk of cancer is the price that we pay for the benefit of multicellularity.

A hallmark of malignant cells is their independence of the exogenous stimuli that promote or inhibit the division rate. This loss of exogenous inhibition leads to the uncontrolled growth of a tumor mass that is primarily limited by the availability of nutrients and oxygen. Not every tumor is malignant. A malignant tumor (cancer) is characterized by the following criteria:

1. Invasiveness

2. Potential to metastasize
3. Failure to undergo terminal differentiation

In some types of cancer, non-malignant tumors may give rise to cancer by the process of accumulation of sequential mutations. This is the case for the tumors of the gut, in which sequential mutations and chromosomal alterations affecting APC (Adenomatous Polyposis Coli), k-Ras, DCC (Deleted in Colon Carcinoma) and p53 genes were shown to accompany the progression from dysplasia to adenoma to adenocarcinoma. In other cases, there is less clinical evidence to support the evolution of a non-malignant precursor into cancer.

The pathway that leads from a normal cell to a malignant one is referred to as carcinogenesis. According to the accepted model, carcinogenesis is a multi-step process that can be broken down into four consequential steps:

- I. Initiation
- II. Promotion
- III. Malignant conversion
- IV. Tumor progression

During the *initiation* step, DNA is mutated or the genome is otherwise altered. This can result from the action of environmental carcinogens, either chemical (e. g. benzopyrene, aflatoxin), physical (ionizing radiation, UV light, asbestos fibers) or viral (e. g. Hepatitis B and C viruses, Human Papilloma virus, Epstein-Barr virus, Human Immunodeficiency virus). Such mutations or alterations are often silent and may persist in the cell population for years or even a lifetime without any phenotypic manifestation.

During the *promotion* step, the replication rate of initiated cells increases in response to extracellular carcinogenic stimuli (such as UV-B light), some chemical carcinogens or mitogenic factors (such as estradiol), or under the conditions of chronic inflammation. Increased division rate leads to faster accumulation of random mutations as a result of DNA replication errors and gives the promoted clone selective advantage over the adjacent cells. Tumor promoters expand the number of cells at risk of *malignant conversion*, the threshold event after which progression of cancer becomes irreversible. Malignant conversion marks the transformation of the genetic and epigenetic changes accumulated during initiation and promotion into the malignant phenotype. At this step a converted cell becomes able, in the process of *tumor progression*, to give rise to a tumor which will possess all the traits of malignancy: invasiveness, ability to spread to distal sites and lack of differentiation. A critical factor in tumor progression is angiogenesis, or the ingrowth of new blood vessels that supply the growing tumor with nutrients and oxygen. It is believed that a tumor larger than 3 mm<sup>3</sup> in size has to establish its own blood supply in order to continue growing. Moreover, neovascularization of tumors provides a gateway for spread of cancer cells to distal sites in the body. Angiogenic vessels usually have thinner walls with less formidable basement membranes than normal vasculature and therefore are easier to penetrate for the intravasating cancer cells.

### Factors affecting tumor behavior

Cancer mortality and morbidity vary greatly with the stage and grade at diagnosis, organ of origin, and the overall physical condition of a patient. Non-melanoma skin cancer and pancreatic adenocarcinoma mark the two extremes, with the former being almost harmless (yet very defacing sometimes), and the latter resulting in nearly 100% mortality within 6 months of diagnosis. The surgical stage of the tumor is a crucial factor that serves as a good prognosticator for the outcome of the disease. Different criteria are used to determine the tumor stage for different types of cancer, but the following factors are invariably considered:

1. Size of the primary tumor
2. Presence of local or distal metastases/invasion through basement membranes

It is obvious that large size and invasiveness of tumors, as well as their ability to spread to lymph nodes and to distal sites, leads to a bleak outlook for survival. In the context of the carcinogenesis model presented above, it is also presumed that these phenotypic traits of a tumor are intimately connected to the set of genes whose function or expression has been altered. It therefore becomes very important to identify and study the factors that lead to, or accompany, the acquisition of a more invasive and metastatic phenotype. A large number of genes have been identified, for which alteration of expression leads to the development of a more invasive and more rapidly metastasizing

tumor. Besides well-known protooncogenes and tumor suppressor genes that represent common targets for accumulation of mutations during early steps of carcinogenesis, alteration of function of other genes is required for tumor progression and generation of distant metastases. Such targets include:

1. Extracellular matrix (ECM) receptors that control cell adhesion and motility
2. Secreted proteases and their receptors
3. Proteins that control responsiveness of a tumor to endocrine and paracrine stimulation, such as hormone receptors and their coactivators, and
4. Factors that regulate neovascularization of tumors, such as VEGF and enzymes involved in angiostatin production.

In the present study I investigated biochemical and structural characteristics of the 67 kDa non-integrin laminin binding protein. This is one of the proteins that are involved in the interaction of a cancer cell with the extracellular matrix, whose expression is altered during cancer progression, and that contributes to the development of the malignant phenotype.

#### 67 kDa Laminin Binding Protein in cancer progression

In order to be able to escape the primary site and start a secondary tumor, a cancer cell has to possess the following traits:

1. Motility, i.e. it should be able to propel itself through the adjacent tissue

2. Ability to degrade the basement membrane that in most cases separates the tumor site from the surrounding stroma, blood, and lymphatic vasculature
3. Ability to stimulate formation of angiogenic vessels by vascular endothelial cells. Establishing an independent blood supply does not only permit further growth of a tumor, but also provides a gateway into the bloodstream.

It is quite natural that proteins that are involved in the development of any of these traits have been thoroughly studied. Such interest has been stimulated not only by natural curiosity to dissect the molecular mechanisms of metastasis, but also by a widely accepted notion that blocking the manifestation of any of these phenotypes will greatly reduce the rate of metastasis and, therefore, will help to save the lives of many patients. A lot of effort has gone into development of therapeutic agents that would either prevent proteolytic degradation of basement membranes, or inhibit angiogenesis. Some of these agents have actually shown promise and are now being tested in clinical trials. Among the many proteins and pathways that researchers attempted to target with antagonists or inhibitors, the 67 kDa laminin binding protein is a unique protein for many reasons. It is ubiquitously expressed and nearly every cell in the body relies on it for survival. It is involved in such diverse processes as protein synthesis and cell adhesion. It interacts with a variety of substrates, ranging from histones to prion proteins. It is an adhesion molecule that is at the same time associated with ribosomes, localizes to the nucleus and is shed in the extracellular medium. It possesses an enzymatic activity. Most of its sequence is

conserved in evolution from archaea to humans. Its upregulation is symptomatic for more invasive and aggressive cancers.

### The story of discovery

In 1983, Lance Liotta and his group discovered a receptor-like moiety on the surface of MCF-7 mammary carcinoma cells that had high affinity for laminin-1. They demonstrated that laminin-1 isolated from Engelbreth-Holm-Swarm (EHS) tumors specifically binds MCF-7 cells (and other cancer cells tested), and mediated their attachment to collagen-IV. The binding had a  $K_d$  of 2-50 nM, with an estimated 10,000-50,000 binding sites per cell. Using limited proteolytic cleavage, they also generated fragments of laminin and showed that the cell-binding site on laminin is located near the intersection of the short arms (181). In a separate study, the same group of authors has isolated the laminin receptor from the membrane extracts of the B16BL6 murine melanoma cells using laminin affinity chromatography (145). The isolated receptor had a molecular weight of approximately 67 kDa. It was able to bind laminin with a  $K_d = 2.0$  nM, which is close to the  $K_d$  of the whole B16BL6 cells or isolated membranes. The number of binding sites was estimated to be approximately 110,000 per cell. At the same time, an independent group of researchers isolated a 69 kDa laminin receptor from the surface of murine fibrosarcoma cells, which, similarly to the receptor isolated in other works, had a  $K_d$  for laminin of 2 nM, identical to that of the intact fibrosarcoma cells

(107). Approximately 50,000 binding sites for laminin were shown to be present on the surface of these cells. In 1986, the laminin receptor from human tissues was further characterized with participation of the same group of researchers. The receptor was isolated from the membrane fraction of a variety of normal and neoplastic tissues using laminin affinity chromatography (199). The procedure included washing the column with 0.3 M NaCl before the laminin receptor was eluted in 1 M NaCl, indicating a high-affinity interaction. It was found to migrate as a single band/spot on one- and two-dimensional SDS-PAGE, demonstrated apparent electrophoretic mobility of 68-72 kDa, depending on the source tissue, and a pI of  $6.4 \pm 0.2$ . While the intact protein appeared to be resistant to direct sequencing, probably due to the blocking of the  $\text{NH}_2$  terminus, the authors succeeded in obtaining a partial sequence by using a cyanogene bromide-generated fragment of the protein. The authors used a previously characterized antibody to the purified laminin receptor (98) to screen a  $\lambda$  phage - based human umbilical vein endothelial cell (HUVEC) cDNA library. By using this strategy they isolated a set of six partial cDNAs, all of which contained the sequence corresponding to the oligopeptide sequenced before. While these cDNA fragments did not represent a complete cDNA for the receptor, the longest one comprised an uninterrupted reading frame which encoded 253 amino acids, while all six fragments covered the common C-terminal 155 amino acids and terminated with a stop codon. The 3'-untranslated region varied in these clones. When this incomplete cDNA was used as a probe in Northern blotting, it hybridized with a ~1700 bp RNA, present in all cell lines tested. Interestingly, the amount of RNA detected on these Northern blots correlated with the metastatic potential of the cell line

tested, and with the amount of laminin receptor protein present on the surface of the cells. However, it was not until two years later that this observation was linked to the role of this protein in metastasis. The first report linking this newly characterized laminin receptor with tumor progression came in 1988, when an independent group identified the laminin receptor cDNA when searching for genes that are differentially expressed in colon carcinoma and normal gut tissue (208). A cDNA clone containing a partial laminin receptor coding sequence hybridized with a single band of ~1200 bp in RNA extracts from normal tissue and surgical gut carcinoma specimens. The signal was up to 9-fold higher in carcinoma RNA extracts, compared to normal tissues. These results were later confirmed by the serial analysis of gene expression (SAGE) analysis (<http://www.sagenet.org/Transcriptome/Table3.htm> and <http://www.sagenet.org/cancer/CTCL-NC/Ctl-nc1.htm>) When total RNA from twenty independent surgical specimens was analyzed, all but one showed an increased level of the putative laminin receptor RNA. Using this partial cDNA clone as a probe, the authors screened a cDNA library produced from a colon carcinoma tissue and thus obtained a full-length cDNA for the laminin receptor. It included a sequence identical to that previously described (199) and contained an open reading frame coding 295 amino acids. Analysis of the primary protein sequence revealed no signal sequence for entry into endoplasmic reticulum and no N-glycosylation signals. A hydropathy plot suggested the presence of hydrophobic regions in the N-terminal part of the protein that may serve to anchor the protein to the membrane. However, no canonical transmembrane domain was detected. The C-terminal part of the deduced protein contained a strongly negatively charged region between

residues 200 and 230 and a overall lack of positively charged residues after residue 225. Thus, the C-terminal 70 aa fragment is extremely acidic, carrying 13 aspartic and glutamic acid residues and not one basic amino acid. Also, the authors reported two repeats of TEDWSAXP (264-271 and 273-280), two repeats of AAAXXA (91-96 and 216-221), three repeats of KEE (11-13, 212-214 and 224-226), two repeats of (E/D)XXX(E/D)XYXY(K/R)XXX(E/D) (31-44 and 196-209), six repeats of (E/D)(E/D)M and one palindromic sequence LMWWML (173-178). Interestingly, the DWS sequence is found twice within the larger repeat mentioned above, and two more times outside of this repeat. Also, there is a related TEW sequence seen in the vicinity of the DWS repeats (284-287). An interesting fact is that the isolated cDNA only coded for a protein with a deduced molecular weight of 32,817 Da, while the previously characterized laminin receptor has an electrophoretic mobility corresponding to 68-72 kDa (199). This finding initially cast doubts on the identity of the protein isolated in earlier work (98, 199) and the putative protein encoded by the isolated cDNA clone. However, the epitopes that were recognized by antibodies directed against purified 67 kDa laminin receptor (200) are entirely present in the deduced protein sequence. It was postulated that the 32 kDa protein encoded by the deduced sequence undergoes a posttranslational modification that results in the increase of molecular weight. Another report, published by the same group that had first described the 67 kDa laminin receptor on the surface of cancer cells in 1986, has presented evidence that this protein plays a critical role in attachment and migration of melanoma cells on a laminin substrate. The authors have found that a polyclonal antibody directed against a C-terminal peptide 270-

290 (which contains 2 TEDWS repeats) significantly inhibited attachment of the A2058 human melanoma cells. Interestingly, the antibody generated against a synthetic peptide corresponding to the another region, 165-184, later shown to be one of the major laminin binding sites (32), did not inhibit cell attachment to the same degree as the antibody against the more C-terminal peptide. It was also shown that antibodies against the purified laminin receptor, as well as antibodies against synthetic peptides, were able to inhibit migration of the A2058 cells in response to laminin (200). At the same time, a specific laminin receptor with a molecular weight of approximately 70 kDa was described on activated macrophages (80, 201). The authors proposed a link between the increased production of laminin by more invasive cancer cells (106, 192) and the ability of activated macrophages to recognize tumor cells, by virtue of the macrophage laminin receptor, and kill them. In a different study, activated macrophages appeared also to express elevated amounts of cell surface-bound laminin (202). These observations fit well into an established paradigm that expressed laminin, being immobilized on the cell surface through a surface-expressed laminin receptor, mediates cell attachment and motility. However, there is no conclusive proof that the described laminin receptor on macrophages is identical to that described in previously mentioned works. In fact, the authors also mention that along with laminin, activated macrophages also express a lectin-binding protein on their surface (202). Since there are several carbohydrate-binding proteins of similar molecular weight (142), it remains unclear which protein was identified as the laminin receptor on macrophages. In recent years, LBP was also implicated in apical ectodermal ridge – mesoderm interaction during embryogenesis in

chicken (77), spermatogenesis in mouse (64), and embryo implantation (191, 211). It was also isolated from various cell types and tissues, including liver (2), muscle (97), platelets (178) and kidney (159).

### 67 kDa LBP and cancer pathology

Upregulation of expression of LBP in cancerous tissues was well documented in the early reports on this protein (see “the story of discovery” section). The function-blocking antibodies against LBP reduce the rate of experimental metastasis (134), cancer cell attachment to laminin, and migration on laminin (98, 200). In addition, expression of LBP correlates with angiogenesis, which is a prerequisite for metastasis, in both tumor and normal organ development (115, 176). This subchapter deals with the implication of the 67 kDa LBP in various forms of cancer.

#### Gut carcinoma

The positive correlation between expression of LBP and progression of colon carcinoma (Duke's stage) was documented relatively early (39, 103). It was shown that the LBP mRNA level is increased in the tumor tissue, compared to the adjacent normal epithelium, in all but one of 21 cases studied, which is compatible with the similar results from another group (208). More interestingly, the ratio of tumor:normal LBP mRNA correlates well with the Duke's stage. Three to ten times more LBP mRNA was found in Duke's D tumors (distant metastases present) than in normal tissue, while in Duke's A

(penetration limited to submucosa) tumors, the level of the LBP mRNA was barely elevated at all. The authors presented evidence of a steady increase in the tumor:normal LBP mRNA ratio spanning the entire range of Duke's stages (A through D). Also, a positive correlation between the number of primary tumors, as well as the presence of distant metastases, and LBP expression was reported. An increased LBP mRNA expression in colon adenocarcinomas was also documented by *in situ* RNA hybridization (23). A positive correlation between LBP expression at the protein level and Duke's stage was also documented (49). In a different work, increased expression of LBP mRNA was found to be inversely correlated with the expression of another non-integrin laminin receptor (termed 31kDa HLBP), which is homologous to the murine galactoside-binding lectin (27). The biological significance of this finding is unclear. The expression of LBP in colon cancers is not only upregulated at the transcriptional level, but also at the protein level, as was demonstrated in a large-scale study involving over 300 samples of normal tissues, polyps, carcinomas, and lymph node metastases (160). Using immunohistochemical staining with a monoclonal anti-LBP antibody, it was shown that the frequency of cells positive for LBP expression increases from normal tissues to adenoma to carcinoma to lymph node metastases. Frequency of LBP expression was also found to correlate with the stage of colorectal carcinomas. These results are compatible with the earlier results of Cioce and coworkers (39), who demonstrated a positive correlation between the 67 kDa LBP expression and Duke's stage in colon carcinomas. Interestingly, no correlation between immunoreactivity with the anti-LBP antibody and histological grade was discovered in this work.

### Lung cancer

The LBP cDNA was isolated from a cDNA library of two lung cancer cell lines and was found to be more abundant in these cells than in a normal lung epithelium (163). Cell surface expression of LBP was also demonstrated in eleven independent small cell lung carcinoma cell lines and a direct correlation between the expression level of 67 kDa LBP and VLA-6 integrins was observed. Interestingly, the expression of LBP was found to correlate with the presence of extracellular laminin in culture (140). Small cell lung carcinomas also showed increased expression of LBP mRNA (162). In clinical studies, the increased expression of the 67 kDa LBP in non-small cell lung carcinomas correlated with nodal involvement, Ki-67 levels, and blood vessel penetration (61). Since all these factors are negative prognostic factors, it can be envisioned that LBP expression also correlates with poorer prognosis in these patients. Partial inhibition of LBP expression by expression of antisense mRNA in murine lung cancer cell line results in lower proliferation rate, weaker adhesion to laminin, substantial decrease of tumor mass, and reduced number of metastases in recipient mice (161). These effects were attributed to the lower neovascularization of LBP-diminished tumors (177). On the other hand, expression of LBP correlates with the tumor infiltration by  $\gamma\delta$  T-lymphocytes, which mediate an antitumor immune response (60). These  $\gamma\delta$  tumor-infiltrating lymphocytes (TILs) specifically kill tumor cells in a process that involves interaction between a TIL and 67 kDa LBP expressed on the tumor cell (59).

### Breast cancer

One of the first descriptions of LBP was made while studying attachment to laminin by two breast cancer cell lines (181), and soon LBP was identified on breast cancer cells in patients (9, 125, 199). Numerous lines of evidence link the 67 kDa LBP to the progression of mammary carcinomas. So, while LBP is almost undetectable by immunostaining in normal breast epithelium, as well as in benign breast tumors, its expression is markedly increased in carcinomas, both invasive and *in situ*, and the amount of LBP present correlates with the invasiveness of the tumor (29, 76, 110, 193) and metastatic potential (122). The analysis of LBP expression in surgical specimens suggests positive correlations with tumor size, lymph node involvement and negative correlation with survival time after surgery (109). In primary breast tumors, overexpression of LBP also correlates with the chance of local recurrence and lymph nodal relapse within metachronous contralateral lesions (51). The prognostic value of LBP correlates with laminin expression, as patients with breast carcinomas expressing both laminin and LBP were shown to have the worst prognosis, while LBP- and laminin - negative tumors appear to be the least dangerous (141). Interestingly, laminin was shown to inhibit mitogenic action of estrogen on estrogen receptor (EsR) positive breast cancer cells (203), which indicates that laminin expression may have either positive or negative influence on tumor behavior, depending on other factors, such as LBP and EsR status. On the contrary, in mammary carcinomas without lymph node involvement, LBP was shown to have no prognostic value as far as survival and disease-free times are concerned, and

positive correlation was observed with the histological grade in these tumors (131). Additionally, in this set of patients, LBP expression correlated with estrogen receptor expression, which is a positive prognostic factor. Expression of LBP was found to be upregulated in breast carcinomas compared to the adjacent normal epithelium and a positive correlation was observed between the invasiveness of tumors and the LBP status (49). In the cell culture model, LBP expression was found to be much higher in a more invasive and aggressive subclone of the T47D breast carcinoma cell line than in the less invasive parental line (166). Contrary to the paradigm of LBP overexpression as a negative prognostic factor in human cancers, some authors found positive correlation between LBP expression and survival or no correlation at all (52, 108), although the identity of the laminin receptor being detected in these studies and LBP is not proven. While the independent prognostic value of LBP expression remains controversial, some authors have suggested a combination of expression of LBP and other mitogenic factors as a good prognosticator (46). A correlation, although not statistically significant, between LBP expression and tumor vascularization was observed in node-negative breast cancers (14, 66), which is consistent with the observation that LBP expression correlates with angiogenesis in a lung cancer experimental system (177).

LBP was shown to be identical to the independently characterized 37 kDa oncofetal antigen of breast carcinomas, acquisition of which by tumor cells correlates with increased invasiveness and suppression of cytotoxic antitumor immune response (45, 152). It is surprising, however, that this protein was previously characterized as a 44 kDa glycoprotein (152), while the 67 kDa LBP does not contain any consensus

glycosylation signals and experimental evidence suggests that this protein is not glycosylated (94).

Expression of LBP was found to be responsive to such breast cancer - relevant mitogens as estradiol and progestins, and in case of estrogen, this effect is mediated by cellular estrogen receptor (31, 166, 190). Interestingly, a positive correlation between LBP expression and EsR status was observed in lymph node-negative breast carcinomas, with 78% of LBP positive tumors being also positive for ER (131). Serial analysis of gene expression (SAGE) data also indicate that expression LBP on mRNA level is upregulated up to 5-fold three hours after estradiol treatment (37) (and <http://sciencepark.mdanderson.org/ggeg/>).

#### Other cancers: thyroid, ovarian, cervical, gastric, nervous and lymphoid tissue

While the role of LBP is best studied in the above mentioned types of cancer, its expression was also found to correlate with negative prognosis and disease progression in thyroid cancers (10, 128), as well as cervical (1), gastric (49, 96), liver (148) and ovarian (187) carcinomas. In case of cervical carcinomas, contradictory evidence emerged, with one report suggesting lack of correlation between LBP expression and invasion (55). Elevated expression of LBP on mRNA level was also described for pancreatic carcinoma (75). LBP was found on a small subset of high grade B cells in lymphomas, both Hodgkin's and non-Hodgkin's, and on approximately 30% of anaplastic large cell lymphomas, of both T- and B-cell origins (25). Relevance of LBP expression in

lymphomas was never elucidated. LBP was found to be differentially expressed on the mRNA level in chronic leukemia, with suppression in the chronic phase and upregulation in the acute phase (50). Interestingly, in this work authors observed a very prominent 5.5 kbp mRNA species in addition to the previously described 1.2 kbp mRNA (103, 199, 208), and the amounts of the 5.5 kbp and 1.2-1.7 kbp mRNAs seemed to be inversely proportional. In the neuroblastoma cell culture model it was shown that differentiation of these cells is accompanied by the decreased expression of LBP, which indicates that this protein may represent a prognostic marker in progression of neuroblastoma (19).

#### Phylogenetic relationships of the LBP

LBP is a member of the family of ribosomal S2p proteins, where "p" denotes homology to prokaryotic S2 proteins to avoid terminological confusion. Homology between LBP and S2p ribosomal protein is limited to the N-terminal two-thirds of the sequence. Mammalian LBP is almost 30% identical to the bacterial S2p in this region. Unlike the N-terminal domain, which is very well conserved in all species studied, the C-terminal domain, which is responsible for laminin binding in higher eukaryotes, is highly divergent. Some conservation of this domain is observed in multicellular organisms which express laminin, while in single-cell organisms this domain can differ a lot from species to species. The distinct separation of functions between the N-terminal domain, which is homologous to S2p proteins, and C-terminal domain, which contains features

necessary for laminin binding, has prompted researchers to hypothesize that LBP of higher eukaryotes has evolved by addition of a novel laminin-binding domain to the S2p progenitor and conservation of the laminin-binding determinants in this domain, such as "peptide G" (see below) (3). The homology between LBP and ribosomal proteins spans residues 1-185 (see figure 4.1). The exact boundaries of the homologous region do not match the intron-exon structure of the gene (85), although an attempt was made to limit the novel laminin-binding domain to exons 5 and 6, which start at position 209 (41) (Positions are given according to the human LBP sequence (163, 199)). There are several proteins that are analogous in function, but not homologous to LBP (116, 117) (and references therein). These include 110 kDa and 180 kDa laminin binding proteins isolated from membranes of neuroblastoma cells (79, 91) and a 30 kDa laminin binding glycoprotein from peripheral nerve membranes (157). There is also a variety of oligosaccharide-binding laminin receptors, such as the 67 kDa elastin/laminin binding protein which apparently binds carbohydrates on these ECM proteins (73, 118, 119, 142), 14 kDa LBP isolated from human melanoma cells (30), and 50 kDa and 18 kDa galectin-like proteins from porcine neutrophils (89). In other species, apparently unrelated laminin receptors were shown to be present on the surface of *C. albicans* (69, 205) and *A. niger* (185) cells and in a variety of bacteria (99, 133, 186, 194).

### Translational regulation

Expression of LBP is thought to be under translational control. It was noticed that the amount of expressed protein may not correlate with the amount of the mRNA present in the cell (95). LBP mRNA was found within RNP particles typical of the "cryptic" (neither translated nor degraded) mRNA and has sequence features in the 5'-UTR characteristic of the RNAs that are under translational control (105, 206).

### Dimerization and cell surface expression

The mRNA for LBP detected in normal and cancer cells is 1.2-1.7 kbp long (103, 199, 208), and the deduced open reading frame codes for a polypeptide with the expected molecular weight of 32 kDa. However, the major surface-expressed protein corresponding to this mRNA has an apparent electrophoretic mobility of 67 kDa (76, 107), and this molecular weight has been later confirmed by mass spectrometry (94). In the cytoplasm, however, this protein is present predominantly in the low molecular weight form, with an electrophoretic mobility corresponding to 37 kDa. The presence of the 37 kDa form in the cytoplasm was demonstrated by immunoblotting (22, 200). According to flow cytometry data, there is approximately 80 times more LBP in the cytoplasm than there is on the cell surface (94). Interestingly, some monoclonal and polyclonal antibodies raised against defined peptides recognized either 37 kDa or 67 kDa forms (21, 32, 146, 200), indicating that a structural rearrangement possibly accompanies

formation of the 67 kDa form. Also of interest, the set of eight monoclonal antibodies raised against recombinant monomeric LBP do recognize the 67 kDa LBP in Western blots, but fail to react with LBP on the cell surface, indicating that non-conformational epitopes exposed in denatured protein and in monomeric LBP may be inaccessible in the membrane-associated 67 kDa protein (21). The cDNA for LBP produced the 32 kDa protein in an *in vitro* translation system, and this was found to be immunologically related to the 67 kDa protein isolated from tissue (146). The hypothesis of precursor-product relationship between 32 kDa and 67 kDa forms was further supported by the pulse-chase experiments, in which radioactivity incorporated into pulse-labeled 32 kDa LBP was traced to the 67 kDa LBP (28). However, it remains unclear whether 67 kDa LBP is a homo- or heterodimer (121). The amino acid composition of the 67 kDa LBP closely matches that of the deduced 32 kDa protein (94), which speaks in favor of the homodimer hypothesis. However, other authors have reported the presence of a lectin epitope with in the 67 kDa LBP, and the recognition of this protein by the antibodies specific for galectin-3 (22). Interestingly, expression of galectin-3 and LBP was found to be inversely regulated in trophoblastic tissue and this expression pattern correlated with the trophoblast invasion (18). The same observation was made for cancer cells (188). In a different study, downregulation of galectin-3 expression was found to correlate with the acquisition of the invasive metastatic phenotype of human breast carcinoma (34) and it was found to be of little importance for the interaction between cancer cells and laminin (189).

The 67 kDa LBP carries covalently associated fatty acid residues of palmitate, stearate and oleate (94). Dimer formation is inhibited by the inhibition of fatty acid synthesis (22), which indicates that acylation of the precursor(s) is necessary for the dimer formation. Boiling of 67 kDa LBP in 1M  $\beta$ -mercaptoethanol for two hours did not cause separation of the dimer, which indicated that dimerization occurs by a mechanism other than disulfide formation (94) (and this dissertation, chapter 3).

Monomeric LBP also binds laminin (64, 169) (and this dissertation, chapter 3), although with an affinity much less than that of the 67 kDa protein (my unpublished observations), and is present on the cell surface (67, 68). Apparently, cell surface expression does not require dimerization of LBP, but may favor it, since in other studies, the 67 kDa form was the predominant one in membrane fractions (see "Story of Discovery" section).

LBP is not only expressed on the cell surface, but is also shed into the extracellular medium. The shedding is stimulated by lactose, and apparently does not involve proteolytic cleavage, since the released protein has the same molecular weight as the affinity-isolated LBP (87). The shed LBP is able to re-bind cell membrane (87) and laminin-1 (173). Drugs that inhibit the ER-Golgi traffic do not affect the shedding of LBP, indicating that the appearance of LBP in the medium is due to shedding rather than active secretion (87). The function of the shed LBP in the extracellular medium is unclear. The results discussed in chapter 3 of this dissertation may provide a clue to its role in the ECM.

### LBP and $\alpha 6$ integrins

Integrins, heterodimeric transmembrane ECM receptors, play important role in cancer cell adhesion and migration. For some integrins, the role in metastasis is well documented and prognostic significance is attributed to some (78). Expression of the  $\alpha 6$  integrins in breast carcinoma inversely correlates with the survival time (63) and directly correlates with the invasiveness of breast carcinoma (5). Expression of  $\alpha 6\beta 1$  integrin positively affects tumorigenicity and metastatic potential of breast cancer cells (198). In a cell culture model system, MDA-MB-435 variant clones which were found to be more tumorigenic and metastatic in mice expressed higher amounts of  $\alpha 6$  than less metastatic variants (130).  $\alpha 6\beta 1$  is the only  $\alpha 6$  integrin in these cells and knocking out its function resulted in substantial loss of laminin adhesion and motility, and an impaired ability to penetrate reconstituted basement membrane (165). The special role of  $\alpha 6$  integrins was noticed for prostate cancer (48, 143), colorectal carcinoma (36), hepatocarcinoma (13, 26, 135, 184), fibrosarcoma (204), pancreatic carcinoma (195) and melanoma (132, 155). Experimental evidence obtained for human leukocytes suggests that avid laminin binding depends on co-expression of VLA-6 ( $\alpha 6\beta 1$ ) and 67 kDa LBP in these cells (24). In pancreatic adenocarcinoma, expression of both  $\alpha 6$  integrin and LBP is upregulated, indicating that both molecules may be involved in the progression of this type of cancer (75). Similar coordinated expression of these two proteins was also documented for non-small cell lung carcinoma (140). Physical association of LBP and  $\alpha 6\beta 1$  integrin was demonstrated by immunostaining (153) and by co-immunoprecipitation of the two

proteins (4). The two laminin receptors were found in the same cytoplasmic particles in resting cells and were transported to the cell surface upon exposure of cells to laminin. It was also shown in a different study that exposure of cancer cells to laminin leads to the increased synchronous expression of both  $\alpha 6$  and LBP, and downregulation of the  $\alpha 6$  by transfection with antisense RNA led to a synchronous decrease in LBP expression (4). Expression of  $\alpha 6$  cDNA in CHO cells leads to concomitant overexpression of LBP and increased shedding of the latter (173).

#### Interaction with laminin

Laminins are one of the major components of the basement membranes and connective tissue. Multiple laminin isoforms have been isolated from different sources. The predominant laminin isoform found in basement membranes of mammals is referred to as laminin-1. All laminins consist of three chains coded  $\alpha$ ,  $\beta$  and  $\gamma$ , arranged in a characteristic cruciform shape (12, 183). Laminin-1 is an important constituent of the extracellular matrix, which is involved in multiple interactions with other components of the ECM, such as nidogen (112, 113), heparan sulfate proteoglycan (90, 112), heparin (170, 175), collagen IV (147), and agrin (57). Laminin-1 is involved in the interaction with cellular receptors through its protein components and associated carbohydrates, and mediates adhesion, spreading and migration of both normal and cancerous cells, as well

as modulating tumor take and the rate of metastasis (7, 17, 35, 38, 54, 82, 114, 151, 179, 180, 182).

LBP specifically binds laminin-1. The diagram of the binding sites for LBP on laminin is shown on figure 1.1. Rotary shadowing experiments have demonstrated that LBP binds multiple sites on laminin, including the globular domain on the long arm of the  $\alpha_1$  chain, globular domain on the short arm of the  $\alpha_1$  chain, the proximal part of the  $\beta_1$  chain, but was most often found bound at the part of the long arm just below the intersection of three chains (40).

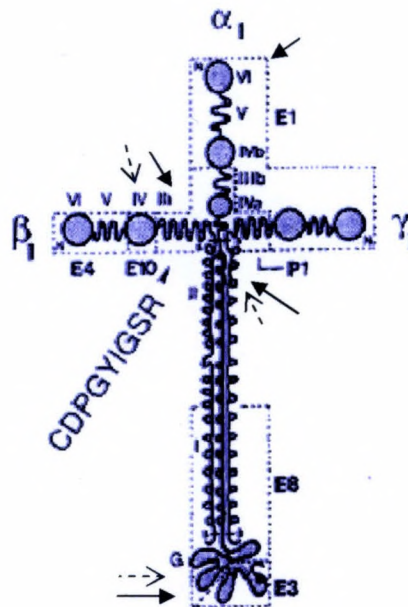


Figure 1.1. Schematics of laminin-1 molecule. Modified from (209). Solid arrows indicate the LBP binding sites as described in (40). Dashed arrows indicate heparin binding sites (172, 173). Fragments derived by elastase (E) and pepsin (P) treatments are indicated. Position of peptide 11 sequence is also shown.

Interestingly, two of these sites were also identified as heparan sulfate-binding sites on laminin (globular domain on the long arm of  $\alpha 1$  chain, and the intersection of the cross) (170). A third heparin sulfate-binding region was located in the globular domain of the short arm of the  $\beta 1$  chain, near the LBP-binding site (40), (171). In a different study, the  $\alpha 3$  fragment of laminin, which comprises the short arms of the  $\alpha 1$ ,  $\beta 1$  and  $\gamma 1$  chains, was shown to retain most of the cell-binding activity of laminin (181).

While the peptide sequences that mediate LBP binding at these sites were not characterized, one peptide from the laminin-1  $\beta 1$  chain was shown to specifically interact with LBP. This peptide CDPGYIGSR, is also referred to as "peptide 11", according to the nomenclature of peptides tested in one of the first reports on this subject (83). The peptide is derived from the proximal part of the short arm of the  $\beta 1$  chain, located approximately three-fifth of the distance between the crosssection of short arms and the middle globular domain of the  $\beta 1$  chain. Most of its activity is attributed to the YIGSR sequence (71). This pentapeptide mediates attachment of endothelial cells and displaces LBP off a laminin affinity column (71), as does the full peptide 11 (70). Similar, but less pronounced effects on cell attachment were observed for hepatocytes, although in this case another laminin peptide from the  $\alpha 1$  chain globular domain was shown to be the preferred cell binding site (44). This was also the case for a mouse trophoblast outgrowth, where the E8 fragment of laminin, which contains the long arm, was shown to support trophoblast sprouting (6). YIGSR also supports migratory behavior of the mesenchymal cells of sea urchin gastrulae (47). YIGSR supports attachment of not only eukaryotic cells, but also some pathogenic bacteria (102, 167), which may indicate that these

pathogens utilize molecular mechanisms for the attachment to host ECM similar to that of mammalian cells.

The YIGSR peptide was found to inhibit the formation of metastatic tumors in mice when coinjected with melanoma cells and reduces the rate of penetration of reconstituted basement membrane in *in vitro* invasion assays (83). It also reduced the rate of secondary colony formation in a system employing leukemic cells (207). This peptide not only inhibits metastatic tumor formation, but also supports cell attachment and spreading (111, 144), and cell attachment to this peptide is inhibited by the anti-LBP antibodies (111). Radiolabeled YIGSR has been successfully used for detection of metastatic tumors in mice. Injected iodinated peptide was found to bind preferentially to the membrane of a subset of metastatic cells, allowing their visualization on microradioautographs (92).

Possibly due to the ability of peptide 11 and YIGSR to support mobility and capillary formation by endothelial cells (72), this peptide also possesses antiangiogenic properties. It inhibited angiogenesis in chick chorioallantoic membrane vascularization assays (158) and inhibited angiogenesis of solid tumors (123, 158).

Crosslinking experiments demonstrated that YIGSR binds two proteins, one of which is thought to be the 67 kDa LBP, and another yet unidentified 116 kDa protein, which possesses a much lower affinity for the peptide. Binding of YIGSR to neuroblastoma cells is accompanied by tyrosine phosphorylation of at least two cellular proteins, which indicates that 67 kDa LBP may act in outside-in signaling (20).

Many research groups have sought to increase the antimetastatic potential of the YIGSR peptide by using various polymer constructs. The major rationale is to increase its half-life in blood by making it less susceptible to proteolytic cleavage. To this end, plain polymeric peptide containing multiple copies of the active sequence (138, 156), as well as peptide conjugated to polyethyleneglycol (86, 101, 210), a polystyrene derivative (129), and chitosan (137) were tested and found to have higher biological activity than the monomeric peptide.

Several studies aimed at elucidating the role of particular amino acid residues in YIGSR peptide demonstrated that the R and Y are absolutely required for the biological activity, and even a conservative R→K substitution is not tolerated (71, 83, 126, 168, 172), while I can be substituted for any other hydrophobic residue (M, L, F) without loss of activity (101). Alanine scan substitution analysis of peptide 11, however, demonstrated that an I→A mutation leads to loss of activity in metastasis inhibition assays, and also showed the importance of the C and D residues (172). Interestingly, a peptide derived from murine EGF with sequence CVIGYSGDRC also binds LBP and inhibits attachment of cancer cells to laminin-1 to the same extent as peptide 11 (136). This indicates that common residues (Y5, G7 and R9 in peptide 11) are most important for these activities, consistent with the data from other groups (71, 83, 172). Both peptide 11 and the EGF33-42 peptide are found in structurally similar domains of the respective proteins (laminin-type EGF-like repeat in laminin and C-loop in EGF) (11, 100, 174). Cyclic peptide 11 (with an added C-terminal C) is far more active in inhibiting the YIGSR-mediated cell adhesion than the linear peptide (102). This observation is consistent with the NMR

solution structure of the free peptide11, which was shown to favor a bent backbone conformation, while less active G<sup>4</sup>→A analog remains linear (139, 172).

Three sites on LBP that are responsible for interaction with laminin-1 were characterized. One is the region called "peptide G", corresponding to positions 161-180 in the mammalian LBP. This peptide specifically binds laminin *in vitro* and elutes LBP from a laminin-1 affinity column (32). Peptide G also inhibits cancer cell attachment to laminin-1 and to endothelial cell monolayers (33). At the same time, pretreatment of laminin-1 with peptide G increases laminin binding to cancer cells and also makes this binding more stable. Cancer cells treated with peptide G are also stimulated to produce more endogenous laminin-1 (104). These effects, however, appear to be mediated through heparan sulfate moieties associated with laminin-1 (74). Peptide G binds heparan sulfate and its binding to laminin-1 is inhibited by an excess of free heparan sulfate. Binding of peptide G to laminin-1 is not affected by the YIGSR peptide (74).

Another site on LBP implicated in laminin binding is the peptide 205-229. This peptide is strongly negatively charged, binds laminin-1 in a YIGSR-inhibitable manner, and modulates the tumor metastasis rate in mice and basement membrane invasion *in vitro* (95).

The third region of LBP involved in interaction with laminin-1 is located in the distal C-terminal part of the protein containing five copies of the DWS and TEWS repeats. Antibodies raised against a larger peptide which includes these repeats partially inhibit cell attachment to laminin (200), as did an excess of free peptide containing the

consensus DWS repeat (88). All three regions were mapped using phage display library screening (88) (see chapter 2 of this dissertation).

### Ribosomal function

As was mentioned above, LBP has extensive homology with the S2p family of ribosomal proteins. Proteins with sequence homologous or identical to the N-terminal part of LBP are found to be components of the small subunit and found in polysomes in a variety of organisms (8, 53, 56, 62, 65, 93, 120, 127, 154). LBP is found in polysomes as a monomer, and repression of protein synthesis results in loss of LBP homologues from ribosomal particles, which may indicate its role as an elongation factor (8). Apparently it is dimerization and possible structural change that accompany dimerization that confer to LBP its laminin receptor function. A more detailed analysis of ribosomal function of LBP is given in the introduction section of chapter 4 of this dissertation.

### LBP as viral and PrP receptor

Besides acting as laminin receptor, 67 kDa LBP also functions as a cell surface receptor for Sindbis virus, a member of the alphavirus family with very a broad spectrum of hosts, ranging from insects to mammals (196).

By utilizing a yeast two-hybrid system, Rieger and coworkers have demonstrated that 37 kDa LBP specifically interacts with prion protein PrP<sup>c</sup> and they have confirmed this interaction in insect and mammalian cells. Accumulation of PrP<sup>sc</sup> in rodent organs correlated well with accumulation of 37 kDa LBP (150). Later, the same group demonstrated that the LBP acts as a surface receptor for the PrP and mediates its internalization. The presence of the 37 kDa form of LBP on the cell membrane was demonstrated by Western blotting of membrane fractions of two different mammalian cell lines. It is not clear whether 67 kDa LBP acts as a PrP receptor, but the role of the 37 kDa monomer in this interaction was very well documented by colocalization of LBP and PrP on the surface of mammalian cells, increased PrP binding to cells overexpressing LBP and by GST pull-down assays (68). Surprisingly, mutational analysis indicated that the same sequence in LBP that is involved in laminin binding ("peptide G") is responsible for the direct interaction with the prion protein. In addition to this sequence, another yet unidentified epitope on LBP is involved in heparan sulfate – mediated PrP binding (81). We, and others, have previously demonstrated the involvement of heparan sulfate in the interaction of LBP with laminin-1 (74, 88). We have also shown the potential involvement of the 205-229 region of LBP in heparan sulfate binding, in addition to that of the previously characterized 161-180 peptide (88). It remains to be elucidated whether the 205-229 peptide is involved in the interaction with PrP in mammalian cells.

### Gene organization

There are no reports of LBP knockouts, either in cell culture or in animal models. This, along with the documented ribosomal function of this protein, tight translational regulation, and significant conservation of a large portion of the protein sequence, leads to the hypothesis that the LBP gene is required for cell viability. The presence of multiple copies of this gene in the genome adds validity to this theory. The mouse genome was shown to have 5-7 copies of the LBP gene, of which at least three are transcriptionally active and produce complete mRNAs (58). In the human genome the number of copies of the LBP gene was reported to be  $26 \pm 2$ , with at least 19 of those bearing features of processed pseudogenes, such as lack of introns, presence of remnants of polyA tails, and numerous genetic lesions, in some cases leading to premature termination of the ORF (84, 164). In another report, the number of genomic copies of LBP coding sequence was estimated as 16 for human and 21 for mouse (15). Three cDNAs were isolated from the human HUVEC cDNA library, which suggests the presence of more than one functional LBP gene in humans (15, 16). The multiple copies of the LBP gene have most likely arisen through retrotransposition events. This notion is supported by the following observations: a) only one LBP gene is present in the chicken genome, and retrotransposition is found much more often in mammals than in birds (197); b) by the comigration of the bands hybridizing with the 5' and 3' probes on the mammalian genomic Southern blots, which indicates lack of interspersions with introns; c) the spread of the LBP pseudogenes throughout the genome in mammals (15). At least one

characterized pseudogene located on the X chromosome has the 18 bp direct repeats on either end, indicating its retroviral origin (149). Active LBP genes from the chicken (42) and human (85) genomes were isolated and characterized. The genes contain seven exons and six introns located in identical or very close ( $\pm 1$  amino acid) positions, and have similar promoter features. Promoters of both genes lack consensus TATA or CAAT boxes, but both contain multiple *sp1* binding sites, AP1 binding site(s), a cyclic AMP response element, and glucocorticoid response element half-sites. In addition, the chicken LBP gene promoter contains enhancer binding protein (C/EBP) binding sites and enhancer core elements previously described for SV40. It should be noted that the promoter region of the chicken gene was sequenced as far as -1500 bp, while the human promoter was sequenced for about -500 bp from the start. An AP1 binding site in the promoter is known to confer responsiveness to a variety of oncogenes, mitogens, growth factors and tumor promoters. Interestingly, TNF- $\alpha$  and IFN- $\gamma$  both repress the promoter activity of the human LBP gene, possibly through the sequestration of AP1, inhibiting its transcriptional activity (43, 124). The biological role of the glucocorticoid response elements (GRE) in the promoters of both chicken and human LBPs is not clear. These sites do not represent complete palindromic responsive elements for the nuclear receptors, and are very dissimilar from the canonical estrogen response element (ERE) or progesterone response element (PRE).

GRE-1 in human LBP promoter: CCTGTTAAACTG (inverted)  
GGACAATTTGAC  
GRE-2 in human LBP promoter: ACGTCATTTCTGC (half-site)  
TGCAGTAAAGGACG  
AGGTCANNNTGACCT -consensus ERE

A comparison of the putative glucocorticoid response elements in the human LBP promoter (85) and the canonical estrogen responsive element is given above. One site is inverted with respect to the canonical sequence, is incomplete and has two substitutions. The second GRE is actually a half-site, and has one substitution. LBP expression is regulated by estrogen and progestin (31, 37, 166, 190) (and our unpublished data), but whether this effect is mediated directly by estrogen or progesterone receptors transactivating LBP gene expression, or whether the effect is mediated by secondary factors, remains to be elucidated. The absence of a TATA box, presence of multiple sp1 binding sites, the location of a cap site within the pyrimidine rich tract, and the very short first exon (located in the 5'-UTR in these genes) are all characteristic of housekeeping genes, including those coding for ribosomal proteins (85).

#### Statement of thesis

In this dissertation project I will investigate the interaction between LBP and laminin-1 mediated through the peptide 11 sequence. I will utilize phage display peptide library screening in order to elucidate the functional relationship between two major laminin-interacting sites in LBP, namely, peptide G and the 205-229 region, and how

these two regions contribute to laminin binding. I will also investigate the possible role of shed LBP in the extracellular medium. This will involve characterization of the sulfhydryl oxidase activity of the LBP *in vitro*. Finally, I will address the possible role of LBP in protein synthesis by modeling the ribosome-binding domain of LBP and attempting to predict its location on the ribosome and interactions with rRNA and other proteins.

REFERENCES CITED

1. al Saleh, W., P. Delvenne, F. A. van den Brule, S. Menard, J. Boniver, and V. Castronovo. 1997. Expression of the 67 KD laminin receptor in human cervical preneoplastic and neoplastic squamous epithelial lesions: an immunohistochemical study. *J.Pathol.* 181:287-293.
2. Anilkumar, N. and P. R. Sudhakaran. 1993. Isolation and characterization of laminin binding protein from regenerating rat liver plasma membrane. *Biochem.Mol.Biol.Int.* 31:201-209.
3. Ardini, E., G. Pesole, E. Tagliabue, A. Magnifico, V. Castronovo, M. E. Sobel, M. I. Colnaghi, and S. Menard. 1998. The 67-kDa laminin receptor originated from a ribosomal protein that acquired a dual function during evolution. *Mol.Biol.Evol.* 15:1017-1025.
4. Ardini, E., E. Tagliabue, A. Magnifico, S. Butó, V. Castronovo, M. I. Colnaghi, and S. Menard. 1997. Co-regulation and physical association of the 67-kDa monomeric laminin receptor and the alpha6beta4 integrin. *J.Biol.Chem.* 272:2342-2345.
5. Arihiro, K., K. Inai, K. Kurihara, S. Takeda, N. Khatun, K. Kuroi, and T. Toge. 1993. A role of VLA-6 laminin receptor in invasion of breast carcinoma. *Acta Pathol.Jpn.* 43:662-669.
6. Armant, D. R. 1991. Cell Interactions with Laminin and its Proteolytic Fragments during Outgrowth of Mouse Primery Trophoblast Cells. *Biol.Reprod.* 45:664-672.
7. Aumailley, M., V. Nurcombe, D. Edgar, M. Paulsson, and R. Timpl. 1987. The cellular interactions of laminin fragments. Cell adhesion correlates with two fragment-specific high affinity binding sites. *J.Biol.Chem.* 262:11532-11538.
8. Auth, D. and G. Brawerman. 1992. A 33-kDa polypeptide with homology to the laminin receptor: Component of translation machinery. *Proc.Natl.Acad.Sci.USA* 89:4368-4372.

9. Barsky, S. H., C. N. Rao, D. Hyams, and L. A. Liotta. 1984. Characterization of a laminin receptor from human breast carcinoma tissue. *Breast Cancer Research and Treatment* 4:181-188.
10. Basolo, F., L. Pollina, F. Pacini, G. Fontanini, S. Mønard, V. Castronovo, and G. Bevilacqua. 1996. Expression of the Mr 67,000 laminin receptor is an adverse prognostic indicator in human thyroid cancer: an immunohistochemical study. *Clin.Cancer Res.* 2:1777-1780.
11. Baumgartner, R., M. Czisch, U. Mayer, E. Poschl, R. Huber, R. Timpl, and T. A. Holak. 1996. Structure of the nidogen binding LE module of the laminin gamma 1 chain in solution. *J.Mol.Biol.* 257:658-668.
12. Beck, K., I. Hunter, and J. Engel. 1990. Structure and function of laminin: anatomy of a multidomain protein. *FASEB J.* 4:148-160.
13. Begum, N., M. Mori, T. Matsumata, K. Sigumachi, and G. Barnard. 1995. Differential Display and Integrin Alpha 6 Messenger RNA Overexpression in Hepatocellular Carcinoma. *Hepatology* 22:1447-1455.
14. Bevilacqua, P., M. Barbareschi, P. Verderio, P. Boracchi, O. Caffo, P. P. Dalla, S. Meli, N. Weidner, and G. Gasparini. 1995. Prognostic value of intratumoral microvessel density, a measure of tumor angiogenesis, in node-negative breast carcinoma--results of a multiparametric study. *Breast Cancer Res.Treat.* 36:205-217.
15. Bignon, C., M. Roux-Dosseto, M. E. Zeigler, M.-G. Mattei, J.-C. Lissitzky, M. S. Wicha, and P.-M. Martin. 1991. Genomic Analysis of the 67-kDa Laminin Receptor in Normal and Pathological Tissues: Circumstantial Evidence for Retroposon Features. *Genomics* 10:481-485.
16. Bignon, C., M. Roux-Dosseto, M. E. Zeigler, M. S. Wicha, and P.-M. Martin. 1992. cDNA Cloning and genomic analysis of a new multigene family sharing common phylogenetic and expression profiles with the laminin receptor gene. *Biochem.Biophys.Res.Comm.* 184:1165-1172.
17. Bresalier, R. S., B. Schwartz, Y. S. Kim, Q.-Y. Duh, H. K. Kleinman, and P. M. Sullam. 1995. The laminin  $\alpha$ 1 chain Ile-Lys-Val-Ala-Val (IKVAV)-containing

- peptide promotes liver colonization by human colon cancer cells. *Cancer Res.* 55:2476-2480.
18. Brule, F. A. v. d., J. Price, M. E. Sobel, R. Lambotte, and V. Castronovo. 1994. Inverse expression of two laminin binding proteins, 67LR and galectin-3, correlates with the invasive phenotype of trophoblastic tissue. *Biochem.Biophys.Res.Comm.* 201:388-393.
  19. Bushkin Harav, I., N. B. Garty, and U. Z. Littauer. 1995. Down-regulation of a 67-kDa YIGSR-binding protein upon differentiation of human neuroblastoma cells. *J.Biol.Chem.* 270:13422-13428.
  20. Bushkin Harav, I. and U. Z. Littauer. 1998. Involvement of the YIGSR sequence of laminin in protein tyrosine phosphorylation. *FEBS Lett.* 424:243-247.
  21. Butó, S., C. Ghirelli, P. Aiello, E. Tagliabue, E. Ardini, A. Magnifico, N. Montuori, M. E. Sobel, M. I. Colnaghi, and S. Ménard. 1997. Production and characterization of monoclonal antibodies directed against the laminin receptor precursor. *Int.J.Biol.Markers* 12:1-5.
  22. Butó, S., E. Tagliabue, E. Ardini, A. Magnifico, C. Ghirelli, F. Van den Brûle, V. Castronovo, M. I. Colnaghi, M. E. Sobel, and S. Ménard. 1998. Formation of the 67-kDa laminin receptor by acylation of the precursor. *J.Cell Biochem.* 69:244-251.
  23. Campo, E., C. Monteagudo, V. Castronovo, A. P. Claysmith, P. L. Fernandez, and M. E. Sobel. 1992. Detection of laminin receptor mRNA in human cancer cell lines and colorectal tissues by in situ hybridization. *Am.J.Pathol.* 141:1073-1083.
  24. Canfield S.M. and Khakoo A. 1999. The non-integrin laminin binding protein (p67 LBP) is expressed on a subset of activated T lymphocytes and together with the integrin VLA-6 mediates avid cellular adherence to laminin. *Arthritis research conference*, Vol.124.
  25. Carbone, A., A. Gloghini, A. Colombatti, V. Castronovo, and S. Mønard. 1995. Expression of the monomeric 67-kd laminin-binding protein in human

lymphomas as defined by MLC5 monoclonal antibody and paraffin section immunohistochemistry. *Hum.Pathol.* 26:541-546.

26. Carloni, V., R. Romanelli, A. M. Mercurio, M. Pinzani, G. Laffi, G. Cotrozzi, and P. Gentilini. 1998. Knockout of  $\alpha 6\beta 1$ -Integrin Expression Reverses the Transformed Phenotype of Hepatocarcinoma Cells. *Gastroenterology* 115:433-442.
27. Castronovo, V., E. Campo, F. A. van den Brule, A. P. Claysmith, V. Cioce, F. T. Liu, P. L. Fernandez, and M. E. Sobel. 1992. Inverse modulation of steady-state messenger RNA levels of two non-integrin laminin-binding proteins in human colon carcinoma. *J.Natl.Cancer Inst.* 84:1161-1169.
28. Castronovo, V., A. P. Claysmith, K. T. Barker, V. Cioce, H. C. Krutzsch, and M. E. Sobel. 1991. Biosynthesis of the 67 kDa high affinity laminin receptor. *Biochem.Biophys.Res.Comm.* 177:177-183.
29. Castronovo, V., C. Colin, A. P. Claysmith, P. H. S. Chen, E. Lifrange, R. Lambotte, H. Krutzsch, L. A. Liotta, and M. E. Sobel. 1990. Immunodetection of the metastasis-associated laminin receptor in human breast cancer cells obtained by fine-needle aspiration biopsy. *American Journal of Pathology* 137:1373-1381.
30. Castronovo, V., F. Luyten, F. van den Brule, and M. E. Sobel. 1992. Identification of a 14-kDa laminin binding protein (HLBP14) in human melanoma cells that is identical to the 14-kDa galactoside binding lectin. *Arch.Biochem.Biophys.* 297:132-138.
31. Castronovo, V., G. Taraboletti, L. A. Liotta, and M. E. Sobel. 1989. Modulation of laminin receptor expression by estrogen and progestins in human breast cancer cell lines. *J.Natl.Cancer Inst.* 81:781-788.
32. Castronovo, V., G. Taraboletti, and M. E. Sobel. 1991. Functional domains of the 67-kDa laminin receptor precursor. *J.Biol.Chem.* 266:20440-20446.
33. Castronovo, V., G. Taraboletti, and M. E. Sobel. 1991. Laminin receptor complementary DNA-deduced synthetic peptide inhibits cancer cell attachment to endothelium. *Cancer Res.* 51:5672-5678.

34. Castronovo, V., F. A. van den Brule, P. Jackers, N. Clause, F. T. Liu, C. Gillet, and M. E. Sobel. 1996. Decreased expression of galectin-3 is associated with progression of human breast cancer. *J.Pathol.* 179:43-48.
35. Chalazonitis, A., V. M. Tennyson, M. C. Kibbey, T. P. Rothman, and M. D. Gershon. 1997. The alpha1 subunit of laminin-1 promotes the development of neurons by interacting with LBP110 expressed by neural crest- derived cells immunoselected from the fetal mouse gut. *J.Neurobiol.* 33:118-138.
36. Chao, C., M. Lotz, A. Clarke, and A. M. Mercurio. 2000. A Function for the Integrin  $\alpha 6\beta 4$  in the Invasive Properties of Colorectal Carcinoma Cells. *Cancer Res.* 56:4811-4819.
37. Charpentier, A. H., Bednarek, A. K., Daniel, R. L., Hawkins, K. A., Laflin, K. J., Gaddis, S., MacLeod, M. C., and Aldaz, C. M. Effects of estrogen on global gene expression: Identification of novel targets of estrogen action. *Cancer Research* 60, 5977-5983. 2000.
38. Chen, L., V. Shick, M. L. Matter, S. M. Laurie, R. C. Ogle, and G. W. Laurie. 1997. Laminin E8 alveolarization site: heparin sensitivity, cell surface receptors, and role in cell spreading. *Am.J.Physiol.* 272:L494-503.
39. Cioce, V., V. Castronovo, B. M. Shmookler, S. Garbisa, W. F. Grigioni, L. A. Liotta, and M. E. Sobel. 1991. Increased expression of the laminin receptor in human colon cancer. *J.Natl.Cancer Inst.* 83:29-36.
40. Cioce, V., I. M. Margulies, M. E. Sobel, and V. Castronovo. 1993. Interaction between the 67 kilodalton metastasis-associated laminin receptor and laminin. *Kidney Int.* 43:30-37.
41. Clause N., Jackers P., and Castronovo V. 1997. The 37 LBP/P40 polypeptide: a multifunctional pleiotropic molecule invlved in tumorigenesis and metastasis. *Belg.J.Zool.* 127:3-11.
42. Clause, N., P. Jackers, P. JarΦs, B. Joris, M. E. Sobel, and V. Castronovo. 1996. Identification of the active gene coding for the metastasis- associated 37LRP/p40 multifunctional protein. *DNA Cell Biol.* 15:1009-1023.

43. Clause, N., F. Van den Brûle, P. Delvenne, N. Jacobs, E. Franzen Detrooz, P. Jackers, and V. Castronovo. 1998. TNF- $\alpha$  and IFN- $\gamma$  down-regulate the expression of the metastasis-associated bi-functional 37LRP/p40 gene and protein in transformed keratinocytes. *Biochem.Biophys.Res.Commun.* 251:564-569.
44. Clement, B., B. Segui-Real, P. Savagner, H. K. Kleinman, and Y. Yamada. 1990. Hepatocyte Attachment to Laminin is Mediated through Multiple Receptors. *J.of Cell Biol.* 110:185-192.
45. Coggin, J. H., Jr., A. L. Barsoum, and J. W. Rohrer. 1999. 37 kiloDalton oncofetal antigen protein and immature laminin receptor protein are identical, universal T-cell inducing immunogens on primary rodent and human cancers. *Anticancer Res.* 19:5535-5542.
46. Colnagi, M. I. 1994. The simultaneous expression of c-erbB-2 oncoprotein and laminin receptor on primary breast tumors has a predicting potential analogous to that of the lymph node status. *Adv.Exp.Med.Biol.* 353:149-154.
47. Crawford, B. D. and R. D. Burke. 1994. YIGSR domain of laminin binds surface receptors of mesenchyme and stimulates migration during gastrulation in sea urchins. *Development* 120:3227-3234.
48. Cress, A. E., I. Rabinovitz, W. Zhu, and R. B. Nagle. 1995. The  $\alpha 6\beta 1$  and  $\alpha 6\beta 4$  integrins in human prostate cancer progression. *Cancer and Metastasis Reviews* 14:219-228.
49. D'Errico, A., S. Garbisa, L. A. Liotta, V. Castronovo, W. G. Stetler Stevenson, and W. F. Grigioni. 1991. Augmentation of type IV collagenase, laminin receptor, and Ki67 proliferation antigen associated with human colon, gastric, and breast carcinoma progression. *Mod.Pathol.* 4:239-246.
50. Daheron, L., S. Salmeron, S. Patri, A. Brizard, F. Guilhot, J. C. Chomel, and A. Kitzis. 1998. Identification of several genes differentially expressed during progression of chronic myelogenous leukemia. *Leukemia* 12:326-332.
51. Daidone, M. G., R. Silvestrini, E. Benini, W. F. Grigioni, and A. D'Errico. 1997. Expression of high-affinity 67-kDa laminin receptors in primary breast cancers

- and metachronous metastatic lesions or contralateral cancers. *Br.J.Cancer* 76:52-53.
52. Daidone, M. G., R. Silvestrini, A. D'Errico, G. DiFronzo, E. Benini, A. M. Mancini, S. Garbisa, L. A. Liotta, and W. F. Grigioni. 1991. Laminin Receptors, Collagenase IV and Prognosis in Node-Negative Breast Cancers. *Int.J.Cancer* 48:529-532.
  53. Davis, S. C., A. Tzagoloff, and S. R. Ellis. 1992. Characterization of a yeast mitochondrial ribosomal protein structurally related to the mammalian 68-kDa high affinity laminin receptor. *J.Biol.Chem.* 267:5508-5514.
  54. Dean, J. W. 3., S. Chandrasekaran, and M. L. Tanzer. 1990. A biological role of the carbohydrate moieties of laminin. *J.Biol.Chem.* 265:12553-12562.
  55. Demeter, L. M., M. H. Stoler, M. E. Sobel, T. R. Broker, and L. T. Chow. 1992. Expression of high-affinity laminin receptor mRNA correlates with cell proliferation rather than invasion in human papillomavirus-associated cervical neoplasms. *Cancer Res.* 52:1561-1567.
  56. Demianova, M., T. G. Formosa, and S. R. Ellis. 1996. Yeast proteins related to the p40/laminin receptor precursor are essential components of the 40 S ribosomal subunit. *J.Biol.Chem.* 271:11383-11391.
  57. Denzer, A. J., T. Schulthess, C. Fauser, B. Schumacher, R. A. Kammerer, J. Engel, and M. A. Ruegg. 1998. Electron microscopic structure of agrin and mapping of its binding site in laminin-1. *EMBO J.* 17:335-343.
  58. Fernandez, M. T., V. Castronovo, C. N. Rao, and M. E. Sobel. 1991. The high affinity murine laminin receptor is a member of a multicopy gene family. *Biochem.Biophys.Res.Comm.* 175:84-90.
  59. Ferrarini, M., S. Heltai, S. M. Pupa, S. Mernard, and R. Zocchi. 1996. Killing of laminin receptor-positive human lung cancers by tumor infiltrating lymphocytes bearing gammadelta(+) t-cell receptors. *J.Natl.Cancer Inst.* 88:436-441.

60. Ferrarini, M., S. M. Pupa, M. R. Zocchi, C. Rugarli, and S. Ménard. 1994. Distinct pattern of HSP72 and monomeric laminin receptor expression in human lung cancers infiltrated by  $\gamma/\delta$  T lymphocytes. *Int.J.Cancer* 57:486-490.
61. Fontanini, G., S. Vignati, S. Chiné, M. Lucchi, A. Mussi, C. A. Angeletti, S. Menard, V. Castronovo, and G. Bevilacqua. 1997. 67-Kilodalton laminin receptor expression correlates with worse prognostic indicators in non-small cell lung carcinomas. *Clin.Cancer Res.* 3:227-231.
62. Ford, C. L., L. Randal-Whitis, and S. R. Ellis. 1999. Yeast proteins related to the p40/laminin receptor precursor are required for 20S ribosomal RNA processing and the maturation of 40S ribosomal subunits. *Cancer Res.* 59:704-710.
63. Friedrichs, K., P. Ruiz, F. Franke, I. Gille, H.-J. Terpe, and B. A. Imhof. 1995. High expression level of  $\alpha 6$  integrin in human breast carcinoma is correlated with reduced survival. *Cancer Res.* 55:901-906.
64. Fulcher, K. D., J. E. Welch, C. M. Davis, D. A. OBrien, and E. M. Eddy. 1993. Characterization of laminin receptor messenger ribonucleic acid and protein expression in mouse spermatogenic cells. *Biol.Reprod.* 48:674-682.
65. Garcia-Hernandez, M., E. Davies, and P. E. Staswick. 1994. Arabidopsis p40 homologue. A novel acidic protein associated with the 40 S subunit of ribosomes. *J.Biol.Chem.* 269:20744-20749.
66. Gasparini, G., M. Barbareschi, P. Boracchi, P. Bevilacqua, P. Verderio, P. Dalla-Palma, and S. Menard. 1995. 67-kDa laminin-receptor expression adds prognostic information to intra-tumoral microvessel density in node-negative breast cancer. *Int.J.Cancer* 60:604-610.
67. Gauczynski, S., C. Hundt, C. Leucht, and S. Weiss. 2001. Interaction of prion proteins with cell surface receptors, molecular chaperones, and other molecules. *Advances in Protein Chemistry* 57:229-272.
68. Gauczynski, S., J. M. Peyrin, S. Haik, C. Leucht, C. Hundt, R. Rieger, S. Krasemann, J. P. Deslys, D. Dormont, C. I. Lasmezas, and S. Weiss. 2001. The 37-kDa/67-kDa laminin receptor acts as the cell-surface receptor for the cellular prion protein. *Embo Journal* 20:5863-5875.

69. Gozalbo, D., I. Gil Navarro, I. Azorin, J. Renau Piqueras, J. P. Martinez, and M. L. Gil. 1998. The cell wall-associated glyceraldehyde-3-phosphate dehydrogenase of *Candida albicans* is also a fibronectin and laminin binding protein. *Infect.Immun.* 66:2052-2059.
70. Graf, J., Y. Iwamoto, M. Sasaki, G. R. Martin, H. K. Kleinman, F. A. Robey, and Y. Yamada. 1987. Identification of an amino acid sequence in laminin mediating cell attachment, chemotaxis, and receptor binding. *Cell* 48:989-996.
71. Graf, J., R. C. Ogle, F. A. Robey, M. Sasaki, G. R. Martin, Y. Yamada, and H. K. Kleinman. 1987. A pentapeptide from the laminin B1 chain mediates cell adhesion and binds the 67,000 laminin receptor. *Biochem.* 26:6896-6900.
72. Grant, D. S., K. Tashiro, B. Segui-Real, Y. Yamada, G. R. Martin, and H. K. Kleinman. 1989. Two different laminin domains mediate the differentiation of human endothelial cells into capillary-like structures in vitro. *Cell* 58:933-943.
73. Grosso, L. E., P. W. Park, and R. P. Mecham. 1991. Characterization of a putative clone for the 67-kilodalton elastin/laminin receptor suggests that it encodes a cytoplasmic protein rather than a cell surface receptor. *Biochem.* 30:3346-3350.
74. Guo, N. H., H. C. Krutzsch, T. Vogel, and D. D. Roberts. 1992. Interactions of a laminin-binding peptide from a 33-kDa protein related to the 67-kDa laminin receptor with laminin and melanoma cells are heparin-dependent. *J.Biol.Chem.* 267:17743-17747.
75. Halatsch, M. E., K. I. Hirsch Ernst, G. F. Kahl, and R. J. Weinel. 1997. Increased expression of alpha6-integrin receptors and of mRNA encoding the putative 37 kDa laminin receptor precursor in pancreatic carcinoma. *Cancer Lett.* 118:7-11.
76. Hand, P. H., A. Thor, J. Schlom, C. N. Rao, and L. Liotta. 1985. Expression of laminin receptor in normal and carcinomatous human tissues as defined by a monoclonal antibody. *Cancer Res.* 45:2713-2719.
77. Hara, K., K. Satoh, and H. Ide. 1997. Apical ectodermal ridge-dependent expression of the chick 67 kDa laminin binding protein gene (cLbp) in developing limb bud. *Zoolog.Sci.* 14:969-978.

78. Honn, K. and D. G. Tang. 1992. Adhesion molecules and tumor cell interaction with endothelium and subendothelial matrix. *Cancer and Metastasis Reviews* 11:353-375.
79. Howard, M. J. and M. D. Gershon. 1998. Development of LBP110 expression by neural crest-derived enteric precursors: migration and differentiation potential in *ls/ls* mutant mice. *J.Neurobiol.* 35:341-354.
80. Huard T., J.Wood, H.Malinoff, K.Mahoney, G.Heppner, and M.Wicha. 1984. Laminin promotes macrophage tumor cell binding by specific plasma membrane receptors. *AACR Proceedings*, Vol. 50. American Association for Cancer Research.
81. Hundt, C., J. M. Peyrin, S. Haik, S. Gauczynski, C. Leucht, R. Rieger, M. L. Riley, J. P. Deslys, D. Dormont, C. I. Lasmezas, and S. Weiss. 2001. Identification of interaction domains of the prion protein with its 37-kDa/67-kDa laminin receptor. *EMBO Journal* 20:5876-5886.
82. Hunt, G. 1989. The role of laminin in cancer invasion and metastasis. *Exp.Cell Biol.* 57:165-176.
83. Iwamoto, Y., F. A. Robey, J. Graf, M. Sasaki, H. K. Kleinman, Y. Yamada, and G. R. Martin. 1987. YIGSR, a synthetic laminin pentapeptide, inhibits experimental metastasis formation [published erratum appears in *Science* 1988 Jan 15;239(4837):245]. *Science* 238:1132-1134.
84. Jackers, P., N. Clause, M. Fernandez, A. Berti, F. Princen, U. Wewer, M. E. Sobel, and V. Castronovo. 1996. Seventeen copies of the human 37 kDa laminin receptor precursor/ p40 ribosome-associated protein gene are processed pseudogenes arisen from retropositional events. *Biochim.Biophys.Acta* 1305:98-104.
85. Jackers, P., F. Minoletti, D. Belotti, N. Clause, G. Sozzi, M. E. Sobel, and V. Castronovo. 1996. Isolation from a multigene family of the active human gene of the metastasis-associated multifunctional protein 37LRP/ p40 at chromosome 3p21.3 [published erratum appears in *Oncogene* 1997 Feb 6;14(5):627]. *Oncogene* 13:495-503.

86. Kaneda, Y., S. Yamamoto, T. Kihira, Y. Tsutsumi, S. Nakagawa, M. Miyake, K. Kawasaki, and T. Mayumi. 1995. Synthetic cell-adhesive laminin peptide YIGSR conjugated with polyethylene glycol has improved anti-metastatic activity due to a longer half-life in blood. *Invasion Metastasis* 15:156-162.
87. Karpatová, M., E. Tagliabue, V. Castronovo, A. Magnifico, E. Ardini, D. Morelli, D. Belotti, M. I. Colnaghi, and S. Ménard. 1996. Shedding of the 67-kD laminin receptor by human cancer cells. *J. Cell Biochem.* 60:226-234.
88. Kazmin, D. A., T. R. Hoyt, L. Taubner, M. Teintze, and J. R. Starkey. 2000. Phage display mapping for peptide 11 sensitive sequences binding to laminin-1. *Journal of Molecular Biology* 298:431-445.
89. Keresztes, M. and Z. Lajtos. 1997. Major laminin-binding and F-actin-linked glycoproteins of neutrophils. *Cell Biol.Int.* 21:543-550.
90. Kleinman, H. K., M. L. McGarvey, J. R. Hassell, V. L. Star, F. B. Cannon, G. W. Laurie, and G. R. Martin. 1986. Basement membrane complexes with biological activity. *Biochem.* 25:312-318.
91. Kleinman, H. K., R. C. Ogle, F. B. Cannon, C. D. Little, T. M. Sweeney, and L. Luckenbill Edds. 1988. Laminin receptors for neurite formation. *Proc.Natl.Acad.Sci.U.S.A.* 85:1282-1286.
92. Kouzi-Koliakos, K, Koliakos, G, Trontos, C, Papageorgiou, A, Iliadis, S, Triantos, A, Dimitriadou, A, and Kanellaki, M. In vivo Binding of the Radioiodinated Peptide YIGSR on B16 Melanoma Cells. *Invasion and Metastasis* 16, 322-329. 1996.
93. Kreader, C. A., C. S. Langer, and J. E. Heckman. 1989. A mitochondrial protein from *Neurospora crassa* detected both on ribosomes and in membrane fractions. Analysis of the gene, the message, and the protein. *J.Biol.Chem.* 264:317-327.
94. Landowski, T. H., E. A. Dratz, and J. R. Starkey. 1995. Studies of the structure of the metastasis-associated 67 kDa laminin binding protein: fatty acid acylation and evidence supporting dimerization of the 32 kDa gene product to form the mature protein. *Biochem.* 34:11276-11287.

95. Landowski, T. H., S. Uthayakumar, and J. R. Starkey. 1995. Control pathways of the 67 kDa laminin binding protein: surface expression and activity of a new ligand binding domain. *Clin.Exp.Metastasis* 13:357-372.
96. Lee, W. A., W. H. Kim, Y. I. Kim, H. K. Yang, J. P. Kim, and H. K. Kleinman. 1996. Overexpression of the 67 kD laminin receptor correlates with the progression of gastric carcinoma. *Pathol.Res.Pract.* 1195-1201.
97. Lesot H., Kuhl U., and von der Mark K. 1983. Isolation of laminin binding protein from muscle cell membranes. *The EMBO Journal* .
98. Liotta, L. A., P. Horan Hand, C. N. Rao, G. Bryant, S. H. Barsky, and J. Schlom. 1985. Monoclonal antibodies to the human laminin receptor recognize structurally distinct sites. *Exp.Cell Res.* 156:117-126.
99. Lopes, J. D., M. dos Reis, and R. R. Brentani. 1985. Presence of laminin receptors in *Staphylococcus aureus*. *Science* 229:275-277.
100. Lu, H. S., J. J. Chai, M. Li, B. R. Huang, C. H. He, and R. C. Bi. 2001. Crystal structure of human epidermal growth factor and its dimerization. *J.Biol.Chem.* 276:34913-34917.
101. Maeda, M., Y. Izuno, K. Kawasaki, Y. Kaneda, Y. Mu, Y. Tsutsumi, S. Nakagawa, and T. Mayumi. 1998. Amino acids and peptides. XXXI. Preparation of analogs of the laminin-related peptide YIGSR and their inhibitory effect on experimental metastasis. *Chem.Pharm.Bull.(Tokyo)* 46:347-350.
102. Maeda, T., K. Titani, and K. Sekiguchi. 1994. Cell-adhesive activity and receptor-binding specificity of the laminin-derived YIGSR sequence grafted onto *Staphylococcal* protein A. *J.Biochem.* 115:182-189.
103. Mafune, K., T. S. Ravikumar, J. M. Wong, H. Yow, L. B. Chen, and G. D. Steele, Jr. 1990. Expression of a Mr 32,000 laminin-binding protein messenger RNA in human colon carcinoma correlates with disease progression. *Cancer Res.* 50:3888-3891.

104. Magnifico, A., E. Tagliabue, S. Butó, E. Ardini, V. Castronovo, M. I. Colnaghi, and S. Ménard. 1996. Peptide G, containing the binding site of the 67-kDa laminin receptor, increases and stabilizes laminin binding to cancer cells. *J.Biol.Chem.* 271:31179-31184.
105. Makrides, S., S. T. Chitpatima, R. Bandyopadhyay, and G. Brawerman. 1988. Nucleotide sequence for a major messenger RNA for a 40 kilodalton polypeptide that is under translational control in mouse tumor cells. *Nucleic.Acids.Res.* 16:2349.
106. Malinoff H., McCoy P., Varani J., and Wicha M. 1986. Metastatic potential of murine fibrosarcoma cells correlates with endogenous, surface receptor bound laminin. 22nd Annual Meeting [ASCB], Vol. 126a. American Society for Cell Biology.
107. Malinoff, H. L. and M. S. Wicha. 1983. Isolation of a cell surface receptor protein for laminin from murine fibrosarcoma cells. *J.Cell Biol.* 96:1475-1479.
108. Marques, L. A., E. L. F. Franco, H. Torloni, M. Brentani, J. Baptista da Silva-Neto, and R. R. Brentani. 1990. Independent prognostic value of laminin receptor expression in breast cancer survival. *Cancer Res.* 50:1479-1483.
109. Martignone, S., S. Menard, R. Bufalino, N. Cascinelli, R. Pellegrini, E. Tagliabue, S. Andreola, F. Rilke, and M. I. Colnaghi. 1993. Prognostic significance of the 67-kilodalton laminin receptor expression in human breast carcinomas. *J.Natl.Cancer Inst.* 85:398-402.
110. Martignone, S., R. Pellegrini, E. Villa, N. N. Tandon, A. Mastroianni, E. Tagliabue, S. Menard, and M. I. Colnaghi. 1992. Characterization of two monoclonal antibodies directed against the 67 kDa high affinity laminin receptor and application for the study of breast carcinoma progression. *Clinical and Experimental Metastasis* 10:379-386.
111. Massia, S. P., S. S. Rao, and J. A. Hubbell. 1993. Covalently immobilized laminin peptide Tyr-Ile-Gly-Ser- Arg (YIGSR) supports cell spreading and co-localization of the 67- kilodalton laminin receptor with alpha-actinin and vinculin. *J.Biol.Chem.* 268:8053-8059.

112. Mayer, U., K. Mann, L. I. Fessler, J. H. Fessler, and R. Timpl. 1997. *Drosophila* laminin binds to mammalian nidogen and to heparan sulfate proteoglycan. *Eur.J.Biochem.* 245:745-750.
113. Mayer, U., R. Nischt, E. Poschl, K. Mann, K. Fukuda, M. Gerl, Y. Yamada, and R. Timpl. 1993. A single EGF-like motif of laminin is responsible for high affinity nidogen binding. *EMBO J.* 12:1879-1885.
114. McCarthy, J. B., M. Basara, S. Palm, D. Sas, and L. T. Furcht. 1985. The role of adhesion proteins - laminin and fibronectin - in the movement of malignant and metastatic cells. *Cancer and Metastasis Reviews* 4:125-152.
115. McKenna, D. J., D. A. C. Simpson, S. Feeney, T. A. Gardiner, C. Boyle, J. Nelson, and A. W. Stitt. 2001. Expression of the 67 kDa laminin receptor (67LR) during retinal development: Correlations with angiogenesis. *Experimental Eye Research* 73:81-92.
116. Mecham, R. P. 1991. Laminin receptors. *Annu.Rev.Cell Biol.* 7:71-91.
117. Mecham, R. P. 1991. Receptors for laminin on mammalian cells. *FASEB J.* 5:2538-2546.
118. Mecham, R. P., A. Hinek, G. L. Griffin, R. M. Senior, and L. A. Liotta. 1989. The Elastin Receptor Shows Structural and Functional Similarities to the 67-kDa Tumor Cell Laminin Receptor. *J.of Biol.Chem* 264:16652-16657.
119. Mecham, R. P., L. Whitehouse, M. Hay, A. Hinek, and M. P. Sheetz. 1991. Ligand affinity of the 67-kD elastin/laminin binding protein is modulated by the protein's lectin domain: visualization of elastin/laminin-receptor complexes with gold-tagged ligands. *J.Cell Biol.* 113:187-194.
120. Melnick, M. B., E. Noll, and N. Perrimon. 1993. The *Drosophila stubarista* phenotype is associated with a dosage effect of the putative ribosome-associated protein D-p40 on spineless. *Genetics* 135:553-564.

121. Ménard, S., V. Castronovo, E. Tagliabue, and M. E. Sobel. 1997. New insights into the metastasis-associated 67 kD laminin receptor. *J.Cell Biochem.* 67:155-165.
122. Menard, S., P. Squicciarini, A. Luini, V. Sacchini, D. Rovini, E. Tagliabue, P. Veronesi, B. Salvadori, U. Veronesi, and M. I. Colnaghi. 1994. Immunodetection of bone marrow micrometastases in breast carcinoma patients and its correlation with primary tumour prognostic features. *Br.J.Cancer* 69:1126-1129.
123. Michigami, T., Nomizu, M., Yamada, Y., Dunstan, C., Williams, P. J., Munday, G. R., and Yoneda, T. Growth and dissemination of a newly-established murine B-cell lymphoma cell line is inhibited by multimeric YIGSR peptide. *Clinical and Experimental Metastasis* 16, 645-654. 1998.
124. Min, W., S. Ghosh, and P. Lengyel. 1996. The interferon-inducible p202 protein as a modulator of transcription: inhibition of NF-kappa B, c-Fos, and c-Jun activities. *Mol.Cell Biol.* 16:359-368.
125. Minafra, S., C. Luparello, I. Pucci-Minafra, M. E. Sobel, and S. Garbisa. 1992. Adhesion of 8701-BC breast cancer cells to type V collagen and 67 kDa receptor. *J.Cell Sci.* 102 ( Pt 2):323-328.
126. Mokotoff, M., Zhao, M., and Kleinman, H. 1991. Synthetic laminin-like peptides and pseudopeptides as potential antimetastatic agents. 12th American Peptide Symposium (Massachusetts), Vol. 925.
127. Montero, M., A. Marcilla, R. Sentandreu, and E. Valentin. 1998. A *Candida albicans* 37 kDa polypeptide with homology to the laminin receptor is a component of the translational machinery. *Microbiology.* 144:839-847.
128. Montuori, N., F. Müller, S. De Riu, G. Fenzi, M. E. Sobel, G. Rossi, and M. Vitale. 1999. Laminin receptors in differentiated thyroid tumors: restricted expression of the 67-kilodalton laminin receptor in follicular carcinoma cells. *J.Clin.Endocrinol.Metab.* 84:2086-2092.

129. Mu, Y., Kamada, H., Kaneda, Y., Yamamoto, Y., Kodaira, H., Tsunoda, S., Tsutsumi, Y., Maeda, M., Kawasaki, K., Nomizu, M., Yamada, Y., and Mayumi, T. Bioconjugation of Laminin Peptide YIGSR with Poly(Styrene Co-maleic Acid) Increases Its Antimetastatic Effect on Lung Metastasis of B16-BL6 Melanoma Cells. *Biochemical and Biophysical Research Communications* 255, 75-79. 1999.
130. Mukhopadhyay, R., R. Theriault, and J. Price. 1999. Increased levels of  $\alpha 6$  integrins are associated with the metastatic phenotype of human breast cancer cells. *Clin.Exp.Metastasis* 17:325-332.
131. Nadji, M., M. Nassiri, M. Fresno, E. Terzian, and A. R. Morales. 1999. Laminin receptor in lymph node negative breast carcinoma. *Cancer* 85:432-436.
132. Nakahara, H., M. Nomizu, S. K. Akiyama, Y. Yamada, Y. Yeh, and W.-T. Chen. 1996. A mechanism for regulation of melanoma invasion. Ligation of  $\alpha 6 \beta 1$  integrin by laminin G peptides. *J.Biol.Chem.* 271:27221-27224.
133. Narasimhan, S., M. Y. Armstrong, K. Rhee, J. C. Edman, F. F. Richards, and E. Spicer. 1994. Gene for an extracellular matrix receptor protein from *Pneumocystis carinii*. *Proc.Natl.Acad.Sci.U.S.A.* 91:7440-7444.
134. Narumi, K., A. Inoue, M. Tanaka, M. Isemura, T. Shimo-Oka, T. Abe, T. Nukiwa, and K. Satoh. 1999. Inhibition of experimental metastasis of human fibrosarcoma cells by anti-recombinant 37-kDa laminin binding protein antibody. *Jpn.J.Cancer Res.* 90:425-431.
135. Nejjari, M., Z. Hafdi, J. Dumortier, A.-F. Bringuier, G. Feldmann, and J.-Y. Scoazec. 1999.  $\alpha 6 \beta 1$  integrin expression in hepatocarcinoma cells: regulation and role in cell adhesion and migration. *Int.J.Cancer* 83:518-525.
136. Nelson, J., W. E. Alien, W. N. Scott, J. R. Bailie, B. Walker, N. V. McFerran, and D. J. Wilson. 1995. Murine epidermal growth factor (EGF) fragment (33-42) inhibits both EGF- and laminin-dependent endothelial cell motility and angiogenesis. *Cancer Res.* 55:3772-3776.
137. Nishiyama, Y., T. Yoshikawa, K. Kurita, K. Hojo, H. Kamada, Y. Tsutsumi, T. Mayumi, and K. Kawasaki. 1999. Regioselective conjugation of chitosan with a

- laminin-related peptide, Tyr-Ile-Gly-Ser-Arg, and evaluation of its inhibitory effect on experimental cancer metastasis. *Chem.Pharm.Bull.(Tokyo)* 47:451-453.
138. Nomizu, M., K. Yamamura, H. K. Kleinman, and Y. Yamada. 1993. Multimeric forms of Tyr-Ile-Gly-Ser-Arg (YIGSR) peptide enhance the inhibition of tumor growth and metastasis. *Cancer Res.* 53:3459-3461.
  139. Ostheimer, G. J., J. R. Starkey, C. G. Lambert, S. L. Helgerson, and E. A. Dratz. 1992. NMR constrained solution structures for laminin peptide 11. Analogs define structural requirements for inhibition of tumor cell invasion of basement membrane matrix. *J.Biol.Chem.* 267:25120-25128.
  140. Pellegrini, R., S. Martignone, S. Ménard, and M. I. Colnaghi. 1994. Laminin receptor expression and function in small-cell lung carcinoma. *Int.J.Cancer* 57 Suppl. 8:116-120.
  141. Pellegrini, R., S. Martignone, E. Tagliabue, D. Belotti, R. Bufalino, N. Cascinelli, S. Menard, and M. I. Colnaghi. 1995. Prognostic significance of laminin production in relation with its receptor expression in human breast carcinomas. *Breast Cancer Res.Treat.* 35:195-199.
  142. Privitera, S., C. A. Prody, J. W. Callahan, and A. Hinek. 1998. The 67-kDa enzymatically inactive alternatively spliced variant of beta-galactosidase is identical to the elastin/ laminin- binding protein. *J.Biol.Chem.* 273:6319-6326.
  143. Rabinovitz, I., R. B. Nagle, and A. E. Cress. 1995. Integrin  $\alpha 6$  expression in human prostate carcinoma cells is associated with a migratory and invasive phenotype *in vitro* and *in vivo*. *Clinical and Experimental Metastasis* 13:481-491.
  144. Ranieri, J. P., R. Bellamkonda, E. J. Bekos, T. G. Vargo, J. A. Gardella, Jr., and P. Aebischer. 1995. Neuronal cell attachment to fluorinated ethylene propylene films with covalently immobilized laminin oligopeptides YIGSR and IKVAV. II. *J.Biomed.Mater.Res.* 29:779-785.
  145. Rao, C. N., S. H. Barsky, V. P. Terranova, and L. A. Liotta. 1983. Isolation of a tumor cell laminin receptor. *Biochem.Biophys.Res.Comm.* 111:804-808.

146. Rao, C. N., V. Castronovo, M. C. Schmitt, U. M. Wewer, A. P. Claysmith, L. A. Liotta, and M. E. Sobel. 1989. Evidence for a precursor of the high-affinity metastasis-associated murine laminin receptor. *Biochem.* 28:7476-7486.
147. Rao, C. N., I. M. Margulies, and L. A. Liotta. 1985. Binding domain for laminin on type IV collagen. *Biochem.Biophys.Res.Comm.* 128:45-52.
148. Rescan, P. Y., B. Clement, Y. Yamada, B. Segui-Real, G. Baffet, C. Guguen-Guillouzo, and A. Guillouzo. 1990. Differential expression of laminin chains and receptor (LBP-32) in fetal and neoplastic hepatocytes compared to normal adult hepatocytes in vivo and in culture. *Am.J.Pathol.* 137:701-709.
149. Richardson, M. P., C. Braybrook, M. Tham, G. E. Moore, and P. Stanier. 1998. Molecular cloning and characterization of a highly conserved human 67-kDa laminin receptor pseudogene mapping to Xq21.3. *Gene* 206:145-150.
150. Rieger, R., F. Edenhofer, C. I. Lasmezas, and S. Weiss. 1997. The human 37-kDa laminin receptor precursor interacts with the prion protein in eukaryotic cells [see comments]. *Nat.Med.* 3:1383-1388.
151. Roberts, D. D., U. M. Wewer, L. A. Liotta, and V. Ginsburg. 1988. Laminin-dependent and laminin-independent adhesion of human melanoma cells to sulfatides. *Cancer Res.* 48:3367-3373.
152. Rohrer, J. W., A. L. Barsoum, D. L. Dyess, J. A. Tucker, and J. H. Coggin, Jr. 1999. Human breast carcinoma patients develop clonable oncofetal antigen-specific effector and regulatory T lymphocytes. *J.Immunol.* 162:6880-6892.
153. Romanov, V., M. E. Sobel, P. Pinto da Silva, S. Menard, and V. Castronovo. 1994. Cell localization and redistribution of the 67 kD laminin receptor and alpha 6 beta 1 integrin subunits in response to laminin stimulation: an immunogold electron microscopy study. *Cell Adhes.Comm.* 2:201-209.
154. Rosenthal, E. T. and L. Wordeman. 1995. A protein similar to the 67 kDa laminin binding protein and p40 is probably a component of the translational machinery in *Urechis caupo* oocytes and embryos. *J.Cell Science* 108:245-256.

155. Ruiz, P., D. Dunon, A. Sonnenberg, and B. A. Imhof. 1993. Suppression of mouse melanoma metastasis by EA-1, a monoclonal antibody specific for alpha 6 integrins [published erratum appears in *Cell Adhes Commun* 1993 Sep;1(2):following 190]. *Cell Adhes.Commun.* 1:67-81.
156. Saiki, I., J. Muratá, T. Iida, N. Nishi, K. Matsuno, and I. Azuma. 1989. Antimetastatic effects of synthetic polypeptides containing repeated structures of the cell adhesive Arg-Gly-Asp (RGD) and Tyr-Ile-Gly-Ser-Arg (YIGSR) sequences. *Br.J.Cancer* 60:722-728.
157. Saito, F., H. Yamada, Y. Sunada, H. Hori, T. Shimizu, and K. Matsumura. 1997. Characterization of a 30-kDa peripheral nerve glycoprotein that binds laminin and heparin. *J.Biol.Chem.* 272:26708-26713.
158. Sakamoto, N., M. Iwahana, N. G. Tanaka, and Y. Osada. 1991. Inhibition of Angiogenesis and Tumor Growth by a Synthetic Laminin Peptide, CDPGYIGSR-NH<sub>2</sub>. *Cancer Res.* 51:903-906.
159. Salas, P. J., M. I. Ponce, M. Brignoni, and M. L. Rodriguez. 1992. Attachment of Madin-Darby canine kidney cells to extracellular matrix: role of a laminin binding protein related to the 37/67 kDa laminin receptor in the development of plasma membrane polarization. *Biol.Cell* 75:197-210.
160. Sanjuán, X., P. L. Fernández, R. Miquel, J. Muñoz, V. Castronovo, S. Ménard, A. Palacín, A. Cardesa, and E. Campo. 1996. Overexpression of the 67-kD laminin receptor correlates with tumour progression in human colorectal carcinoma. *J.Pathol.* 179:376-380.
161. Satoh, K., K. Narumi, T. Abe, T. Sakai, T. Kikuchi, M. Tanaka, T. Shimo-Oka, M. Uchida, M. Tezuka, M. Isemura, and T. Nukiwa. 1999. Diminution of 37-kDa laminin binding protein expression reduces tumour formation of murine lung cancer cells. *Br.J.Cancer* 80:1115-1122.
162. Satoh, K., K. Narumi, M. Isemura, T. Sakai, T. Abe, K. Matsushima, K. Okuda, and M. Motomiya. 1992. Increased expression of the 67kDa-laminin receptor gene in human small cell lung cancer. *Biochem.Biophys.Res.Comm.* 182:746-752.

163. Satoh, K., K. Narumi, T. Sakai, T. Abe, T. Kikuchi, K. Matsushima, S. Sindoh, and M. Motomiya. 1992. Cloning of 67-kDa laminin receptor cDNA and gene expression in normal and malignant cell lines of the human lung. *Cancer Lett.* 62:199-203.
164. Segui-Regal, B., Rhodes, C., and Yamada, Y. The human genome contains a pseudogene for the Mr=32000 laminin binding protein. *Nucleic Acids Research* 17[3], 1257. 1989.
165. Shaw, L. M., C. Chao, U. M. Wewer, and A. M. Mercurio. 1996. Function of the integrin  $\alpha 6 \beta 1$  in metastatic breast carcinoma cells assessed by expression of a dominant-negative receptor. *Cancer Res.* 56:959-963.
166. Shi, Y. E., J. Torri, L. Yieh, M. E. Sobel, Y. Yamada, M. E. Lippman, R. B. Dickson, and E. W. Thompson. 1993. Expression of 67 kDa laminin receptor in human breast cancer cells: regulation by progestins. *Clin.Exp.Metastasis* 11:251-261.
167. Silva, F. C. E., J. Ortega-López, and R. Arroyo. 1998. YIGSR is the preferential laminin-1 residing adhesion sequence for *Trichomonas vaginalis*. *Exp.Parasitol.* 88:240-242.
168. Sivanandaiah, K. M., V. V. Babu, S. C. Shankaramma, M. Lakshmana, R. Babu, M. A. Arif, and M. Kumar. 1996. Synthetic peptides related to laminin pentapeptide (YIGSR) fragment. *Indian J.Exp.Biol.* 34:658-662.
169. Siyanova E. Yu. 1992. Expression of LBP 32/67 kD human gene in *E. coli* and analysis of its binding with laminin. *Byulleten' Eksperimental'noi Biologii i Meditsini* 113:70-72.
170. Skubitz, A. P., J. B. McCarthy, A. S. Charonis, and L. T. Furcht. 1988. Localization of three distinct heparin-binding domains of laminin by monoclonal antibodies. *J.Biol.Chem.* 263:4861-4868.
171. Skubitz, A. P., J. B. McCarthy, A. S. Charonis, and L. T. Furcht. 1989. Novel synthetic heparin binding peptides of laminin and fibronectin which promote the adhesion of melanoma cells. *Invasion Metastasis* 9:89-101.

172. Starkey, J. R., S. Dai, and E. A. Dratz. 1998. Sidechain and backbone requirements for anti-invasive activity of laminin peptide 11. *Biochim.Biophys.Acta Protein Struct.Mol.Enzymol.* 1429:187-207.
173. Starkey, J. R., S. Uthayakumar, and D. L. Berglund. 1999. Cell surface and substrate distribution of the 67-kDa laminin-binding protein determined by using a ligand photoaffinity probe. *Cytometry* 35:37-47.
174. Stetefeld, J., U. Mayer, R. Timpl, and R. Huber. 1996. Crystal structure of three consecutive laminin-type epidermal growth factor-like (LE) modules of laminin gamma1 chain harboring the nidogen binding site. *J.Mol.Biol.* 257:644-657.
175. Sung, U., J. J. O'Rear, and P. D. Yurchenco. 1997. Localization of heparin binding activity in recombinant laminin G domain. *Eur.J.Biochem.* 250:138-143.
176. Tanaka, M., K. Narumi, M. Isemura, M. Abe, Y. Sato, T. Abe, Y. Saijo, T. Nukiwa, and K. Satoh. 2000. Expression of the 37-kDa laminin binding protein in murine lung tumor cell correlates with tumor angiogenesis. *Cancer Lett.* 153:161-168.
177. Tanaka, M., K. Narumi, M. Isemura, M. Abe, Y. Sato, T. Abe, Y. Saijo, T. Nukiwa, and K. Satoh. 2000. Expression of the 37-kDa laminin binding protein in murine lung tumor cell correlates with tumor angiogenesis. *Cancer Lett.* 153:161-168.
178. Tandon, N. N., E. A. Holland, U. Kralisz, H. K. Kleinman, F. A. Robey, and G. A. Jamieson. 1991. Interaction of human platelets with laminin and identification of the 67 kDa laminin receptor on platelets. *Biochem.J.* 274:535-542.
179. Tashiro, K., G. C. Sephel, B. Weeks, M. Sasaki, G. R. Martin, H. K. Kleinman, and Y. Yamada. 1989. A synthetic peptide containing the IKVAV sequence from the A chain of laminin mediates cell attachment, migration, and neurite outgrowth. *J.Biol.Chem.* 264:16174-16182.
180. Terranova, V. P., L. A. Liotta, R. G. Russo, and G. R. Martin. 1982. Role of laminin in the attachment and metastasis of murine tumor cells. *Cancer Res.* 42:2265-2269.

181. Terranova, V. P., C. N. Rao, T. Kalebic, I. M. Margulies, and L. A. Liotta. 1983. Laminin receptor on human breast carcinoma cells. *Proc.Natl.Acad.Sci.U.S.A.* 80:444-448.
182. Terranova, V. P., D. H. Rohrbach, and G. R. Martin. 1980. Role of laminin in the attachment of PAM 212 (epithelial) cells to basement membrane collagen. *Cell* 22:719-726.
183. Timpl, R., H. Rohde, P. G. Robey, S. I. Rennard, J. M. Foidart, and G. R. Martin. 1979. Laminin--a glycoprotein from basement membranes. *J.Biol.Chem.* 254:9933-9937.
184. Torimura, T., T. Ueno, M. Kin, S. Inuzuka, H. Sugawara, S. Tamaki, R. Tsuji, K. Sujaki, M. Sata, and K. Tanikawa. 1997. Coordinated Expression of Integrin  $\alpha 6\beta 1$  and Laminin in Hepatocellular Carcinoma. *Hum.Pathol.* 28:1131-1138.
185. Tronchin, G., K. Esnault, G. Renier, R. Filmon, D. Chabasse, and J. P. Bouchara. 1997. Expression and identification of a laminin-binding protein in *Aspergillus fumigatus* conidia. *Infect.Immun.* 65:9-15.
186. Valkonen, K. H., T. Wadström, and A. P. Moran. 1997. Identification of the N-acetylneuraminylactose-specific laminin-binding protein of *Helicobacter pylori*. *Infect.Immun.* 65:916-923.
187. Van den Brûle, F. A., A. Berchuck, R. C. Bast, F. T. Liu, C. Gillet, M. E. Sobel, and V. Castronovo. 1994. Differential expression of the 67-kD laminin receptor and 31-kD human laminin-binding protein in human ovarian carcinomas. *Eur.J.Cancer* 30A:1096-1099.
188. van den Brule, F. A., C. Buicu, A. Berchuck, R. C. Bast, M. Deprez, F. T. Liu, D. N. Cooper, C. Pieters, M. E. Sobel, and V. Castronovo. 1996. Expression of the 67-kD laminin receptor, galectin-1, and galectin-3 in advanced human uterine adenocarcinoma. *Hum.Pathol.* 27:1185-1191.
189. van den Brule, F. A., C. Buicu, M. E. Sobel, F. T. Liu, and V. Castronovo. 1995. Galectin-3, a laminin binding protein, fails to modulate adhesion of human melanoma cells to laminin. *Neoplasma* 42:215-219.

190. Van den Brûle, F. A., J. Engel, W. G. Stetler Stevenson, F. T. Liu, M. E. Sobel, and V. Castronovo. 1992. Genes involved in tumor invasion and metastasis are differentially modulated by estradiol and progestin in human breast-cancer cells. *Int.J.Cancer* 52:653-657.
191. Van den Brûle, F. A., J. Price, M. E. Sobel, R. Lambotte, and V. Castronovo. 1994. Inverse expression of two laminin binding proteins, 67LR and galectin-3, correlates with the invasive phenotype of trophoblastic tissue. *Biochem.Biophys.Res.Comm.* 201:388-393.
192. Varani, J., E. J. Lovett, III, J. P. McCoy, Jr., S. Shibata, D. E. Maddox, I. J. Goldstein, and M. Wicha. 1983. Differential expression of a lamininlike substance by high- and low-metastatic tumor cells. *Am.J.Pathol.* 111:27-34.
193. Viacava, P., A. G. Naccarato, P. Collecchi, S. Mønard, V. Castronovo, and G. Bevilacqua. 1997. The spectrum of 67-kD laminin receptor expression in breast carcinoma progression. *J.Pathol.* 182:36-44.
194. Vicentini, A. P., J. Z. Moraes, J. L. Gesztesi, M. F. Franco, W. de Souza, and J. D. Lopes. 1997. Laminin-binding epitope on gp43 from *Paracoccidoides brasiliensis* is recognized by a monoclonal antibody raised against *Staphylococcus aureus* laminin receptor. *J.Med.Vet.Mycol.* 35:37-43.
195. Vogelmann, R., E. Kreuser, G. Adler, and M. Lutz. 1999. Integrin  $\alpha 6\beta 1$  role in metastatic behavior of human pancreatic carcinoma cells. *Int.J.Cancer* 80:791-795.
196. Wang, K. S., R. J. Kuhn, E. G. Strauss, S. Ou, and J. H. Strauss. 1992. High-affinity laminin receptor is a receptor for Sindbis virus in mammalian cells. *J.Virol.* 66:4992-5001.
197. Weiner, A. M., P. L. Deininger, and A. Efstratiadis. 1986. Nonviral retroposons: genes, pseudogenes, and transposable elements generated by the reverse flow of genetic information. *Annu.Rev.Biochem.* 55:631-661.
198. Wewer, U., L. M. Shaw, R. Albrechtsen, and A. M. Mercurio. 1997. The Integrin  $\alpha 6\beta 1$  Promotes the Survival of Metastatic Human Breast Carcinoma Cells in Mice. *Am.J.Pathol.* 151:1191-1198.

199. Wewer, U. M., L. A. Liotta, M. Jaye, G. A. Ricca, W. N. Drohan, A. P. Claysmith, C. N. Rao, P. Wirth, J. E. Coligan, and R. Albrechtsen. 1986. Altered levels of laminin receptor mRNA in various human carcinoma cells that have different abilities to bind laminin. *Proc.Natl.Acad.Sci.U.S.A.* 83:7137-7141.
200. Wewer, U. M., G. Taraboletti, M. E. Sobel, R. Albrechtsen, and L. A. Liotta. 1987. Role of laminin receptor in tumor cell migration. *Cancer Res.* 47:5691-5698.
201. Wicha M.S., Herbert L., Malinoff H., and Huard T.K. Laminin receptors on macrophages - a mechanism for metastatic tumor recognition. [AACR Proceedings], 35. 1983. American Association for Cancer Research.
202. Wicha, M. S. and T. K. Huard. 1983. Macrophages express cell surface laminin. *Exp.Cell Res.* 143:475-479.
203. Woodward, T. L., H. Lu, and S. Z. Haslam. 2000. Laminin inhibits estrogen action in human breast cancer cells. *Endocrinology* 141:2814-2821.
204. Yamamoto, H., A. Irie, Y. Fukushima, T. Ohnishi, N. Arita, T. Hayakawa, and K. Sekiguchi. 1996. Abrogation of lung metastasis of human fibrosarcoma cells by ribozyme-mediated suppression of integrin  $\alpha 6$  subunit expression. *Int.J.Cancer* 65:519-524.
205. Yan, S., R. G. Rodrigues, D. Cahn Hidalgo, T. J. Walsh, and D. D. Roberts. 1998. Hemoglobin induces binding of several extracellular matrix proteins to *Candida albicans*. Identification of a common receptor for fibronectin, fibrinogen, and laminin. *J.Biol.Chem.* 273:5638-5644.
206. Yenofsky, R., S. Cereghini, A. Krowczynska, and G. Brawerman. 1983. Regulation of mRNA utilization in mouse erythroleukemia cells induced to differentiate by exposure to dimethyl sulfoxide. *Mol.Cell Biol.* 3:1197-1203.
207. Yoshida, N., Ishii, E., Nomizu, M., Yamada, Y., Mohri, S., Kinukawa, N., Matsuzaki, A., Oshima, K., Hara, T., and Miyazaki, S. The laminin-derived peptide YIGSR (Tyr-Ile-Gly-Ser-Arg) inhibits human pre-B leukaemic cell

- growth and dissemination to organs in SCID mice. *British Journal of Cancer* 80, 1898-1904. 1999.
208. Yow, H. K., J. M. Wong, H. S. Chen, C. G. Lee, S. Davis, G. D. Steele, Jr., and L. B. Chen. 1988. Increased mRNA expression of a laminin-binding protein in human colon carcinoma: complete sequence of a full-length cDNA encoding the protein [published erratum appears in *Proc Natl Acad Sci U S A* 1989 Sep;86(18):7032]. *Proc.Natl.Acad.Sci.U.S.A.*, 85:6394-6398.
209. Yurchenco, P. D. and J. C. Schittny. 1990. Molecular architecture of basement membranes. *FASEB J.* 4:1577-1590.
210. Zalipsky, S., B. Puntambekar, P. Boulikas, C. M. Engbers, and M. C. Woodle. 1995. Peptide attachment to extremities of liposomal surface grafted PEG chains: preparation of the long-circulating form of laminin pentapeptide, YIGSR. *Bioconjug.Chem.* 6:705-708.
211. Zhang, C., E. Duan, Y. Cao, G. Jiang, and G. Zeng. 2000. Effect of 32/67 kDa laminin-binding protein antibody on mouse embryo implantation. *Reprod.Fertil.* 137-142.

## CHAPTER 2

## PHAGE DISPLAY MAPPING FOR PEPTIDE 11 SENSITIVE SEQUENCES

## BINDING TO LAMININ-1

Abstract

We utilized a 9-mer random phage display library to identify sequences which bind to laminin-1 and elute with heparan sulfate or peptide 11. Laminin-1 derivatized plates were used for biopanning. Three consecutive rounds of low pH elutions were carried out, followed by three rounds of specific elutions, each consisting of a heparan sulfate elution followed by a peptide 11 (CDPGYIGSR) elution. The random sequence inserts were sequenced for phage populations eluted at low pH, by heparan sulfate and by peptide 11. Specifically eluted phage populations exhibited three classes of mimotopes for different regions in the cDNA derived amino acid sequence of the 67 kDa laminin binding protein (LBP). These regions were 1) a palindromic sequence known as peptide G, 2) a predicted helical domain corresponding to LBP residues 205-229, and 3) TEDWS-containing C-terminal repeats. All elution conditions also yielded phage with putative heparin binding sequences. We modeled the LBP<sup>205-229</sup> domain, which is strongly predicted to have a helical secondary structure, and determined that this region likely possesses heparin-binding characteristics located to one side of the helix, while the

opposite side appears to contain a hydrophobic patch where peptide 11 could bind. Using ELISA plate assays, we demonstrated that peptide 11 and heparan sulfate individually bound to synthetic LBP<sup>205-229</sup> peptide. We also demonstrated that the QPATEDWSA peptide could inhibit tumor cell adhesion to laminin-1. These data support the proposal that the 67 kDa LBP can bind the  $\beta$ -1 laminin chain at the peptide 11 region, and suggest that heparan sulfate is a likely alternate ligand for the binding interactions. Our results also confirm previous data (73) suggesting that the most C-terminal region of the LBP, which contains the TEDWS repeats, is involved in cell adhesion to laminin-1, and we specifically implicate the repeat sequence in that activity.

### Introduction

Many clinical studies on solid tumors show a strong positive correlation of high expression of the 67 kDa LBP with poor prognosis (9-11, 17, 48, 57, 58, 68, 70, 71). The 67 kDa LBP was originally described as "the laminin receptor", but, with the subsequent description of laminin binding integrin receptors, the apparent common intracellular trafficking (54) and co-overexpression of the LBP and the  $\alpha$ 6 $\beta$ 1 integrin in some solid tumors (22), as well as a demonstrated association of the 67 kDa LBP with the  $\alpha$ 6 $\beta$ 4 integrin (2), it is now considered much more likely that the LBP modulates cell:basement membrane adhesion rather than mediating it. The fact that the LBP is shed from tumor cells in culture in large amounts proportional to the invasive potential of the cells (30,

63), and subsequently binds laminin-1 containing matrix substrates (63), is most consistent with an activity modifying cell:extracellular matrix interactions. The cDNA sequence of the LBP can only code for a non-glycosylated protein of about half the mass of that observed for the mature membrane and shed forms of the LBP. While the mature protein has been shown to be lipid acylated (4, 36), studies by this lab (36) and others (7) have failed to produce any evidence for N- or O - linked glycosylation. There is experimental evidence that the high molecular weight mature form of the protein represents a dimer, but no conclusive evidence, as yet, demonstrating either a homo- or a hetero- dimer (36, 43, 51). The LBP cDNA sequence shares a very high homology with the S2 ribosomal class of proteins, so much so that the existence of functions for the LBP outside of those associated with ribosomal activities has been questioned by some investigators (26). However, a detailed study of the evolutionary genomics of the 67 kDa LBP, revealed that a unique evolution of the protein occurred in the C-terminal domain in parallel with the appearance of laminin and laminin -like molecules (1). The subsequent very high conservation of this domain has the hallmark of the acquisition of a new and important function for the protein (1). Therefore, the most likely scenario is that the modern protein is multifunctional, having a role as a ribosomal protein (16), and also having acquired a more recent function as a laminin binding protein (1). An interesting hypothesis is that the evolution of extracellular matrix binding activity could have occurred via a chaperone function for laminins (1). Two peptides derived from the C-terminal domain sequence, LBP residues 205-229 (37) and LBP residues 161-180 (peptide G) (41), have been shown to bind to laminin-1. In the case of peptide G, there is

evidence that laminin-1 binding may be mediated via heparin or heparan sulfate (21). Potential involvement of heparin/heparan sulfate in laminin-1 binding by the LBP<sup>205-229</sup> peptide, however, has not been evaluated to date.

Laminin-1 is one of the major components of basement membranes (33). It is a large glycoprotein molecule (MW  $\approx$  800 kDa), consisting of three polypeptide chains ( $\alpha$ 1,  $\beta$ 1 and  $\gamma$ 1), arranged in a characteristic cruciform shape. It contains multiple sites for polymerization, interaction with other components of basement membrane, such as collagen IV, nidogen and heparan sulfate proteoglycan (32, 49), as well as numerous cell adhesion molecules, such as integrins (6, 60) and non-integrin laminin receptors, including the 67 kDa laminin binding protein (LBP) (75). Laminin-1 also contains numerous heparan sulfate/heparin binding sites (23, 46, 65).

The peptide 11 sequence, CDPGYIGSR, which is found in the LE (laminin epidermal growth factor like) repeat region of the short arm of the  $\beta$ 1 laminin chain, was described as the ligand binding sequence for the 67 kDa LBP shortly after the initial descriptions of that protein (19, 28, 52). The proposed ligand function was deduced from the ability of the synthetic peptide to alter or mimic laminin-1 mediated cellular activities (27, 42). Associated with these activities were the ability to block tumor cell invasion of basement membrane, the ability to greatly reduce tumor lung colonization (28, 37), and the ability to block tumor angiogenesis (56). Anti-LBP antibodies have also been shown to interfere with cell spreading on immobilized YIGSR (42). However, compelling proof of interaction of the 67 kDa LBP with laminin-1 at this site is still lacking. Indeed, rotary shadowing experiments appear to show a predominance of binding by the 67 kDa LBP to

the long arm of laminin-1 just below the intersection of the cross (6). This is a short distance from the peptide 11 sequence in the short arm of the  $\beta$ 1 chain. Since the 67 kDa LBP has been shown to bind to laminin-1 via heparin or heparan sulfate (21), and since purified laminin-1 retains some heparan sulfate bound to it (21), the 67 kDa LBP is likely to be able to associate with isolated laminin-1 at more than one site via the residual laminin-bound glycosaminoglycan (GAG) moieties. Synthetic peptide 11, and its C-terminal YIGSR peptide, are currently being actively evaluated by several groups, including us, as potential anti-cancer drug leads (38, 39, 44, 62). Should the peptide 11-containing domain of laminin-1 fail to interact in a major way with the 67 kDa LBP, then it would be essential to describe alternative amino acid sequences with which peptide 11 does show a significant interaction.

The current study uses phage display mapping to derive information about ligand binding interactions at the peptide 11 site in laminin-1. Since this sequence comprises only about 0.1% of the total length of the three chains of laminin-1, it was obvious that specific elution with free peptide 11 would be needed to enrich for phage whose binding to laminin-1 occurred in this region. Several experiments have been reported in which successful elution was performed using specific competition elution conditions instead of extreme pH (18, 47, 72). Our experimental design utilized three initial rounds of selection for phage exhibiting any type of binding affinity for laminin-1. This was accomplished with low pH elution which does not put any qualitative constraints on the nature of the binding. By initially eliminating all phage which failed to bind to laminin-1, we felt that this would favor the statistical likelihood of eventually isolating phage

which bound to the peptide 11 -containing LE repeat region.

In order to assess the biological relevance of the phage LBP mimotope sequences, we evaluated the ability of phage displaying LBP mimotopes to bind to isolated laminin-1. We also synthesized a peptide with the LBP homologous sequence of a repeatedly isolated mimotope, and tested its ability to inhibit cell adhesion to laminin-1. The nature of ligand interactions at the LBP<sup>205-229</sup> domain was probed using 1) a photoactivatable crosslinking analog of peptide 11 (63) to assess the ability of peptide 11 to bind directly to the synthetic LBP<sup>205-229</sup> helix peptide, and 2.) using a sequence specific antibody for the LBP<sup>205-229</sup> helix peptide (37) to evaluate the ability of synthetic LBP<sup>205-229</sup> peptide to bind to isolated heparan sulfate.

## Materials and Methods

### Cell lines and tissue culture conditions

The highly invasive and metastatic murine melanoma cell line, B16BL6 (50), was obtained from the Mason Research Institute, Worcester, MA. The B16BL6 cells were propagated in RPMI 1640 medium (Sigma) supplemented with 10% fetal bovine serum (Gibco), 5 µg/ml insulin and cover antibiotics. The DG44 variant of the CHO (Chinese hamster ovary) cell line was kindly provided by Dr. L. Chasin of Columbia University. These cells are double mutants for the dihydrofolate reductase gene, and are used for

methotrexate amplification of expression systems previously introduced along with a dhfr expression vector. Wild type cells were propagated in  $\alpha$ MEM medium (Sigma) containing 10% fetal bovine serum, hypoxanthine and thymidine, 5  $\mu$ g/ml insulin and cover antibiotics. Generation of the DG44CHO  $\alpha$ 6 $\beta$ 1 cells which overexpress the human  $\alpha$ 6 and  $\beta$ 1 integrin chains is fully described in Starkey et al., 1999. Since these cells are methotrexate amplified for G418 -selectable expression vectors, they are propagated in  $\alpha$ MEM containing 60  $\mu$ M methotrexate and 400  $\mu$ g/ml G418 as well as 10% dialyzed fetal bovine serum, 5  $\mu$ g/ml insulin and cover antibiotics. Both the DG44CHO and the DG44CHO $\alpha$ 6 $\beta$ 1 cell lines are highly invasive and metastatic in *SCID* mice.

#### The 9-mer random sequence phage display library

The J404 random sequence phage display library was generously donated by its creator, Dr. Jim Burritt, Montana State University. The library was constructed by insertion of 27 bp synthetic oligonucleotides coding for random amino acids at the amino terminus of the minor phage coat protein III (3). The chemical diversity of the library is estimated to be  $5.7 \times 10^8$ . The library was provided as primary unamplified stock. Unmodified M13 phage was used as the wild type in our experiments. J404 is expressed in the phage display vector, M13KBst, a filamentous M13 bacteriophage carrying a gene for kanamycin resistance. The bacteriophage was propagated in K91 *E. coli* cells, and plaque assays were used to titrate the phage.

Reagents used in the biopanning and ELISA assays

Mouse EHS laminin-1 was purchased from Gibco Life Technologies (Grand Island, NY). Bovine kidney heparan sulfate was purchased from Sigma Chemical Co. (St. Louis, MO), and heparan sulfate from bovine lens capsule was isolated by us as described in (53). Peptide 11 (CDPGYIGSR) was synthesized at the Montana State University peptide synthesis facility on a Milligen 9050 automated peptide synthesizer using standard Fmoc chemistry with an amide carboxy terminus using PAL resin. The peptide was purified to homogeneity using a C18 reverse phase HPLC column (Vydac, Hesperia, CA), and the molecular weight verified using electrospray mass spectrometry. Peptide QPATEDWSA was purchased from Commonwealth Biotechnologies (Richmond, VA), and peptide LBP<sup>205-229</sup> (RDPEEIEKEEQAAA EKAVTKEEFQG), laminin-1 peptide AFSTLEGRPSAY, scrambled peptide 11 (SRYDGGICP) and scrambled QPATEDWSA (WAQADSTPE) were purchased from Macromolecular Resources (Ft. Collins, CO). As described in (63), we synthesized an ultraviolet light photoactivatable crosslinker based on the peptide 11 sequence by replacing the tyrosine in the peptide 11 ligand with 4-benzoyl-L-phenylalanine. We also added a biotinylated lysine at the – terminus of the peptide, and included three glycines as a spacer between the biotinylated residue and the peptide 11 sequence to facilitate avidin binding. Bovine serum albumin (BSA, heat shock fraction IV) was purchased from Boehringer Mannheim (Indianapolis, MN). Glycine was purchased from Gibco Life Technologies, and Tris was purchased from Bio-Rad (Hercules, CA). All other chemicals were from Sigma

Chemicals Co. (St. Louis, MO). For biopanning, 60mm Falcon® bacteriological Petri dishes (Becton Dickinson, Franklin Lakes, NJ) were used. Immulon® 2HB 96 well plates used for direct phage binding assay were from Dynex Technologies, Inc. (Chantilly, VA). Positively charged Primaria® and standard Falcon® tissue culture (Becton Dickinson, Franklin Lakes, NJ) microtiter plates were used for the direct peptide interaction ELISA assays as indicated elsewhere.

#### Screening of the phage display peptide library

Screening of the phage display peptide library for peptide inserts exhibiting binding affinity for laminin-1 was based on standard protocols described elsewhere (61). One hundred µg of mouse laminin-1 in 2 ml of 0.1M NaHCO<sub>3</sub> buffer was adsorbed to the surface of a 60mm polystyrene Petri plate (Falcon®) during an incubation of 10 hours at +4°C in a humidity chamber with constant agitation. The plates were then blocked by incubation with 5 mg/ml dialyzed BSA (heat shock fraction IV, Boehringer Mannheim, MO) in 0.1M NaHCO<sub>3</sub> buffer, before being washed seven times with 2 ml TTBS (Tris buffered saline containing 0.5% Tween-20). For the first round of selection, an aliquot of the phage display library representing  $5 \times 10^{12}$  phage was added to the plate. In consecutive rounds, aliquots of 30 to 50 µl of amplified phage ( $\sim 10^{10}$  PFU/µl) from the previous round were used. The aliquots of amplified phage were added in TTBS, and unbound phage were removed with seven washes of 2 ml TTBS. Bound phage were

eluted using 0.1M HCl-glycine, pH = 2.2, for 5 minutes with agitation. Eluted phage were immediately transferred to a fresh tube, and the solution was neutralized by addition of 1M Tris. Eluted phage were amplified and re-planned on immobilized laminin-1. This procedure was repeated three times. In rounds 4, 5 and 6, we applied two consecutive specific elutions at neutral pH. These consisted of an elution with 700µg/ml mixture of heparan sulfates (50:50 by weight) from bovine kidney and bovine lens capsule in TBS, followed by an elution using 5mM peptide 11 in TBS. The combined specific selection cycle was repeated two more times, to give a total of six rounds of phage selection and amplification. We tested a variety of inorganic buffers to achieve the maximal stringency of washing, and determined that Dulbecco's TPBS (phosphate buffered saline containing 0.5% Tween-20) was the most effective. Therefore, Dulbecco's TPBS was used for the washes in rounds 4, 5 and 6. Eluted phages were amplified in *E. coli* K-91, and titers of phage were monitored using a standard plaque forming assay. Phage elutions using an irrelevant laminin-1 bioactive peptide, AFSTLEGRPSAY, and scrambled peptide 11, SRYDGGICP, were used to assess the specificity of peptide 11 eluted sequences.

#### ELISA assay for direct binding of phage to laminin-1

The wells of a 96-well tissue culture plate were incubated with 100µl of a 25 µg/ml laminin-1 in 0.1 M NaHCO<sub>3</sub> buffer for 6 hours at room temperature, followed by 3 hours of incubation at 37<sup>0</sup>C. The wells were then blocked by incubation with 150µl of

1% BSA in PBS for 12 hours. Phage stocks were titered immediately prior to use. Before adding these to the plate, the phage were diluted in PBS, and then  $10^{10}$ ,  $10^9$  and  $10^8$  pfu in 100 $\mu$ l were added per well. Phage were allowed to bind for 10 hours at room temperature. Unbound phage were removed and the plates were washed 6 times in PBS/0.1% Tween-20. Rabbit anti-M13 antiserum was generously provided by Dr. Algirdas Jesaitis, Montana State University. The IgG fraction was purified using immobilized protein A columns (Pierce, Rockford, IL), and was diluted in PBS/1% BSA. The working antibody dilution was determined empirically. One hundred  $\mu$ l of diluted anti-M13 antibody was loaded per well and allowed to react for 4 - 6 hours at room temperature. The plates were then rinsed as described above. Goat anti-rabbit IgG (H+L chain) alkaline phosphatase conjugated antibody (Bio-Rad) was diluted 1:1000 in PBS/1% BSA, and 100  $\mu$ l was loaded per well and allowed to react for 4 - 6 hours at room temperature. Then plates were again washed as described above. One hundred  $\mu$ l of enzyme substrate solution (0.5 mg/ml disodium p-nitrophenyl phosphate (Sigma) in 9.8% diethanolamine, 0.5mM  $MgCl_2$ ) was added per well, and absorbance readings at 405 nm were taken at several time points from 5 minutes to 2 hours. The effectiveness of binding was determined by taking the ratio of the averages of absorbencies in replicate wells for the phage being tested and for wild-type phage in  $10^{10}$  pfu/well dilution. Specificity of binding was determined by comparing the "phage/wt" ratios for wells coated with laminin and wells without laminin.

Direct binding and crosslinking of the photoactivatable peptide 11 analog to LBP<sup>205-229</sup> peptide

Positively charged 96-well Primaria® plates were treated with 100 µl of the LBP<sup>205-229</sup> synthetic peptide per well at dilutions of 0.5 mg/ml, 0.25 mg/ml, 0.125 mg/ml and 0.0625 mg/ml in Dulbecco's phosphate buffered saline (PBS). Four replicates were used per dilution. The microwell plate was then incubated overnight at 4°C. After this, the peptide -containing solution was removed from the wells, 150 µl of PBS containing 1% BSA was added to block the plate, and the plate was incubated at room temperature for a further 2 hours. The blocking solution was then removed, and the plate washed three times with PBS. For the assay, 80 µl of the photoactivatable peptide 11 analog (63), freshly dissolved at a concentration of 0.167 mg/ml in PBS, was added per well. The plate was then subjected to a 2 minute irradiation with 350 nm long wave U.V. light (black light) as described in (63) to crosslink the peptide 11 analog to any binding sites. The analog -containing solution was then removed and the plate washed three times with PBS. One hundred µl of a 1:1000 dilution of avidin neutralite (Molecular Probes, Eugene, OR) in PBS was then added to each well, and the plate was incubated at room temperature for one hour. After the avidin neutralite solution was removed, the plate was washed six times with PBS and 100 µl of a 1:1000 dilution of biotinylated alkaline phosphatase (Bio-Rad) in PBS was added per well. The plate was then incubated for one hour at room temperature. Following removal of the biotinylated

alkaline phosphatase and six washes with PBS, 100  $\mu$ l of p-nitrophenyl phosphate chromogenic substrate was added. The quantity of peptide 11 analog which bound and crosslinked to the LBP<sup>205-229</sup> peptide was assessed using an ELISA plate reader measuring light absorption at 405 nm. Absorption from wells treated with BSA but no LBP<sup>205-229</sup> peptide was subtracted from the final readings. Three individual assays were conducted, and each gave similar results.

#### Heparan sulfate binding assay

Positively charged 96-well Primaria® microtiter plates were coated with heparan sulfate in increasing concentrations in PBS, pH = 7.0, and incubated for 3 hours at room temperature. The residual heparan sulfate solution was then removed, the wells were rinsed 3 times with PBS and blocked with 1% gelatin (Bio-Rad, ACS grade) in PBS for 3 hours at room temperature. The gelatin solution was then removed, wells washed 7 times and 100  $\mu$ l of the LBP<sup>205-229</sup> peptide in PBS (0.5 mg/ml) was loaded per well. The peptide was allowed to bind for 15 hours at room temperature. The wells were then washed multiple times with PBS, and binding of the peptide to heparan sulfate was detected using anti-LBP<sup>205-229</sup> rabbit antibodies (37) followed by alkaline phosphatase-conjugated goat anti-rabbit IgG (H+L chain) (Bio-Rad) (1:1000) in PBS. Chromogenic reaction with p-nitrophenyl phosphate was monitored by absorption at 405 nm. To assess the specificity of LBP<sup>205-229</sup> peptide binding to heparan sulfate, an irrelevant peptide from

the protein kinase C<sub>β1</sub> sequence, H-C-(STYTANPEFVIANV-OH) (Calbiochem, San Diego, CA) was used in place of the LBP<sup>205-229</sup> peptide in this assay. A rabbit antibody specific for this peptide (Calbiochem) was used in place of our rabbit anti-LBP<sup>205-229</sup> antibody, and then the assay was developed as indicated above.

#### Cell adhesion inhibition assay

Ninety-six well microtiter plates (Falcon®) were coated with 100µl laminin-1 (50 µg/ml in Dulbecco's's PBS) and incubated for 3 hours at 37 °C. The wells were then blocked by addition of 6% BSA solution to give a final concentration of 3% BSA, and were incubated for 15 hours at +4 °C. The wells were briefly rinsed with Dulbecco's's PBS immediately before use. Monodispersed suspensions of cells were obtained using minimal trypsin exposure. 10<sup>4</sup> cells were loaded per well in serum-free, protein-free medium with or without the QPATEDWSA peptide (100 µg/ml) and were incubated in a tissue culture incubator at 37 °C. After set time intervals, unattached cells were removed, the wells were washed twice with serum-free, and fresh medium was added. After the end of the adhesion period, medium in all wells was replaced with fresh medium containing MTT (0.25 mg/ml) and incubation was continued for 3 hours. The medium was then removed and the MTT metabolite was dissolved in DMSO. Absorbency readings were taken at 580 nm using a microtiter plate reader. Sequence specificity for bioactivity of the QPATEDWSA peptide was evaluated by substituting a peptide with

scrambled sequence, WAQADSTPE, in the adhesion assay.

#### Computer-based modeling of a potential 3D structure for the LBP<sup>205-229</sup> peptide

A model for the LBP<sup>205-229</sup> region was built in an  $\alpha$ -helical backbone conformation using the program, InsightII (MSI, Inc.). The initial structure was then energy minimized using the "steepest descents" then "conjugate gradients" algorithms in Discover (MSI, Inc.). Since the total energy of the structure was still relatively high and had not converged well, a molecular dynamics simulation was carried out using the Discover software package. The CVFF forcefield was employed for 200 ps of molecular dynamics with steps of 1 fs at 300 K. Charges and cross terms were omitted from the potentials and harmonic bond stretching potentials were used. The lowest energy structure was then further energy minimized using "steepest descents" followed by "conjugate gradients" algorithms to give a final structure exhibiting a forty-fold reduction in total energy compared to the initial structure. This was considered to be a reasonable potential structure for the peptide.

## Results

Phage clones which bound to laminin-1 via peptide 11 sensitive mechanisms were obtained, but heparan sulfate binding phage clones could not be eliminated from the selected population

The bacteriophage display peptide library, J404 (12), was screened for phage that selectively bound laminin-1 at the peptide 11, CDPGYIGSR, sequence. Our experimental design utilized multiple initial rounds of selection for phage with any type of affinity for laminin-1. These rounds were followed by specific elutions of laminin-1 - bound phage with excess heparan sulfate then excess peptide 11. Titers of phage were obtained for all washes and eluates, providing information on the relative efficiency of heparan sulfate and peptide 11 elutions. Titers from the elution rounds 4, 5 and 6 showed that we succeeded in obtaining an enrichment for phage preferentially eluted by peptide 11. By round 5, peptide 11 eluted phage were significantly more numerous than the mock buffer (TBS) eluted phage, and this effect was maintained in round 6 (Table 2.1).

The relative titers for elutions using heparan sulfate compared to the subsequent peptide 11 elutions are interesting because they stabilize by round 5. In the first round of the double specific selection (round 4), we found that the titer of phage in the heparan sulfate elution was 10.1 times higher than that in the peptide 11 elution. However, in round 5, this ratio decreased to 5.3, and in the sixth round was found to be essentially unchanged at 5.7 (Table 2.1).

The proportional decrease in the numbers of phage which were eluted by heparan sulphate in the fifth round indicated that we had succeeded in reducing the contribution of heparan sulfate binding phage to the specifically eluted populations. However, in later rounds, we did not see any further relative decrease in the numbers of heparan sulfate - binding phage. Therefore, some fraction of the heparan sulfate sensitive binding appeared to be linked to peptide 11 sensitive binding.

	Round 4	Round 5	Round 6
% phage eluted by heparan sulfate	91	84	85
% phage eluted by peptide 11	9	16	15
% phage specific for peptide 11 <sup>2</sup>	1.2	18.5	42.3

<sup>1</sup>Titers were derived from standard plaque forming assays using *E.Coli* K-91.

<sup>2</sup>Calculated by subtracting the % phage eluted by TBS under identical conditions.

Table 2.1. Comparisons of the numbers<sup>1</sup> of phage specifically eluted from laminin-1 by heparan sulfate and by peptide 11 in the last three rounds of selection

To evaluate the overall specificity of the peptide 11 eluted phage sequences, starting with the low pH eluted phage population, three rounds of sequential heparan sulfate/peptide elutions were carried out using 1) scrambled peptide 11 (SRYDGGICP) and 2) an unrelated bioactive laminin-1 peptide, AFSTLEGRPSAY (66). For both of these control peptides, the contribution of heparan sulfate -binding phage to the final specific elution populations was very much smaller than was the case for the peptide 11

experiments. This finding supports specificity of the proposed link between heparan sulfate sensitive and peptide 11 sensitive phage binding.

Sequence analysis of specifically eluted phage reveals inserts with similarities for three regions of the 67 kDa LBP

We sequenced the recombinant inserts of 27 randomly picked phage clones eluted by heparan sulfate, as well as 66 phage clones eluted by peptide 11. Thirty eight of the peptide 11 eluted phage clones were from round 6, and 28 were from earlier rounds. In addition, we sequenced the inserts from 20 phage clones eluted by low pH during the initial three non-specific elutions, as well as inserts from 42 phage clones eluted by the irrelevant laminin-1 peptide and 41 phage clones eluted by scrambled peptide 11. The only informative sequences from the low pH eluted phage were five clones bearing inserts with two positively and no negatively charged residues (data not shown). Three of these sequences also contained tryptophan residues (data not shown). Heparan sulfate/heparin binding motifs are often characterized by an enrichment in basic amino acids juxta positioned to tryptophan residues (5, 20), and we concluded that these sequences likely represented heparan sulfate -binding peptides. Considering the fact that laminin-1 has numerous heparin/heparan sulfate binding sites, and isolated laminin-1 still has some residual glycosaminoglycan associated with it (21), recovery of potential heparin/heparan sulfate -binding sequences from the non-specific elutions was expected.

Sequence homology <sup>2</sup> with:	Sequences from phage eluted by peptide 11 <sup>1</sup> <sub>a</sub>	Sequences eluted by heparan sulfate <sup>1</sup>
LBP <sup>205-229</sup>	RDPEEIEK <u>EEQ</u> <u>AAAEKAVTK</u> <u>EEFQ</u> G  GM <u>KAVR</u> IQG G <u>KAM</u> <u>LD</u> <u>DRAS</u> SH <u>ATV</u> <u>KAAV</u>	RDPEEIEK <u>EEQ</u> <u>AAAEKAVTK</u> <u>EEFQ</u> G  <u>DR</u> <u>TAMQ</u> <u>VAA</u> <u>DR</u> <u>TAMQ</u> <u>VAA</u> <u>VV</u> <u>KI</u> <u>SEAG</u> GG <u>SVA</u> <u>FRAG</u>
LBP - Peptide G	IPCNNKGAHSVGL <u>MW</u> <u>WMLAREV</u> LRMR  KP <u>WWR</u> <u>TNTA</u> (6) WHRT <u>MWW</u> <u>WP</u> (8) <u>PWW</u> <u>MTR</u> <u>HW</u> <sup>3</sup>	IPCNNKGAHSVGL <u>MW</u> <u>WMLAREV</u> LRMR  GPG <u>AW</u> <u>W</u> <u>GSA</u>
LBP - C-terminal DWS containing repeats	<u>QP</u> <u>ATE</u> <u>DWS</u>  <u>QN</u> <u>TD</u> <u>W</u> <u>LG</u> <u>NL</u> (3)	QPATEDWS  None
Putative heparin binding sequences <sup>4</sup>	HARSHYPWY KWKWPDRPK SLEHRAFRN GKLNLG <sup>5</sup> GYK KM <sup>5</sup> NKGVVNP	SKMHRNSWF AKIPAGRDR KM <sup>5</sup> NKGVVNP

<sup>1</sup> Residues contributing to the homology are shown in bold and underlined.

<sup>2</sup> Residues showing homology with the mimotopes are underlined.

<sup>3</sup> Previous sequence in reverse order.

<sup>4</sup> Positively charged residues in putative heparin binding peptides are shown in bold.

<sup>5</sup> Number of multiple isolations are shown in parentheses.

Table 2.2. Sample mimotopes and putative heparin binding sequences obtained from phage specifically eluted from laminin-1 by peptide 11 or by heparan sulfate.

Table 2.2. shows informative phage sequences which were obtained from the

specific elutions with peptide 11 and heparan sulfate. Phage clones carrying sequences mimicking three different regions of the 67 kDa LBP sequence were obtained. These regions are: the LBP<sup>205-229</sup> putative helical domain, the LBP peptide G domain and the C-terminal DWS -containing repeats. Since antibodies have been independently raised to synthetic peptides containing the sequences of all three LBP regions (37, 73), the random phage displayed sequences which mimic these antigenic sequences can be classified as mimotopes. Amongst the sequenced inserts of the phage clones eluted by peptide 11 in round 6, we found six independent isolates containing inserts coding for the sequence, KPWWRTNA, which shows a homology with the sequence of peptide G. Three individual isolates of phage carrying identical inserts coding for the sequence, QNTDWLGNL, were also identified from the round 6 peptide 11 elution. This sequence is reminiscent of the sequences of DWS -containing repeats which are found in the C-terminal portion of the 67 kDa LBP. The LBP peptide G region and the LBP<sup>205-229</sup> domain have both been previously shown to be involved in binding to laminin-1, while an antibody, raised to the C-terminal LBP region containing the DWS repeats, modified cellular interactions with laminin-1. Our phage display results suggested that the DWS containing repeats could themselves bind to laminin-1. Heparan sulfate eluted numerous phage clones carrying sequences reminiscent of heparin/heparan sulfate -binding domains found in other proteins (5, 20) (Table 2.2). As indicated earlier, this was to be expected. Surprisingly, however, peptide 11 was also quite efficient at eluting phage carrying these inserts, even in round 6 when the elution pattern had apparently stabilized. This suggests that some peptide 11 and heparan sulfate binding phage are interdependent in their

binding to laminin-1. No phage insert sequences mimicking any LBP sequence domains were obtained with the irrelevant laminin-1 peptide, AFSTLEGRPSAY, while only a single sequence mimicking part of the LBP<sup>205-229</sup> domain was obtained with scrambled peptide 11, SRYDGGICP. We were not surprised to obtain this mimic since a scrambled YIGSR sequence peptide has previously been shown to retain some, albeit much reduced, activity in other experiments (74).

BLAST searches for similarities to phage LBP mimotope and putative heparin -binding sequences support specific relationships to the LBP sequence

BLAST searches were run against the Owl composite sequence database (218,197 sequences) for all of the phage insert sequences shown in Table 2.2 to look for sequence matches in other proteins. None of the phage LBP<sup>205-229</sup> mimotope sequences eluted by peptide 11 were found in identical form in the database, and no more than three poor matches in other proteins were found for any of these sequences. No matches were found for one of the phage LBP<sup>205-229</sup> mimotope sequences eluted by heparan sulfate. The other two yielded poor sequence matches in two and seven proteins respectively. Somewhat better matches were found for phage mimotopes of the LBP peptide G domain. Two modest and nine poor sequence matches were found for the WHRTMWWWP peptide eluted by peptide 11, and two modest and four poor sequence matches were found for the GPGAWWWSA peptide eluted by heparan sulfate. Only four

poor sequence matches were found for the QNTDWLGNL peptide, a Mimotope for the LBP DWS containing repeats. No matches at all were found for two of the putative heparin binding sequences, and between two and nine poor sequence matches were obtained for the remaining six phage sequences. In all cases, the proteins in which the limited sequence matches were found were of very diverse functions. Overall, the very limited pattern of “match” sequences obtained in the Blast searches confirm the likely specificity of the phage sequence mimotopes for the LBP sequence.

#### Phage clones carrying LBP mimotopes re-bind directly to laminin-1

In order to confirm the binding specificity of phage populations specifically eluted from laminin-1, we chose six such phage clones and compared their abilities to bind to laminin-1 with the wild type phage population in an ELISA plate assay. The phage clones from the specific elutions were chosen to represent phage carrying insert sequences mimicking each of the three regions for which LBP mimotopes were obtained (Table 2.2). As shown in Figure 2.1, all clones that were tested displayed significantly higher affinity for laminin-1 than the wild-type phage. These data suggest that all three regions of the LBP identified by the existence of mimotopes in the peptide library may play a role in binding to laminin-1, and that each of them may be independently capable of binding.

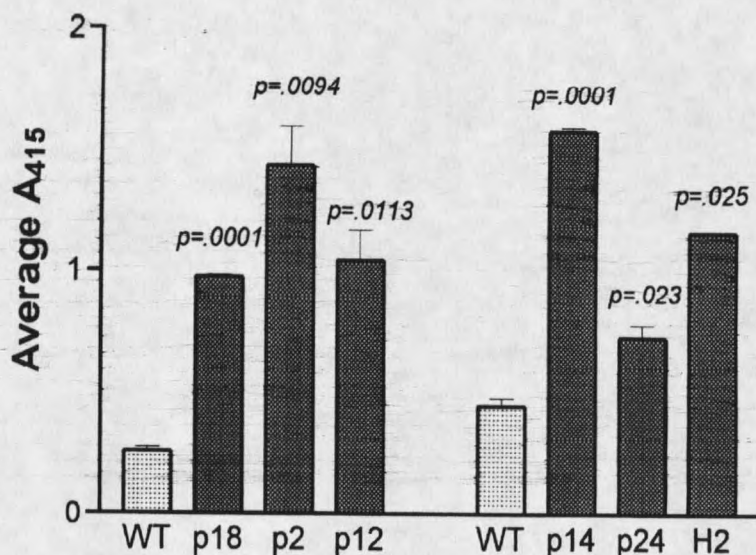


Figure 2.1. ELISA assays showing the ability of specifically eluted phage clones to bind to laminin-1. The assays were carried out as described in the Materials and Methods, and the data shown is the average of replicate wells  $\pm$  S.D. Wild type M13 phage were used as a control. We tested two clones containing peptide G mimotopes (p18, KPWWRTNTA; p24, WHRTMWWWP), three clones containing mimotopes for LBP<sup>205-229</sup> (p14, GKAMLDRAS; p2, GMKAVRIQG and h2, DRTAMQVAA) and a clone with the mimotope for the DWS -containing C-terminal repeats (p12, QNTDWLGNL). Clones with a "p" designation were eluted with peptide 11 and the clone with an "h" designation was eluted with heparan sulfate.

#### Peptide 11 binds and crosslinks the LBP<sup>205-229</sup> peptide in a dose-dependent manner

To further investigate the possibility that the LBP<sup>205-229</sup> domain could bind directly to laminin-1 at the peptide 11 site, as has been implicated previously by us (37), we examined the ability of a photoactivatable crosslinking analog of peptide 11 (63) to

bind and crosslink synthetic LBP<sup>205-229</sup> peptide in an ELISA assay, as described in Materials and Methods. In our previous studies (63), we demonstrated the exquisite specificity of the peptide 11 -based photoprobe. Using a Western protocol, we showed that, of the very large number of proteins present in an NP-40 detergent extract of tumor cell membranes, only one was biotinylated by this reagent. The biotinylated protein was of the correct molecular weight for the LBP. Figure 2.2 shows the dose dependent crosslinking of the peptide 11 analog to the LBP<sup>205-229</sup> peptide.

We repeated this assay three times, and, in each case, maximal crosslinking was obtained close to the LBP<sup>205-229</sup> peptide concentration shown in Figure 2.2, with crosslinking decreasing appreciably at higher concentrations. We have examined the LBP<sup>205-229</sup> peptide using circular dichroism (C.D.) spectroscopy and two dimensional proton NMR spectroscopy. At modest concentrations, the peptide exhibits a C.D. spectrum consistent with predominantly alpha helical structure (data not shown). However, at the higher concentrations needed for NMR spectroscopy, the NMR spectrum suggested significant aggregation of the peptide (data not shown). Such aggregation might be expected from the highly charged nature of the peptide, and it would also be expected to interfere with binding interactions to other ligands. We feel that the decrease in apparent ligand binding at higher LBP<sup>205-229</sup> peptide concentrations in the ELISA assay is probably due to aggregation of the LBP<sup>205-229</sup> peptide. Nevertheless, at favorable concentrations, the peptide 11 analog clearly bound and crosslinked to the LBP<sup>205-229</sup> peptide in a dose dependent and reproducible manner.

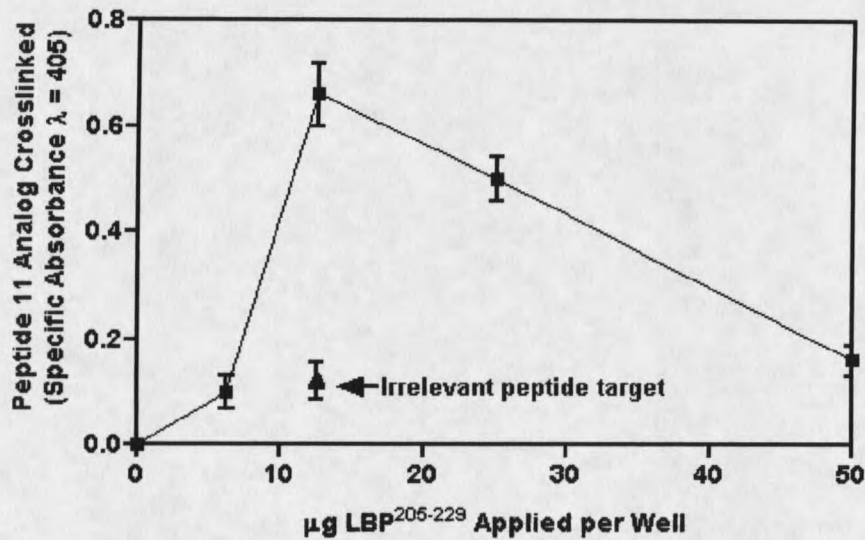


Figure 2.2. ELISA plate assay showing binding and crosslinking of the peptide 11 based photo-activatable analog to synthetic LBP<sup>205-229</sup> peptide. Synthetic LBP<sup>205-229</sup> peptide was allowed to bind to positively charged Primaria® plates as described in the Materials and Methods. The peptide 11 based photoprobe was added, and the plates U.V. irradiated as described in the Materials and Methods. Bound photoprobe was quantitated using avidin neutralite followed by biotinylated alkaline phosphatase and disodium p-nitrophenyl phosphate chromogenic substrate. Four replicates were used per dilution and the data shown is the average of the replicates  $\pm$  S.D.

### Modeling of the LBP<sup>205-229</sup> peptide sequence reveals potential heparin binding characteristics

Heparin binding protein domains are frequently helical with positive charges occurring close together on one side of the helix (5, 13). The LBP<sup>205-229</sup> region is predicted to be mainly alpha helical (37), and a synthetic peptide with this sequence gives

a strong  $\alpha$ -helical signal by C.D. (data not shown). When a helical wheel plot of the relevant sequence was evaluated, we found that three positively charged Lys residues occurred on one side of the helix (Figure 2.3). Negatively charged Glu residues flank two of the Lys residues in the helical conformation (Figure 2.3). By examining the linear sequence and the helical wheel plot, we could not readily anticipate the likely relationship of the three positively charged Lys sidechains to each other, and to the sidechains of the negatively charged Glu residues. We, therefore, modeled the three-dimensional structure using the InsightII and Discover programs (MSI). After running a molecular dynamics experiment and conducting energy minimization on the resultant structures, as described in Materials and Methods, we evaluated the final low energy structure as an example of a possible conformation for this domain of the 67 kDa LBP. Opposite sides of this potential structure are shown in Figure 2.4. Overall, the structure exhibited a helical backbone bent into a shallow comma shape (data not shown). Figure 2.4, panel A shows the putative heparin/heparan sulfate -binding side of the helix. From this type of modeling, we were able to deduce that the sidechains of the three positively charged Lys residues discussed above are likely to project together in a longitudinal linear array down one face of the helix. Negatively charged sidechains flank this linear array. We concluded that this side of the helix probably could bind heparin or heparan sulfate. However, the closeness of the negatively charged residues would likely reduce the avidity of binding, and could provide for conformationally dependent binding. The other side of the helix (Figure 2.4, panel B) shows a relative paucity of positively charged residue sidechains. Towards the C-terminus, there exists a hydrophobic patch including a

phenyl alanine sidechain. This hydrophobic patch is compatible with a docking site for peptide 11. It is known that the tyrosine residue in peptide 11 must be solvent exposed for bioactivity (31, 40, 62, 76), and it is very likely that its sidechain docks to peptide 11 binding proteins (62).

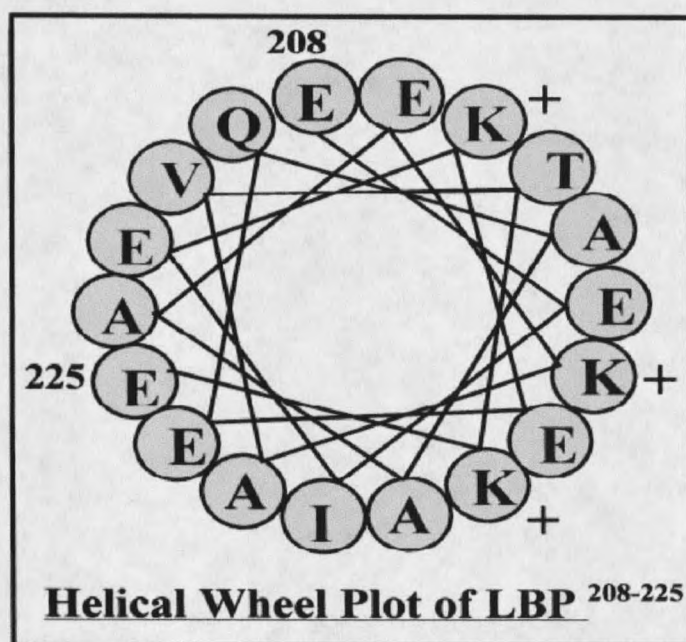


Figure 2.3. Helical wheel plot for LBP<sup>208-225</sup>. The start and end residues as well as the positively charged Lys residues are indicated by residue number or + as appropriate

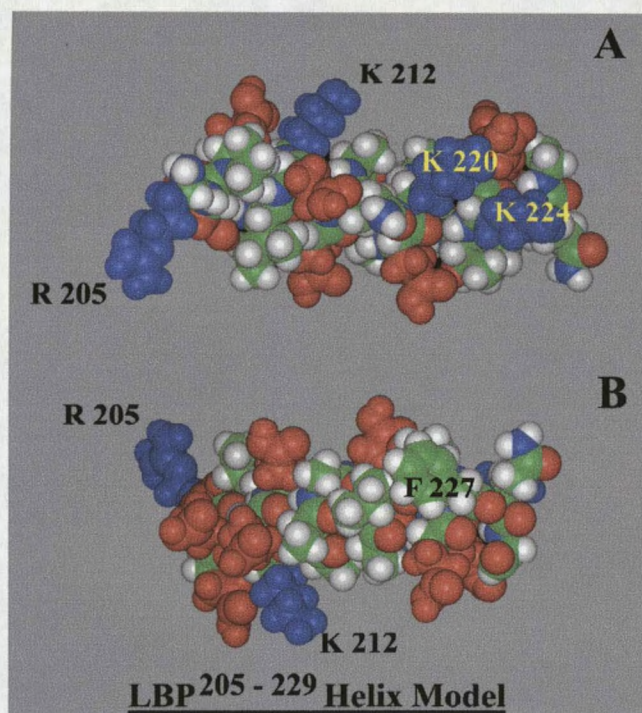


Figure 2.4. Computer based model of the LBP<sup>205-229</sup> domain. The structure is shown after a molecular dynamics simulation and extensive energy minimization. Panel A shows the putative heparin-binding side, and panel B shows the putative peptide 11 binding side. Residues with positively charged sidechains are shown in blue and residues with negatively charged sidechains are shown in red.

Synthetic LBP<sup>205-229</sup> peptide binds to isolated heparan sulfate

We utilized an ELISA plate assay to determine if isolated heparan sulfate could bind to synthetic LBP<sup>205-229</sup>. Increasing concentrations of isolated heparan sulfate were allowed to bind to positively charged Primaria© tissue culture 96-well plates as described

in the Materials and Methods. One hundred  $\mu\text{g}$  synthetic LBP<sup>205-229</sup> peptide was added per well, and the amount bound determined using our rabbit sequence specific antibody raised against this peptide (36, 37). An irrelevant peptide from the protein kinase C $\beta_1$  sequence, H-C-(STYTANPEFVIANV-OH), and an antibody specific for this peptide were used to assess the potential for non-specific binding to heparan sulfate in the ELISA assay. Minimal binding to the target plate was observed for this peptide, and binding did not increase with increasing amounts of heparan sulfate. Specific binding of the LBP<sup>205-229</sup> peptide to heparan sulfate was observed, and increased with increasing concentration of heparan sulfate to a plateau at 4  $\mu\text{g}$  heparan sulfate per well (Figure 2.5).

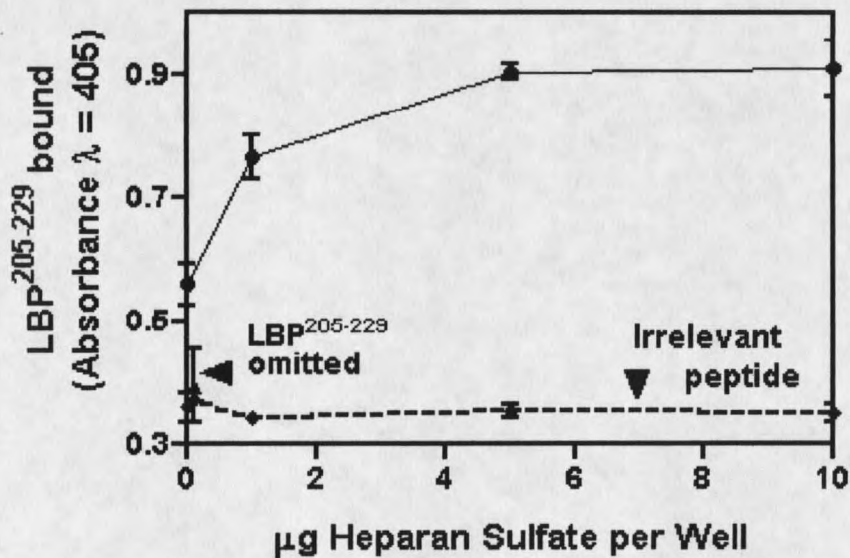


Figure 2.5. ELISA plate assay showing binding of synthetic LBP<sup>205-229</sup> peptide to heparan sulfate bound to a positively charged Primaria® plate. Binding of the synthetic LBP<sup>205-229</sup> peptide was quantitated using our LBP<sup>205-229</sup> specific rabbit antibody, followed by alkaline phosphatase conjugated anti-rabbit IgG and the chromogenic p-nitrophenyl phosphate substrate. Each data point represents the average of six replicates  $\pm$  S.E.M.

This experiment was repeated twice with similar results, and indicates that synthetic LBP<sup>205-229</sup> peptide can bind isolated heparan sulfate as is predicted by the phage display experiments and modeling studies reported in this manuscript.

### Synthetic QPATEDWSA peptide inhibits cell adhesion to laminin-1

In the course of sequencing of the recombinant inserts of the 38 phage specifically eluted by peptide 11 in round 6, we observed a sequence QNTDWLGNL in 3 individual isolates (Table 2.2). This peptide exhibits a sequence similarity to the TEDWS sequence which is repeated with minor variations five times within the most C-terminal domain of the LBP. To determine the biological relevance of this sequence, we synthesized a peptide derived from the LBP with the sequence of the third repeat, QPATEDWSA, and tested its ability to interfere with cell adhesion to laminin-1.

Laminin-1 was coated on the wells of a 96-well tissue culture plate as described in Materials and Methods, and the QPATEDWSA peptide was used at a concentration of 100 µg/ml. Cell attachment was measured at several time points from 5 to 120 minutes after cell addition using the MTT (3-[4,5-dimethylthiazol-2-yl]-2,5-diphenyltetrazolium bromide) metabolite to quantitate adherent cells. Three tumor cell lines were assayed. B16BL6 mouse melanoma cells were used as a representative highly invasive and metastatic cell line, and DG44CHOwt and DG44CHO $\alpha$ 6 $\beta$ 1 as chinese hamster ovary cell variants exhibiting modest and high co-expression of the 67 kDa LBP and the  $\alpha$ 6 $\beta$ 1

laminin -specific integrin (63). For B16BL6 cells, a clear inhibition of attachment was evident by 10 minutes after addition of the cells in the presence of the synthetic peptide, and this became more intense by 15 minutes after addition of the cells (Figure 2.6). At later time points, the difference between peptide treated and control cells gradually diminished. A similar profile for inhibition of the rate of attachment was seen for DG44CHOwt cells in the presence of the QPATEDWSA peptide (Figure 2.6).

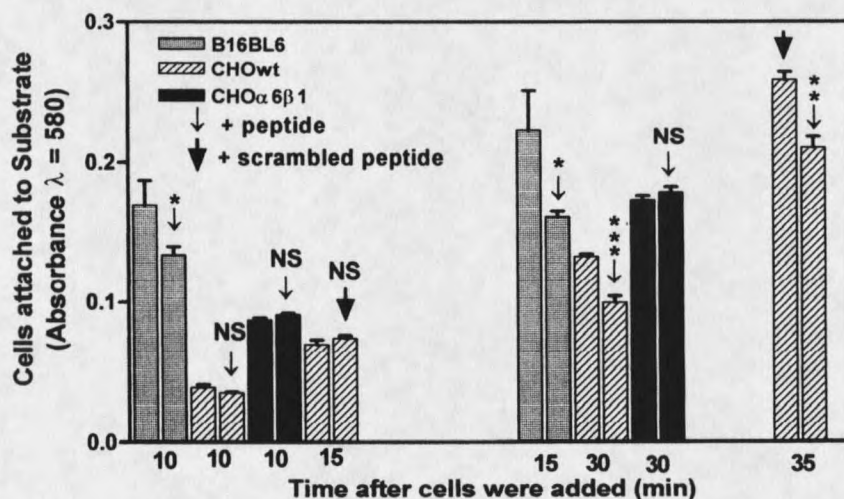


Figure 2.6. Cell adhesion assay to laminin-1 coated on a 96-well tissue culture plate as described in the Materials and Methods. Data is shown for B16BL6 mouse melanoma cells and for two variants of the DG44CHO chinese hamster ovary cell line. The number of adherent cells was quantitated using the MTT assay, and data is shown for various time points in the presence and the absence of the QPATEDWSA synthetic peptide. The scrambled sequence peptide, WAQADSTPE, was used as a sequence specificity control. The data shown is the average of six replicate wells  $\pm$  S.E.M. Results from cells in the presence of the synthetic peptide are indicated with an asterisk.

The scrambled peptide, WAQADSTPE did not inhibit binding of DG44CHOwt cells to laminin-1 (Figure 2.6), supporting the importance of the QPATEDWSA sequence to bioactivity of the peptide.

DG44CHO cells attach more slowly to laminin-1 than do B16BL6 cells. Therefore, the 30 minute time point for DG44CHO cells is roughly equivalent to the 15 minute time point which is shown for B16BL6 cells. The synthetic peptide had no apparent effect of the attachment of DG44CHO $\alpha$ 6 $\beta$ 1 cells (Figure 2.6). Since these cells express much more 67 kDa LBP and  $\alpha$ 6 $\beta$ 1 integrin receptor than the DG44CHOwt cells (63), the simplest explanation for their lack of sensitivity to the effects of the QPATEDWSA peptide, is that the amount of peptide present was insufficient to affect the large number of laminin binding proteins expressed by these cells. These results support a direct interaction of the QPATEDWSA peptide with cellular laminin-1 binding proteins, but does not indicate whether the 67 kDa LBP or the  $\alpha$ 6 $\beta$ 1 integrin is involved.

### Discussion

Screening of random sequence phage display peptide libraries is a powerful technique which allows for mapping of the regions on a protein surface which are involved in protein-protein interactions (12, 29, 69). Since it was first described in 1990 (14, 59), it has rapidly become a tool of choice for investigators seeking to identify

interfacial sequences between proteins (12, 29) and for epitope mapping (15, 25, 55, 67). Phage display experiments have been used in a variety of systems, including mapping of protein-protein interactions involved in cell adhesion (24, 34, 35, 45, 55, 72). Our preliminary data indicated that populations of phage eluted by peptide 11 immediately after the non-specific elution rounds expressed inserts which were dominated by sequences containing tryptophans, aromatic and positively charged residues. Heparan/heparin -binding motifs are often characterized by enrichment in basic amino acids juxta positioned to tryptophan residues (5, 21), and it appeared likely that these sequences represented heparin-binding peptides. By employing serial specific elutions, consisting of heparan sulfate followed by peptide 11 elutions, we managed to eliminate a subpopulation of phage whose binding to laminin-1 is dependent on GAG. In this way, we largely overcame the predominance of putative heparin -binding phage recovered from elution with peptide 11. Putative heparin -binding phage dominated the early rounds of elution from laminin-1, to the extent that in the first round of specific selection 91% of the total eluted phage were recovered in the heparan sulfate fraction. Further selection with peptide 11 elution resulted in a significant reduction of phage in the heparan sulfate eluate. However, a heparan sulfate labile population persisted in the later rounds suggesting that peptide 11 itself could destabilize binding of this class of phage. Additional studies will be needed to ascertain if these particular phage clones bind to one or more sites on isolated laminin-1 and its residual associated GAG.

The majority of displayed peptide sequences from phage eluted with heparan sulfate in round six revealed multiple short stretches of linear homology with the R<sup>205</sup>-

G<sup>229</sup> region of the LBP. As indicated earlier, this region probably is of alpha-helical conformation. Therefore, we analyzed the sequences of these phage inserts both from the point of view of linear sequence homology, and for mimicking spatial epitopes formed by residues three or four apart in the primary sequence, a spacing which would place them adjacent in a helical fold. This analysis revealed additional sites of homology, mostly based on localization of charged residues (data not shown).

Of the sequenced inserts from the phage eluted by peptide 11 in round six, we found one insert, KPWWRTNA, with a homology to the palindromic sequence within LBP peptide G. We also found a number of sequences with homology to the R<sup>205</sup>-G<sup>229</sup> region of LBP. Amongst these, some phage displayed linear sequence homology (Table 2.2), while others appeared to be mimicking the spatial distribution of charged residues on the surface of the presumed alpha helix structure of this region (data not shown). The sequence, QNTDWLGNL, was found in three independent isolates. This sequence is reminiscent of the DWS -containing repeats which are found in the C-terminal portion of the LBP. Although an antibody raised to a 20 residue long LBP peptide containing a single DWS repeat has been shown to disrupt cell binding to laminin-1 (73), no bioactivity had been ascribed to the repeat sequence itself. In the current report, we show that a peptide consisting of only this sequence does reduce the rate of cell binding to laminin-1 (Figure 2.6), so the repeat sequence is likely responsible for bioactivity of this region.

All residues involved in protein:protein interactions need not be mimicked by a single recombinant phage insert. The primary limitation is the size of the insert in the

phage display peptide library that is utilized. It has been reported that some interacting surfaces simply cannot be adequately mapped using libraries with short (6 residues long) inserts, while libraries with longer (12-20 residues) inserts produce reliable mapping (64). In the current project, we used a library with 9-mer inserts, which carries some limitation on the size of epitope that can be mimicked by a single phage. We observed stretches of homology covering, at best, five continuous residues. Further, the sequences that we did obtain fell into the class of mimotopes. Amongst the phage that mimic the LBP<sup>205-229</sup> region most homology is found with the region comprised by the K<sup>220</sup>AVT<sup>223</sup> residues. Interestingly, this same quadruplet is mimicked both by phage eluted by peptide 11 and by phage eluted by heparan sulfate. While heparan sulfate did elute some phage with putative heparin binding characteristics, none of these had any linear sequence homology with the LBP<sup>205-229</sup>. It is not clear why numerous sequences with homology to the LBP<sup>205-229</sup> were found in the heparan sulfate eluate from round six. It is possible that excess free heparan sulfate might interact with the heparin binding site in the proximal globular domain on the laminin  $\beta$ 1 chain, causing a structural change in the LE repeats where the peptide 11 sequence is located. Such a conformational change might result in release of phage bound to the LE repeat through LBP<sup>205-229</sup>-like sequences.

We obtained mimotopes for part of the LBP<sup>161-180</sup> region (peptide G). Interestingly, these mimotopes were seen in inserts from phage isolated from both peptide 11 and heparan sulfate eluates. As indicated earlier, we expected to see sequences with similarities to peptide G in the heparan sulfate eluates. Their presence in phage from the peptide 11 eluates was not expected, especially since peptide G was

previously shown to interact with laminin-1 in a YIGSR - independent manner (8). One possible explanation for this apparent discrepancy with our phage display findings could result from effects which peptide G is suspected to have on the conformation of laminin-1 (41). These conformational changes have been proposed to explain the fact that pre-treatment of laminin with peptide G in solution increases its binding to the cell surface, probably by exposing conditional receptor binding sites within laminin-1 (41). Elution of LBP<sup>205-229</sup> - like sequences from the peptide 11 - containing site on laminin-1 could cause conformational changes in the nearby heparan sulfate binding domain of the laminin  $\beta$ 1 chain. However, ligand photo-crosslinking and site-directed mutagenesis experiments will be needed to determine if one or more binding sites in laminin-1 are involved in binding by the phage clones examined in the current study.

The phage display mapping reported in this manuscript strongly suggests that peptide 11 interacts with the LBP<sup>205-229</sup> region. To test how these observations can be accommodated by the likely structure of this region, we performed computer simulated modeling experiments of this region. As shown in Figure 2.4, panel A, hydrophobic stretches <sup>216</sup>AAA<sup>218</sup> and <sup>221</sup>AVT<sup>223</sup> contribute residues to a hydrophobic pocket on the surface of the  $\alpha$ -helix. The aromatic F<sup>227</sup> sidechain also faces into this pocket. On the - terminal side, this pocket is flanked by K<sup>212</sup>, and on the C- terminal end by <sup>225</sup>E. Peptide 11, CDPGYIGSR, contains a negatively charged residue in the second position and a C-terminal positively charged residue. Both charged residues are required for bioactivity (62) and may contribute to ligand binding. Therefore, it is possible that LBP residues K<sup>212</sup> and E<sup>225</sup> provide electrostatic attraction for peptide 11. The binding could be further

stabilized by stacking of the aryl rings of peptide 11 Y<sup>5</sup> and LBP F<sup>227</sup>. Our hypothesis that LBP<sup>205-229</sup> is indeed a binding site for peptide 11 is supported by these simulations, and by the results of our ELISA experiment showing direct binding of the peptide 11 photo-crosslinking analog with the LBP<sup>205-229</sup> peptide (Figure 2.2).

As indicated in the results section, the opposite side of the LBP<sup>205-229</sup> helix demonstrates some features expected in a heparin - binding domain. A primary requirement for a "canonical" heparin binding site is significant enrichment in basic amino acids, and the binding domain is frequently helical in conformation (5). The basic amino acids appear on the same side of the helix, forming a positively charged surface (5). As shown in Figure 2.4, panel A, K<sup>212</sup>, K<sup>220</sup> and K<sup>224</sup> face the same side of the helix to form a linear array of positive charges. Therefore, this side of the LBP<sup>205-229</sup> helix could, theoretically, bind heparin or heparan sulfate. Our ELISA assay confirmed that synthetic LBP<sup>205-229</sup> could bind to immobilized heparan sulfate. From previous reports (21) we know that the binding of LBP to laminin via peptide G is mediated by heparan sulfate. Hence the presence of potential heparan sulfate binding domain on the "reverse" side of the LBP<sup>205-229</sup> helix may also be biologically relevant.

Overall, the results presented in this manuscript indicate that binding of the 67 kDa LBP to laminin-1 is likely to be more complex than was previously thought. Heparan sulfate is probably an important alternative ligand, interacting not only with the peptide G sequence but also with LBP<sup>205-229</sup>. Based on the fact that peptide 11 can elute mimotopes of sequences found in the cDNA for the LBP, the peptide 11 sequence in laminin-1 would appear to be a binding site for the LBP. This has been questioned based on the results of rotary shadowing experiments where the dominant site for binding was shown to be on the long arm of laminin-1 at a short distance from the peptide 11 site (6). In this earlier experiment, the fact that the LBP might exhibit binding to more than one site on this very large molecule was not fully considered. Indeed, the several heparin-binding sites present in laminin-1 make it likely that an isolated protein with heparin-binding characteristics would bind to multiple sites, albeit perhaps with different affinities. The most convincing argument for the importance of the peptide 11 sequence is the bioactivity of the synthetic peptide in inhibiting cellular activities dependent on interaction with laminin-1. If this sequence did not interact with the 67 kDa LBP, it would be necessary to postulate the involvement of another peptide 11 binding protein(s). Our own studies have shown that a photo-crosslinking peptide 11 analog only reacts with one detergent-extractable membrane protein with a mass appropriate for the 67 kDa LBP (63). However, although this finding and the evidence presented in the current manuscript strongly supports interaction of the 67 kDa LBP with the peptide 11-containing region of laminin-1, other approaches including additional analytical crosslinking experiments will need to be pursued to conclusively prove this.

REFERENCES CITED

1. Ardini, E., G. Pesole, E. Tagliabue, A. Magnifico, V. Castronovo, M. E. Sobel, M. I. Colnaghi, and S. Menard. 1998. The 67-kDa laminin receptor originated from a ribosomal protein that acquired a dual function during evolution. *Mol.Biol.Evol.* 15:1017-1025.
2. Ardini, E., E. Tagliabue, A. Magnifico, S. Butó, V. Castronovo, M. I. Colnaghi, and S. Menard. 1997. Co-regulation and physical association of the 67-kDa monomeric laminin receptor and the alpha6beta4 integrin. *J.Biol.Chem.* 272:2342-2345.
3. Burritt, J. B., C. W. Bond, K. W. Doss, and A. J. Jesaitis. 1996. Filamentous phage display of oligopeptide libraries. *Anal.Biochem.* 238:1-13.
4. Butó, S., E. Tagliabue, E. Ardini, A. Magnifico, C. Ghirelli, F. Van den Brúle, V. Castronovo, M. I. Colnaghi, M. E. Sobel, and S. Ménard. 1998. Formation of the 67-kDa laminin receptor by acylation of the precursor. *J.Cell Biochem.* 69:244-251.
5. Cardin, A. D. and H. J. Weintraub. 1989. Molecular modeling of protein-glycosaminoglycan interactions. *Arteriosclerosis* 9:21-32.
6. Castronovo, V. 1993. Laminin receptors and laminin-binding proteins during tumor invasion and metastasis. *Invasion Metastasis* 13:1-30.
7. Castronovo, V., A. P. Claysmith, K. T. Barker, V. Cioce, H. C. Krutzsch, and M. E. Sobel. 1991. Biosynthesis of the 67 kDa high affinity laminin receptor. *Biochem.Biophys.Res.Commun.* 177:177-183.
8. Castronovo, V., G. Taraboletti, and M. E. Sobel. 1991. Functional domains of the 67-kDa laminin receptor precursor. *J.Biol.Chem.* 266:20440-20446.
9. Colnagi, M. I. 1994. The simultaneous expression of c-erbB-2 oncoprotein and laminin receptor on primary breast tumors has a predicting potential analogous to that of the lymph node status. *Adv.Exp.Med.Biol.* 353:149-154.

10. Daidone, M. G., R. Silvestrini, E. Benini, W. F. Grigioni, and A. D'Errico. 1997. Expression of high-affinity 67-kDa laminin receptors in primary breast cancers and metachronous metastatic lesions or contralateral cancers. *Br.J.Cancer* 76:52-53.
11. De Manzoni, G., A. Guglielmi, G. Verlato, A. Tomezzoli, G. Pelosi, I. Schiavon, and C. Cordiano. 1998. Prognostic significance of 67-kDa laminin receptor expression in advanced gastric cancer. *Oncology (Basel)* 55:456-460.
12. DeLeo, F. R., L. Yu, J. B. Burritt, L. R. Loetterle, C. W. Bond, A. J. Jesaitis, and M. T. Quinn. 1995. Mapping sites of interaction of p47-phox and flavocytochrome b with random-sequence peptide phage display libraries. *Proc.Natl.Acad.Sci.U.S.A.* 92:7110-7114.
13. Deprez, P. N. and N. C. Inestrosa. 1995. Two heparin-binding domains are present on the collagenic tail of asymmetric acetylcholinesterase. *J.Biol.Chem.* 270:11043-11046.
14. Devlin, J. J., Panganiban, L. C., and Devlin, P. E. Random peptide libraries: A source of specific protein binding molecules. *Science* 249, 404-406. 1990.
15. Fack, F., B. Hügler-Dorr, D. Song, I. Queitsch, G. Petersen, and E. K. Bautz. 1997. Epitope mapping by phage display: random versus gene-fragment libraries. *J.Immunol.Methods* 206:43-52.
16. Ford, C. L., L. Randal-Whitis, and S. R. Ellis. 1999. Yeast proteins related to the p40/laminin receptor precursor are required for 20S ribosomal RNA processing and the maturation of 40S ribosomal subunits. *Cancer Res.* 59:704-710.
17. Gasparini, G., M. Barbareschi, P. Boracchi, P. Bevilacqua, P. Verderio, P. Dalla-Palma, and S. Menard. 1995. 67-kDa laminin-receptor expression adds prognostic information to intra-tumoral microvessel density in node-negative breast cancer. *Int.J.Cancer* 60:604-610.
18. Gho, Y. S., J. E. Lee, K. S. Oh, D. G. Bae, and C. B. Chae. 1997. Development of antiangiogenic peptide using a phage-displayed peptide library. *Cancer Res.* 57:3733-3740.

19. Graf, J., Y. Iwamoto, M. Sasaki, G. R. Martin, H. K. Kleinman, F. A. Robey, and Y. Yamada. 1987. Identification of an amino acid sequence in laminin mediating cell attachment, chemotaxis, and receptor binding. *Cell* 48:989-996.
20. Guo, N. H., H. C. Krutzsch, E. NØgre, T. Vogel, D. A. Blake, and D. D. Roberts. 1992. Heparin- and sulfatide-binding peptides from the type I repeats of human thrombospondin promote melanoma cell adhesion. *Proc.Natl.Acad.Sci.U.S.A.* 89:3040-3044.
21. Guo, N. H., H. C. Krutzsch, T. Vogel, and D. D. Roberts. 1992. Interactions of a laminin-binding peptide from a 33-kDa protein related to the 67-kDa laminin receptor with laminin and melanoma cells are heparin-dependent. *J.Biol.Chem.* 267:17743-17747.
22. Halatsch, M. E., K. I. Hirsch Ernst, G. F. Kahl, and R. J. Weinel. 1997. Increased expression of alpha6-integrin receptors and of mRNA encoding the putative 37 kDa laminin receptor precursor in pancreatic carcinoma. *Cancer Lett.* 118:7-11.
23. Hall, H., R. Deutzmann, R. Timpl, L. Vaughan, B. Schmitz, and M. Schachner. 1997. HNK-1 carbohydrate-mediated cell adhesion to laminin-1 is different from heparin-mediated and sulfatide-mediated cell adhesion. *Eur.J.Biochem.* 246:233-242.
24. Healy, J. M., O. Murayama, T. Maeda, K. Yoshino, K. Sekiguchi, and M. Kikuchi. 1995. Peptide ligands for integrin alpha v beta 3 selected from random phage display libraries. *Biochem.* 34:3948-3955.
25. Henderikx, P., Kandilogiannaki, M., Petrarca, C., von Mensdorff-Pouilly, S., Hilgers, J. H. M., Krambovitis, E., Arends, J. W., and Hoogenboom, H. R. Human single-chain Fv antibodies to MUC1 core peptide selected from phage display libraries recognize unique epitopes and predominantly bind adenocarcinoma. *Cancer Research* 58, 4324-4332. 1998.
26. Hung, M., E. rosenthal, B. Boblett, and S. Benson. 1995. Characterization and localized expression of the laminin binding protein/p40 (LBP/p40) gene during sea urchin development. *Exp.Cell Res.* 221:221-230.

27. Iwamoto, Y., J. Graf, M. Sasaki, H. K. Kleinman, D. R. Grotzinger, G. R. Martin, F. A. Robey, and Y. Yamada. 1988. Synthetic pentapeptide from the B1 chain of laminin promotes B16F10 melanoma cell migration. *J. Cell Physiol.* 134:287-291.
28. Iwamoto, Y., F. A. Robey, J. Graf, M. Sasaki, H. K. Kleinman, Y. Yamada, and G. R. Martin. 1987. YIGSR, a synthetic laminin pentapeptide, inhibits experimental metastasis formation [published erratum appears in *Science* 1988 Jan 15;239(4837):245]. *Science* 238:1132-1134.
29. James, M., Man, N. T., Edwards, Y. H., and Morris, G. The molecular basis for cross-reaction of an anti-dystrophin antibody with alpha-actinin. *Biochim. Biophys. Acta* 1360, 169-176. 1997.
30. Karpatová, M., E. Tagliabue, V. Castronovo, A. Magnifico, E. Ardini, D. Morelli, D. Belotti, M. I. Colnaghi, and S. Ménard. 1996. Shedding of the 67-kD laminin receptor by human cancer cells. *J. Cell Biochem.* 60:226-234.
31. Kawasaki, K., T. Murakami, M. Namikawa, T. Mizuta, Y. Iwai, Y. Yamashiro, T. Hama, S. Yamamoto, and T. Mayumi. 1994. Amino acids and peptides. XXI. Laminin-related peptide analogs including poly(ethylene glycol) hybrids and their inhibitory effect on experimental metastasis. *Chem. Pharm. Bull. (Tokyo)* 42:917-921.
32. Kleinman, H. K., M. L. McGarvey, L. A. Liotta, P. G. Robey, K. Tryggvason, and G. R. Martin. 1982. Isolation and Characterization of Type IV Procollagen, Laminin, and Heparan Sulfate Proteoglycan from the EHS Sarcoma. *Biochem.* 21:6188-6193.
33. Kleinman, H. K., B. Weeks, H. W. Schnaper, M. C. Kibbey, K. Yamamura, and D. S. Grant. 1993. The laminins: A family of basement membrane glycoproteins important in cell differentiation and tumor metastases. *Vitamins and Hormones* 47:161-186.
34. Koivunen, E., B. Wang, and E. Ruoslahti. 1994. Isolation of a highly specific ligand for the  $\alpha_5\beta_1$  integrin from a phage display library. *J. Cell Biol.* 124:373-380.

35. Kraft, S., Diefenbach, B., Mehta, R., Jonczyk, A., Luckenbach, G. A., and Goodman, S. L. Definition of an unexpected ligand recognition motif for  $\alpha\beta 6$  integrin. *Journal of Biological Chemistry* 274, 1979-1985. 1999.
36. Landowski, T. H., E. A. Dratz, and J. R. Starkey. 1995. Studies of the structure of the metastasis-associated 67 kDa laminin binding protein: fatty acid acylation and evidence supporting dimerization of the 32 kDa gene product to form the mature protein. *Biochem.* 34:11276-11287.
37. Landowski, T. H., S. Uthayakumar, and J. R. Starkey. 1995. Control pathways of the 67 kDa laminin binding protein: surface expression and activity of a new ligand binding domain. *Clin.Exp.Metastasis* 13:357-372.
38. Maeda, M., Y. Izuno, K. Kawasaki, Y. Kaneda, Y. Mu, Y. Tsutsumi, S. Nakagawa, and T. Mayumi. 1998. Amino acids and peptides. XXXI. Preparation of analogs of the laminin-related peptide YIGSR and their inhibitory effect on experimental metastasis. *Chem.Pharm.Bull.(Tokyo)* 46:347-350.
39. Maeda, M., K. Kawasaki, Y. Mu, H. Kamada, Y. Tsutsumi, T. J. Smith, and T. Mayumi. 1998. Amino acids and peptides - XXXIII. A bifunctional poly(ethylene glycol) hybrid of laminin-related peptides. *Biochem.Biophys.Res.Commun.* 248:485-489.
40. Maeda, T., K. Titani, and K. Sekiguchi. 1994. Cell-adhesive activity and receptor-binding specificity of the laminin-derived YIGSR sequence grafted onto *Staphylococcal* protein A. *J.Biochem.* 115:182-189.
41. Magnifico, A., E. Tagliabue, S. Butó, E. Ardini, V. Castronovo, M. I. Colnaghi, and S. Ménard. 1996. Peptide G, containing the binding site of the 67-kDa laminin receptor, increases and stabilizes laminin binding to cancer cells. *J.Biol.Chem.* 271:31179-31184.
42. Massia, S. P., S. S. Rao, and J. A. Hubbell. 1993. Covalently immobilized laminin peptide Tyr-Ile-Gly-Ser- Arg (YIGSR) supports cell spreading and co-localization of the 67- kilodalton laminin receptor with alpha-actinin and vinculin. *J.Biol.Chem.* 268:8053-8059.

43. Ménard, S., V. Castronovo, E. Tagliabue, and M. E. Sobel. 1997. New insights into the metastasis-associated 67 kD laminin receptor. *J.Cell Biochem.* 67:155-165.
44. Nomizu, M., K. Yamamura, H. K. Kleinman, and Y. Yamada. 1993. Multimeric forms of Tyr-Ile-Gly-Ser-Arg (YIGSR) peptide enhance the inhibition of tumor growth and metastasis. *Cancer Res.* 53:3459-3461.
45. O, N. K. T., W. F. DeGrado, S. A. Mousa, N. Ramachandran, and R. H. Hoess. 1994. Identification of recognition sequences of adhesion molecules using phage display technology. *Methods Enzymol.* 245:370-386.
46. Parthasarathy, N., L. F. Gotow, J. D. Bottoms, T. E. Kute, W. D. Wagner, and B. Mulloy. 1998. Oligosaccharide sequence of human breast cancer cell heparan sulfate with high affinity for laminin. *J.Biol.Chem.* 273:21111-21114.
47. Pasqualini, R., E. Koivunen, and E. Ruoslahti. 1995. A peptide isolated from phage display libraries is a structural and functional mimic of an RGD-binding site on integrins. *J.Cell Biol.* 130:1189-1196.
48. Pei, D. P., Y. Han, D. Narayan, D. Herz, and T. S. Ravikumar. 1996. Expression of 32-kDa laminin-binding protein mRNA in colon cancer tissues. *J.Surg.Res.* 61:120-126.
49. Poschl, E., U. Mayer, J. Stetefeld, R. Baumgartner, T. A. Holak, R. Huber, and R. Timpl. 1996. Site-directed mutagenesis and structural interpretation of the nidogen binding site of the laminin gamma1 chain. *EMBO J.* 15:5154-5159.
50. Poste, G., J. Doll, I. R. Hart, and I. J. Fidler. 1980. In vitro selection of murine B16 melanoma variants with enhanced tissue-invasive properties. *Cancer Res.* 40:1636-1640.
51. Rao, C. N., V. Castronovo, M. C. Schmitt, U. M. Wewer, A. P. Claysmith, L. A. Liotta, and M. E. Sobel. 1989. Evidence for a precursor of the high-affinity metastasis-associated murine laminin receptor. *Biochem.* 28:7476-7486.
52. Rao, C. N., I. M. Margulies, T. S. Tralka, V. P. Terranova, J. A. Madri, and L. A.

- Liotta. 1982. Isolation of a subunit of laminin and its role in molecular structure and tumor cell attachment. *J.Biol.Chem.* 257:9740-9744.
53. Robertson, N. P., J. R. Starkey, S. Hamner, and G. G. Meadows. 1989. Tumor Cell Invasion of Three-dimensional Matrices of Defined Composition: Evidence for a Specific Role for Heparan Sulfate in Rodent Cell Lines. *Cancer Res.* 49:1816-1823.
  54. Romanov, V., M. E. Sobel, P. Pinto da Silva, S. Menard, and V. Castronovo. 1994. Cell localization and redistribution of the 67 kD laminin receptor and alpha 6 beta 1 integrin subunits in response to laminin stimulation: an immunogold electron microscopy study. *Cell Adhes.Commun.* 2:201-209.
  55. Ryan, S. T., G. Chi-Rosso, L. L. C. Bonmycastle, J. K. Scott, V. Koteliansky, S. Pollard, and P. J. Gotwals. 1998. Epitope mapping of a function-blocking  $\beta 1$  integrin antibody by phage display. *Cell Adhes.Commun.* 5:75-82.
  56. Sakamoto, N., M. Iwahana, N. G. Tanaka, and Y. Osada. 1991. Inhibition of Angiogenesis and Tumor Growth by a Synthetic Laminin Peptide, CDPGYIGSR-NH<sub>2</sub>. *Cancer Res.* 51:903-906.
  57. Sanjuán, X., P. L. Fernández, R. Miquel, J. Muñoz, V. Castronovo, S. Ménard, A. Palacín, A. Cardesa, and E. Campo. 1996. Overexpression of the 67-kD laminin receptor correlates with tumour progression in human colorectal carcinoma. *J.Pathol.* 179:376-380.
  58. Satoh, K., K. Narumi, M. Isemura, T. Sakai, T. Abe, K. Matsushima, K. Okuda, and M. Motomiya. 1992. Increased expression of the 67kDa-laminin receptor gene in human small cell lung cancer. *Biochem.Biophys.Res.Commun.* 182:746-752.
  59. Scott, J. K. and G. P. Smith. 1990. Searching for peptide ligands with an epitope library. *Science* 249:386-390.
  60. Shaw, L. M. and A. M. Mercurio. 1994. Regulation of cellular interactions with laminin by integrin cytoplasmic domains: the A and B structural variants of the alpha 6 beta 1 integrin differentially modulate the adhesive strength, morphology, and migration of macrophages. *Mol.Biol.Cell* 5:679-690.

61. Smith, G. P. and J. K. Scott. 1993. Libraries of peptides and proteins displayed on filamentous phage. *Methods Enzymol.* 217:228-57:228-257.
62. Starkey, J. R., S. Dai, and E. A. Dratz. 1998. Sidechain and backbone requirements for anti-invasive activity of laminin peptide 11. *Biochim.Biophys.Acta Protein Struct.Mol.Enzymol.* 1429:187-207.
63. Starkey, J. R., S. Uthayakumar, and D. L. Berglund. 1999. Cell surface and substrate distribution of the 67-kDa laminin- binding protein determined by using a ligand photoaffinity probe. *Cytometry* 35:37-47.
64. Stephen, C. W., Helminen, P., and Lane, D. P. Characterisation of epitopes on human p53 using phage-displayed peptide libraries: Insights into antibody-peptide interactions. *J.Mol.Biol.* 248, 58-78. 1995.
65. Sung, U. 1997. Heparin binding of laminin: contribution of the triple helix in the rod domain to the formation of cryptic and active sites in the globular domain. *Mol.Cells* 7:272-277.
66. Tanaka, M., K. Narumi, M. Isemura, M. Abe, Y. Sato, T. Abe, Y. Saijo, T. Nukiwa, and K. Satoh. 2000. Expression of the 37-kDa laminin binding protein in murine lung tumor cell correlates with tumor angiogenesis. *Cancer Lett.* 153:161-168.
67. Tarassishin, L., Szawlowski, P., McLay, J., Kidd, A. H., and Russell, W. C. Adenovirus core protein VII displays a linear epitope conserved in a range of human adenoviruses. *J.Gen.Virol.* 80, 47-50. 1999.
68. Van den Brûle, F. A., A. Berchuck, R. C. Bast, F. T. Liu, C. Gillet, M. E. Sobel, and V. Castronovo. 1994. Differential expression of the 67-kD laminin receptor and 31-kD human laminin-binding protein in human ovarian carcinomas. *Eur.J.Cancer* 30A:1096-1099.
69. van Zonneveld, A. J., B. M. van den Berg, M. van Meijer, and H. Pannekoek. 1995. Identification of functional interaction sites on proteins using bacteriophage-displayed random epitope libraries. *Gene* 167:49-52.

70. Viacava, P., A. G. Naccarato, P. Collecchi, S. Menard, V. Castronovo, and G. Bevilacqua. 1997. The spectrum of 67-kD laminin receptor expression in breast carcinoma progression. *J.Pathol.* 182:36-44.
71. Waltregny, D., L. de Leval, S. Menard, J. de Leval, and V. Castronovo. 1997. Independent prognostic value of the 67-kd laminin receptor in human prostate cancer. *J.Natl.Cancer Inst.* 89:1224-1227.
72. Welply, J. K., C. N. Steininger, M. Caparon, M. L. Michener, S. C. Howard, L. E. Pegg, D. M. Meyer, P. A. De Cicchi, C. S. Devine, and G. F. Casperson. 1996. A peptide isolated by phage display binds to ICAM-1 and inhibits binding to LFA-1. *Proteins* 26:262-270.
73. Wewer, U. M., G. Taraboletti, M. E. Sobel, R. Albrechtsen, and L. A. Liotta. 1987. Role of laminin receptor in tumor cell migration. *Cancer Res.* 47:5691-5698.
74. Yoshida, N., Ishii, E., Nomizu, M., Yamada, Y., Mohri, S., Kinukawa, N., Matsuzaki, A., Oshima, K., Hara, T., and Miyazaki, S. The laminin-derived peptide YIGSR (Tyr-Ile-Gly-Ser-Arg) inhibits human pre-B leukaemic cell growth and dissemination to organs in SCID mice. *British Journal of Cancer* 80, 1898-1904. 1999.
75. Yow, H. K., J. M. Wong, H. S. Chen, C. G. Lee, S. Davis, G. D. Steele, Jr., and L. B. Chen. 1988. Increased mRNA expression of a laminin-binding protein in human colon carcinoma: complete sequence of a full-length cDNA encoding the protein [published erratum appears in *Proc Natl Acad Sci U S A* 1989 Sep;86(18):7032]. *Proc.Natl.Acad.Sci.U.S.A.* 85:6394-6398.
76. Zhao, M., H. K. Kleinman, and M. Mokotoff. 1994. Synthetic laminin-like peptides and pseudopeptides as potential antimetastatic agents. *J.Med.Chem.* 37:3383-3388.

## CHAPTER 3

## EVIDENCE FOR SULFHYDRYLOXIDASE ACTIVITY OF LBP

Introduction

This chapter will discuss the findings that implicate LBP in the modulation of the redox status of thiols and disulfides in substrate proteins and peptides. This activity places LBP in a functional relationship with a well characterized family of dithiol/sulfhydryl oxidoreductases. The best studied subset of this diverse family encompasses the proteins with homology to thioredoxin, of which eukaryotic protein disulfide isomerase is a classical example. LBP is not a member of this family. It has no sequence similarity with these proteins and lacks the organization of the active site characteristic of this family. However, LBP possesses some activities similar to PDI and related proteins. Therefore, this introduction will focus primarily on the biology and chemistry of proteins in the PDI family, for lack of closer analogs. While LBP and PDI are probably very different in many respects, thorough description of the biochemistry of PDI and related proteins is certainly needed to understand the biochemistry of LBP. The term "PDI" is used interchangeably to define a particular protein of endoplasmic reticulum (for instance, PDI1, EC 5.3.4.1), as well as any protein which performs disulfide isomerization, depending on the context.

### Basic mechanism of PDI function

Role of active site cysteines Maintenance of the redox state of protein thiols is instrumental to cell viability. Disulfide bonds can be viewed as natural constraints of the conformational entropy of a polypeptide, which help to maintain its conformation and to define its active tertiary and quaternary structure. Disulfide formation can happen concomitantly with polypeptide synthesis, as well as post-translationally (32). Disulfide formation, however, is a statistical process, guided in part by the thermodynamic viability of the resulting structure. Incorrect disulfide formation does occur, and it takes a catalyst-dependent rearrangement of disulfides to reach the final active conformation. For instance, in RNase or hirudin, early folding intermediates are dominated by random disulfides, which need to be rearranged in order for maturation to proceed (19) (57) (14). Oxidative folding and rearrangement of incorrectly formed disulfides is the primary function of a class of enzymes collectively called thiol/disulfide oxidoreductases. This family includes protein disulfide isomerase (PDI), thioredoxin, DsbA, B, C, D, G and many other enzymes. The catalytic properties of the enzymes of this family may be very different. For instance, thioredoxin has a tendency to reduce disulfide bonds under physiological conditions, while DsbA of *E. coli*, on the contrary, has a very strong oxidative potential. Eukaryotic PDI performs both disulfide bond breaking and making equally well, depending on the substrate it is presented with. Most of these enzymes are characterized by the presence of a CXXC motif in the active site. The two cysteines are involved in catalysis of disulfide bond formation, reduction and rearrangement (76). The classical mammalian PDI of the endoplasmic reticulum consists of two domains with

similar tertiary structure, each of which contains the CGHC active site. These domains, however, are non-equivalent. It was shown that C-terminal active site possesses a lower  $k_{cat}$  than the N-terminal one ( $0.24 \text{ min}^{-1}$  vs.  $0.72 \text{ min}^{-1}$ ), and its inactivation has no effect on the  $k_{cat}$  of the protein. It was also shown that N-terminal active site has lower substrate (reduced and denatured RNaseA) binding affinity ( $K_m$  of  $29 \mu\text{M}$  vs.  $7.1 \mu\text{M}$  for the C-terminal domain), and its loss does not affect the overall  $K_m$  of the protein (65). Notably, a mutant with all four active cysteines removed still displays low, but detectable PDI activity (0.5% of that of the wild-type). Redox properties of CXXC active sites in PDI and related proteins are determined in large part by the internal residues flanked by the two active cysteines. Consistent with this notion, the oxidative potential of DsbA, a potent dithiol oxidizer of *E. coli*, depends in large part on the two residues flanked by cysteines in the active site. Replacement of the CPHC active site sequence with CPPC results in a change of oxidation constant (measured as the equilibrium constant in the reaction of reduction of glutathione) from 0.12 mM to 0.2M, that is, effectively reversing the oxidative potential (35). Generally, the dipeptide sequence between the cysteines in the active site determines the  $K_{ox}$  of the protein in this family. Replacement of this dipeptide in a protein with a dipeptide from another protein in this family results in a redox potential for the chimera close to that of the protein from which the dipeptide sequence originated (64). In the current model, the intermediate residues within the active site influence the pKa of the N-terminal cysteine, which is involved in the formation of intermolecular disulfide intermediates with the substrate (see below). The pKa of this cysteine correlates well with the redox potential of the protein (35).

It was shown that thioredoxin, whose active sites have the CGPC configuration, possesses a lower redox potential (-270mV) than PDI (CGHC, -190mV) (63) (58). Replacement of proline with histidine in the active site of *E. coli* thioredoxin (P34H), making it mimic the sequence of active sites of PDI, results in an increase of the redox potential by approximately 35 mV, which accounts for about half of the difference in redox potentials between thioredoxin and PDI. Similarly, the P34H mutation of thioredoxin results in substantial (10-fold) increase of dithioloxidase activity, accounting for about half of the difference in such activity between thioredoxin and PDI (64). Interestingly, this mutation also confers disulfide isomerization activity, which is almost non-detectable in wild type thioredoxin. Therefore, it is apparent that the catalytic properties of CXXC-containing enzymes depend, in part, on the sequence of the active site, and in part on other factors, such as protein conformation, substrate binding affinity and microenvironment in the vicinity of the active site. For example, it has been demonstrated that replacement of a distant cis-proline P151 in DsbA, which has its active site at residues 30-33, by alanine, results in more than 50% loss of activity in an in vivo oxidative folding assay (13). The absence of the cis backbone configuration changes the microenvironment of the active site and affects its conformation, although does not affect the pKa of the active site C30.

Studies of some proteins of the PDI family involved in oxidative folding provide a valuable insight into the roles of the two CXXC cysteines in catalysis. PDI, a resident protein of endoplasmic reticulum plays a role similar to that performed by DsbA in the periplasm of *E. coli*, namely, assisting in oxidative folding of newly synthesized proteins.

The N- and C- terminal cysteines in the active site appear to play different roles in catalysis. Replacement of the N-terminal cysteine by serine in PDI destroys both sulfhydryl oxidase and disulfide rearrangement activities in the absence of a glutathione redox buffer, while removal of the C-terminal cysteine selectively destroys the ability of PDI to catalyze *de novo* disulfide formation, while preserving low, but measurable isomerase activity (approximately 10% of that of the wild-type) (107).

Mechanism of catalysis Based on the current evidence (108), it is most likely that PDI does not guide a protein into a specific structure. Rather, it catalyzes the formation of intramolecular disulfides and rearrangement of "incorrect" disulfides by scanning for them, breaking, isomerizing, and repeating this cycle until the correct conformation is found. Most likely, the formation of "correct" disulfides is gauged by the reactivity of substrate disulfide with a substrate cysteine sulfhydryl. The isomerization begins by attack of the deprotonated thiol of reduced PDI on the disulfide of the substrate with the formation of intermolecular mixed disulfide and a deprotonated thiol within the substrate. This step is reversible. In the next step, the substrate thiol should find a disulfide within the same molecule of substrate and react with it, forming a new disulfide within the substrate and releasing reduced PDI. Therefore, release of PDI from the intermolecular complex is entirely dependent on the reactivity of the substrate thiol formed in the first step of the reaction. If the formed substrate thiol is slow to react for reasons of thermodynamic or spatial (conformational) hindrance, the PDI would be trapped in a covalent complex with the misfolded substrate. The second, C-terminal

cysteine in the active site serves to rescue the PDI from such complexes by donating its proton to the substrate, thus breaking the intermolecular bond and releasing oxidized PDI and partially reduced substrate. The C-terminal cysteine can be viewed as a molecular clock, which provides a certain time period for the propagation of a disulfide rearrangement within the substrate and then rescues the oxidized PDI if such a rearrangement does not succeed (108). Conversely, in case of oxidation catalysis, the same general mechanism applies, except that in this case thiol of the substrate attacks the active site disulfide in PDI, forming a covalent intermolecular intermediate with the N-terminal cysteine of the PDI. The C-terminal cysteine then accepts the proton from the substrate and transfers it to the N-terminal cysteine, thus releasing reduced PDI from the complex. Consistent with this model, addition of glutathione redox buffer rescues the activity of PDI mutants that have a C-terminal active cysteine replaced by a serine (109) (108).

Structural organization of the catalytic domain All known proteins that modulate the redox status of thiols and disulfides through the classical CXXC active site possess the same structural motif, referred to as a thioredoxin fold. This fold, represented in figure 3.1, is characterized by at least four (sometimes five) beta-strands, all but one of which are parallel, and at least three (sometimes four) alpha helices, two of which are located on one side of the beta-sheet, and another on the opposite side, the latter roughly perpendicular to the direction of the beta-strands (68).

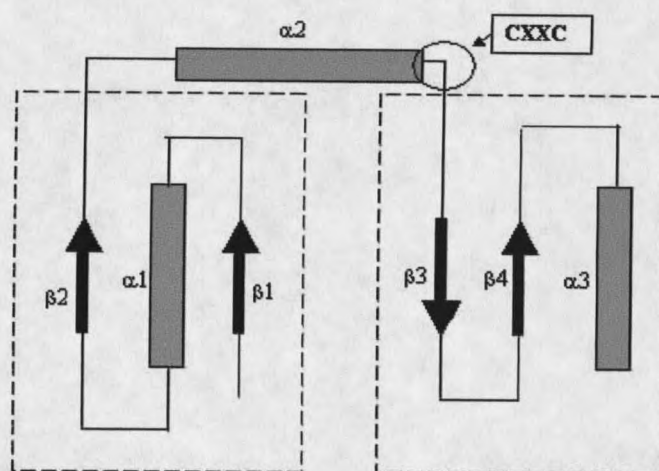


Figure 3.1. Thioredoxin fold. Adapted from (68).

The fold may be quite variable, with additions of intervening elements of secondary structure and additional domains. The active site is located at the C-terminal end of the connecting helix 2. In most cases, one cysteine is located within the helix, while the other is in the adjacent flexible loop. This fold is conserved in all members of thioredoxin family, including thioredoxin (49) (39), glutaredoxin (93), mammalian PDI (52) (51), glutathione S-transferase (8), glutathione peroxidase (60) (26), thioredoxin reductase (106), DsbA (69), DsbC (70) and other enzymes. Mammalian PDI is a homodimer of two 55 kDa subunits, each of which has an "a-a'-b-b'-c" domain organization. Only the "a" and "a'" domains contain the active site. However, "b" domains are structurally very similar to the "a" domains, although they are catalytically inactive (53). Some dithiol/disulfide oxidoreductases do not possess the thioredoxin fold

of the catalytic domain. Structures of these proteins may be quite variable, depending on the presence of cofactor and the arrangement of catalytically active cysteines.

Substrate recognition It is not immediately clear how thioredoxin and related enzymes recognize their respective targets. Experiments in which peptides and misfolded proteins were chemically crosslinked to recombinant PDI consisting of various combinations of a, b, a', b' and c domains, demonstrated that b' domain of PDI is indispensable for substrate binding. This domain is sufficient for binding of small peptides, such as D-somatostatin, but binding of larger substrates, such as scrambled RNaseA or bovine pancreatic trypsin inhibitor fragment 4-31 requires the presence of other domains, especially a' (56). As was mentioned before, "b" domains possess the same thioredoxin fold as do "a" domains, but lack the CXXC active site. While the binding of peptides by the b' domain is independent of the presence of cysteines in the substrate or in the b' domain itself (55), cysteine-containing peptides bind to the PDI more avidly than cysteine-less ones. This indicates the formation of intermolecular disulfide intermediates with the involvement of catalytic a and a' domains. No complete structure of the mammalian PDI is available at this time, although structures of some individual domains have been solved. It is therefore unknown how catalytic and non-catalytic domains are arranged in space to provide for synchronized binding and catalysis. Some clue to the topology of the binding site of proteins with a thioredoxin fold can be derived from the studies of thioredoxin itself. A recent X-ray structure of thioredoxin in complex with the substrate peptide shows the binding of the substrate in

the hydrophobic cleft on the surface of human thioredoxin delineated by the active-site loop, helices alpha 2, alpha 3 and alpha 4, and strands beta 3 and beta 4 (85) (Figure 3.2).

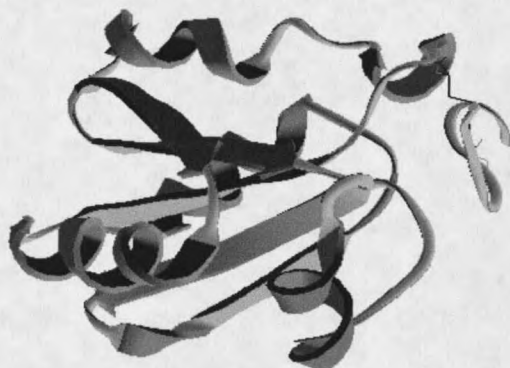


Figure 3.2. Mixed disulfide intermediate between a thioredoxin single cysteine mutant and a substrate peptide. Genbank accession number 1MDI, (85).

Glycine 91 is located on the loop connecting strand 4 and helix 3 and faces into the binding cleft. Interestingly, substitution of Gly91 for aspartic acid abolishes the interaction between *E. coli* thioredoxin and T7 DNA polymerase, indicating that this region is a universal binding site for the large array of thioredoxin's substrates (46). Comparison of reduced and oxidized forms of *E. coli* (25) and human thioredoxins (111) reveals very subtle differences in the conformation between the two states. These differences are mostly evident in the immediate proximity of the active site, and propagate further through the structure, resulting in a slight change in orientation of alpha helices 2 and 4 with respect to the beta sheet (84). The cleft between the active site and

two opposing loops is increased by approximately 10% in the oxidized state compared to the reduced state. Only the reduced form of thioredoxin or C→S mutants are able to bind T7 DNA polymerase, but not oxidized thioredoxin. This implies that, while cysteines are not immediately involved in the interaction with the core polymerase, the conformational change in the binding cleft between reduced and oxidized states, however subtle, is substantial enough to allow discrimination of substrates. Since the experimental evidence for conformational change during catalysis and substrate recognition exists only for thioredoxin, it is difficult to judge whether the same mechanism exists for all members of the family, or is specific for thioredoxin only. However, taking into account conservation of tertiary structure and active site configuration, it seems possible to cautiously extrapolate the concept of substrate discrimination by thioredoxin to other members of this family.

Chaperone and antichaperone activities of PDI PDI does not only forms and rearranges disulfides, but also acts as a chaperone *in vivo* in the endoplasmic reticulum and *in vitro* in cell-free assays. It has been shown that PDI in the ER of intestinal epithelial cells works as a redox-dependent chaperone to unfold the cholera toxin (CT) A1 subunit, after it has been released from the accompanying B subunits. In the reduced state PDI binds the CT A1, trapping it in the ER, while in oxidized state it releases it, allowing the retrograde transport to cytosol, where the biological target of CT A1 is localized (104). PDI also functions as a quality control chaperone in the endoplasmic

reticulum, binding and discriminating properly folded secretory proteins from misfolded ones, and directing the latter to retrograde translocation to the cytoplasm, while the former are directed to the Golgi (33). In addition to chaperone activity, under certain conditions *in vitro*, PDI catalyses the formation of large insoluble disulfide-crosslinked complexes which include terminally misfolded substrate protein and PDI. This behavior is referred to as antichaperone activity and depends on the relative concentrations of PDI and the substrate protein (82). Interestingly, another chaperone of the ER, BiP, also displays the antichaperone activity if presented with excessive amount of denatured lysozyme *in vitro* and is incorporated into insoluble aggregates in competition with PDI (81). Unlike PDI, which is a redox-dependent chaperone, the chaperone activity of BiP is driven by the hydrolysis of ATP. While chaperone/disulfide isomerase activity of PDI involves intact active site cysteines, antichaperone activity does not involve formation of mixed disulfide intermediates, since a mutant PDI variant with all four active site cysteines mutated exhibits the same antichaperone activity as the wild-type (83). Antichaperone activity is manifested under certain conditions, namely, at concentrations of substrate (reduced and denatured lysozyme) about 10 times higher than the concentration of PDI on a molar basis. Normal chaperone activity is exhibited when lower or higher substrate:PDI ratios are utilized (82). This "schizophrenic" (82) behavior of PDI explains a number of earlier observations, such as the necessity for a relatively high concentration of PDI in the ER (on the order of mM) and transient accumulation of disulfide-crosslinked aggregates in the ER during expression of disulfide-rich proteins (21) (67). This may also represent a mechanism of quality control, which results in ER

retention of misfolded secretory proteins. It is interesting that aggregates formed *in vitro* are very stable and need to be treated with urea to dissociate, while similar aggregates formed in the ER *in vivo* (in response to DTT treatment of cells) can be salvaged and correctly folded when DTT is washed out (102) (10).

#### Other functions of PDI-related proteins

Modulation of cell-ECM interactions PDI not only acts as an ER chaperone, but is also secreted into the extracellular space and associates with the cell membrane. It has been shown that cell surface expressed PDI is involved in the disulfide exchange in the  $\text{Ca}^{2+}$  binding loops and C-terminal globular domain of thrombospondin. This disulfide shuffling leads to a structural rearrangement in the thrombospondin molecule that results in the exposure of a cryptic RGD domain. This sequence is the recognition site for a number of integrin receptors. Treatment of isolated thrombospondin with purified human PDI results in increased RGD-dependent adhesion of bovine aortic endothelial cells to thrombospondin (44). PDI-catalyzed rearrangement of disulfides in thrombospondin-1 also alters its binding to neutrophil cathepsin D (45).

PDI is expressed on the surface of both resting (27) and activated (15) platelets and is released in the extracellular medium by platelets upon activation (17). It is suggested that plasma PDI, which is immunologically identical to platelet PDI, is involved in the formation of disulfide-crosslinked vitronectin-thrombin-antithrombin complexes (29). PDI is also involved in platelet aggregation by acting on the disulfides

of GPIIa/IIIb fibrinogen receptor complex, converting it into a fibrinogen-binding state (28).

Shedding of surface-expressed proteins Surface expressed PDIs may also be involved in the regulation of shedding of other proteins into the extracellular medium. A PDI expressed on human leukocytes was implicated in the regulation of proteolytic L-selectin shedding. Treatment of cells with an arsenic modifier of proximal thiols or bacitracin, a known inhibitor of PDI, induces L-selectin shedding by leukocytes (5). Treatment with thiol oxidizing agents leads to the same effect. Inhibition of shedding increases leukocyte recruitment to the inflamed tissue (36). Cell surface PDI is also apparently involved in the release of the thyrotropin receptor ectodomain from the surface of thyroid follicle cells. The mature surface receptor consists of two subunits, linked by a disulfide, only one of which ( $\beta$ ) is membrane-spanning. The release of the  $\alpha$  subunit is inhibited by bacitracin and anti-PDI antibodies (18) (74).

Nitrositol transfer In addition to platelets and thyroid endothelial cells, PDI has been found on the surface of several other cell types, including pancreatic exocrine cells (which also shed PDI into acinar lumen) (2), B lymphocytes (59) and magakaryocytes (16). Cell surface – expressed PDI has been implicated by several groups in the catalysis of transmembrane transfer of nitric oxide (NO). NO is a free radical signal molecule with a wide range of physiological effects, including regulation of platelet function, blood pressure control, and lymphocyte activation. One of the primary targets of NO is soluble

guanylyl cyclase, which is activated by NO. For a long time it was thought that NO penetrates the plasma membrane of effector cells by passive diffusion. However, it must first be released from the S-nitrositols, a diverse set of carrier complexes, which serve as a serum reservoir of NO. Recent data implicate PDI in the release of NO from such complexes. Partial inhibition of PDI surface expression by overexpression of antisense PDI cDNA in human erythroleukemia cells results in a 2.5-fold decrease in the synthesis of cGMP, but not cAMP, indicating a decrease of NO concentration within the cell. PDI is also able to abstract NO from S-nitrositols and bind NO in the molar ratio PDI:NO=1:2. PDI is also able to catalyze the reaction of transnitrosylation and so attach NO to free thiols or hydroxyls in other biological molecules (114). It has also been shown, using a fluorescent probe, that PDI on the surface of lung fibroblasts and umbilical vein endothelial cells catalyses the denitrosylation of BSA-NO (one of the common NO carrier complexes in serum), and that NO is transferred inside the cell in the form of  $N_2O_3$ , where it nitrosylates cytoplasmic targets (86). Therefore, PDI or related proteins on the cell surface do not only modulate the thiol redox state, but also are involved in other physiological responses, such as regulation of NO signaling.

Transcription and replication control      Recently, a chloroplast PDI was implicated in the regulation of gene expression. In this system, an excited electron from photosystem II is transferred to ferredoxin and to ferredoxin/thioredoxin reductase, which then reduces chloroplast PDI. This, in turn, reduces a disulfide pair in the transcription factor cPABP, thereby activating it. cPABP specifically activates the *psbA* gene, which

codes for the photosynthetic reaction center protein D1. In the absence of illumination, cPDI is phosphorylated, which leads to "locking in" the oxidized state and reversal of cPABP activation. (54) (24).

Another thiol/disulfide oxidoreductase, thioredoxin, is involved in replication of T7 DNA. *E. coli* thioredoxin associates with T7 DNA polymerase, conferring high processivity to this otherwise inactive enzyme. Only reduced thioredoxin acts a processivity factor; oxidized thioredoxin or thioredoxin with alkylated cysteines are defective in association with the T7 DNA polymerase (46) (1). Both cysteines, however, can be mutated without loss of this function, which indicates that disulfide formation is not involved in the maintenance of processivity (46). Mutation complementation analysis showed that thioredoxin binds the putative polymerization domain and the putative 3'-to-5' exonucleolytic domain of T7 DNA polymerase (37). Insertion of the thioredoxin binding domain of T7 DNA polymerase into *E. coli* DNA polymerase I, which possesses very low processivity, confers processivity comparable to that of T7 DNA polymerase (4). It is unclear what the molecular mechanism of thioredoxin function in the polymerase complex is. Thioredoxin and T7 DNA polymerase associate in 1:1 stoichiometric ratio, and one and probably both active site cysteines of thioredoxin stay reduced and solvent-exposed, since their alkylation is possible within the complex. Polymerase DNA substrates alter the accessibility of thioredoxin sulfhydryls, making them more protected from alkylation (1). So far, this is the only reported case of sulfhydryl/thiol modulators being intimately involved in DNA synthesis.

Other members of the family. FAD-containing proteins

Some thiol/disulfide oxidoreductases perform catalysis in a different manner from PDI, thioredoxin or Dsb proteins. These enzymes carry a FAD moiety in the active site and belong to the pyridine nucleotide-disulfide oxidoreductase family of enzymes (112). The well characterized members of this family include lipoamide dehydrogenase (EC.1.8.1.4), glutathione reductase (EC. 1.6.4.2), thioredoxin reductase (EC. 1.6.4.5), cystine reductase (EC. 1.6.4.1), sulfhydryl oxidase from *Aspergillus niger*. With a few exceptions (including sulfhydryl oxidase), all enzymes in this family catalyze electron transfer between NAD(P)(H) and disulfide/dithiol. Some of enzymes in this class lack the canonical CXXC motif seen in "classic" thiol/disulfide oxidoreductases, but all possess two active cysteine residues which are involved in catalysis. Some proteins that utilize FAD as a cofactor, however, have the CXXC motif with redox-active cysteines, involved in catalysis (42) (40) (43). These enzymes include a sulfhydryl oxidase isolated from the hen egg white of and numerous homologues of quiescin Q6, a protein involved in growth regulation and fibroblast quiescence in organisms as diverse as humans and *C. elegans*. Sulfhydryl oxidase of hen egg white does not utilize NAD(P)(H) as a source of redox equivalents in catalysis. Oxidation of DTT by this enzyme is accompanied by generation of hydrogen peroxide in aerobic solution, suggesting oxygen as an acceptor of protons (41).

Dithiol-disulfide oxidoreductases that lack the CXXC motif

Some proteins that demonstrate protein disulfide isomerase activity lack the canonical CXXC motif and do not utilize FAD as a cofactor. An example of such type of thiol/disulfide oxidoreductases is elongation factor EF-Tu of *E. coli* (87). This protein is active in oxidative refolding of reduced and denatured RNaseA, refolding of scrambled oxidized denatured RNaseA, and in catalyzing reduction of insulin in the presence of DTT. However, EF-Tu does not have a canonical CXXC motif. Instead, it has three cysteine residues, one of which is solvent-exposed, the second of which can be titrated in the absence of GTP (EF-Tu is a GTPase), and the third of which is buried. The biological relevance of the PDI activities demonstrated *in vitro* remains unclear. Another example is the yeast protein Eug1p. This protein is homologous to the yeast PDI and appears to have the same domain organization (100). But the active site sequence CXXC of PDI is replaced by CXXS in Eug1p. However, mutants of Eug1p, with both CXXS active sites replaced by CXXC, demonstrate much higher activity in RNase oxidation and disulfide isomerization than the wild-type Eug1p (78). The latter is active in these assays, but not nearly as active as the CXXS→CXXC mutants. The wild-type protein is inactive in catalysis of insulin reduction. As can be predicted from the basic mechanism of catalysis by a thioredoxin-like PDI, catalysis only requires the more N-terminal cysteine, while the second cysteine is not required for disulfide isomerization, especially in the presence of glutathione redox buffer. PDI mutants with CGHS active sites retain about half of the disulfide isomerization activity of the wild-type enzyme, but are almost devoid of the dithiol oxidase activity. In addition, such mutants tend to get trapped in intermolecular

disulfide complexes with the substrate (109). Sulfhydryl oxidation, however, requires the presence of both active site cysteines in PDI, at least in the absence of oxidized form of glutathione, GSSG. Also, in case of *E. coli* protein DsbA, a potent sulfhydryl oxidase, the C-terminal active site cysteine is dispensable for oxidation of DTT and protein substrates in the presence of GSSG. About half of the activity of the wild-type DsbA is retained by these mutants (113). The two proteins that lack the CXXC configuration of the active site (EF-Tu and Eug1p), are active in the oxidation of the reduced RNaseA and disulfide rearrangement in the presence of GSSG. It is not clear whether the catalysis by these enzymes would occur without GSSG. This would shed light on the mechanism of catalysis, since if two cysteines are involved, sulfhydryl oxidation catalysis is likely to be observed, even in the absence of GSSG.

### Materials and methods

#### RNase refolding assays

Denatured and reduced RNaseA (drRNaseA) was prepared as described in (12) (79). Bovine pancreatic RNaseA (Boehringer Mannheim-Roche) was dissolved in 3 mL of water at 20 mg/mL and dialyzed against 250 mL of 6M Guanidinium chloride/0.15M DTT/0.1M Tris-HCl pH 8.6 overnight at room temperature. Reduced and denatured RNaseA (rdRNaseA) was then purified by gel filtration on Sephadex G25 equilibrated in 0.1% acetic acid. Column parameters were: height: 30 cm, bed volume: 75 mL, flow rate:

7 ml/min. All solutions were treated with diethylpyrocarbonate (DEPC) and autoclaved, all glassware was autoclaved and baked at 200°C overnight to minimize RNase contamination. Purified rdRNaseA was lyophilized, dissolved in degassed 0.1% acetic acid and the solution was sparged with argon. rdRNaseA was aliquoted and stored at -80°C. The RNaseA renaturation assays were performed according to the method of Crook et al. (20) with modifications (12). Briefly, 30 µM rdRNaseA was diluted into 0.1M Tris-HCl/1mM EDTA pH 7.4 and mixed with the protein being tested for the chaperone activity. Refolding mixes were incubated at room temperature. At time points indicated, aliquots of the refolding mixture were tested for RNaseA activity by mixing with 0.1 mg/mL 2':3'cCMP (Sigma) in 0.1M Tris-HCl/0.1M NaCl pH 7.5. RNaseA activity was determined by the rate of conversion of 2':3'cCMP into 2'CMP as monitored by the increase of absorbance at 284 nm.

#### Insulin reduction assays

The ability of LBP to catalyze the DTT-driven reduction of insulin was tested according to the procedure of Holmgren (38). Proteins being tested for this activity were mixed with 0.13 M human recombinant insulin (Boehringer Mannheim/Roche) in 50 mM potassium phosphate pH 7.4 in the presence of 0.3 mM DTT. Insulin reduction was determined by precipitation of separated B chains turbidimetrically at 640 nm.

### LBP cloning and expression

Hamster LBP cDNA was a gift of Dr. J. H. Strauss. The coding sequence was amplified using the following primers containing 5' extensions with incorporated BamHI restriction endonuclease recognition sequences:

LBP-BamHI-FOR-2: 5'-TTAGGATCCCATGTCCGGAGCCCTTG

LBP-BamHI-REV: 5'-TTAGGATCCAGTCAGGACCACTCAGTGGTG

Amplification reactions were carried out in 50  $\mu$ l volumes with: 1X GeneAmp PCR buffer I (PE Applied Biosystems), 1.5 mM MgCl<sub>2</sub>, 100 nM primers, 200  $\mu$ M dNTPs, 2.5 U Taq polymerase, and 0.1 ng template per reaction. PCR parameters were: 5 min at 94°C, followed by 3 cycles of 1 min at 94°C, 1 min at 40°C, 1 min at 72°C, followed by 27 cycles of 1 min at 94°C, 1 min at 45°C, 1 min at 72°C, followed by 1 cycle of 7 min at 72°C. Amplified product was purified using a PCR purification kit (Qiagen) and treated with BamHI endonuclease (New England Biolabs). pET15b vector (Novagen) was linearized with BamHI and dephosphorylated using calf intestinal alkaline phosphatase (Promega). Linearized dephosphorylated vector was resolved on a 0.8% agarose gel, retrieved from the gel and purified using the PCR purification kit. The LBP PCR product was also purified using the same kit. LBP cDNA insert and vector were mixed in 1:10 molar ratio and ligated overnight at 14°C with 3 Weiss units of T4 DNA ligase (Promega). Ligation products were ethanol precipitated, washed with 70% ethanol, dissolved in 10  $\mu$ L ddH<sub>2</sub>O and transformed into Top10F' *E. coli* (Invitrogen) by electroporation. Transformants were plated on LB agar medium supplemented with 60

$\mu\text{g/mL}$  ampicillin. Plasmid DNA from selected clones was isolated using modified alkaline lysis procedure of Birnboim and Doly (7). Orientation of the insert was determined by SacI restriction digest, and clones that carried the LBP insert in the correct orientation were kept. Plasmid DNA from the selected clones was sequenced using T7 promoter and T7 terminator primers to ensure the integrity of the vector-insert junctions. The expression construct was transformed into the C-41(DE3) expression host (110), which is a modified version of the BL21(DE3)pLysS strain (Invitrogen). Cells were grown overnight in 3 mL cultures and transferred in the morning into 250-500 mL of LB/Ap60 and grown at 37°C with intensive aeration. Expression of LBP was induced at  $\text{OD}_{600}$  0.3-0.6 by addition of isopropyl- $\beta$ -D-thiogalactopyranoside (IPTG) to 1mM final concentration. Pilot expression indicated that maximum expression was achieved at 7 hours after induction (figure 3.3).

#### Purification of recombinant LBP

After expression, cells were harvested by centrifugation, and recombinant LBP (rLBP) was purified under native or denaturing conditions on either Talon (Clontech) or Ni-NTA (Qiagen) metal affinity matrices. Cells were resuspended in 1/10 of the culture volume of the lysis and binding buffer and incubated at room temperature for 30 min. If purification under denaturing conditions was to be performed, cells were treated with lysozyme prior to lysis. Cells were lysed either by sonication or by hydraulic mechanical disruption ("French press"). In the latter case, chromosomal DNA was sheared by

forceful passing of the lysate through a 27-gauge syringe needle. The lysate was centrifuged for 20 min at 10000 rpm in a Sorvall S-34 rotor. Cleared lysate was then mixed with 1-2 mL bed volume of the metal affinity resin and allowed to bind for 1 hour (Talon) or 3 hours to overnight (Ni-NTA) with mixing. The resin was loaded in columns, washed until the absorbance at 280 nm decreased to baseline and then bound proteins were eluted (see table 3.1 for buffer compositions). Eluted material was dialyzed against several changes of cPBS pH 7.5/10 mM  $\beta$ -mercaptoethanol (BME) (2 L) with decreasing concentrations of urea (6M, 4M, 2M, 1M) for at least 48 hours at 4<sup>0</sup>C to allow slow renaturation of the protein and to avoid aggregation. The polyhistidine tag was removed by treatment with biotinylated thrombin (Novagen), allowing 1U of thrombin per 1 mg of protein for 20 hours at room temperature. Biotinylated thrombin was removed by incubation with streptavidin agarose followed by centrifugation. Any recombinant protein that retained the polyhistidine tag was removed by re-purification on the metal affinity column under denaturing conditions. The flow-through fraction was collected and dialyzed as described above. In the final step, BME was dialyzed out against at least 5 changes of cPBS pH 7.5, 2 L each.

Buffer	Talon (immobilized cobalt)		Ni-NTA (immobilized nickel)	
	Native conditions**	Denaturing conditions	Native conditions**	Denaturing conditions
Lysis and binding	50 mM Na <sub>2</sub> HPO <sub>4</sub> 0.5M NaCl pH 8.0	6M GuCl 20mM Na <sub>2</sub> HPO <sub>4</sub> 0.5M NaCl pH 8.0	50mM NaH <sub>2</sub> PO <sub>4</sub> 10mM Tris HCl 300mM NaCl 10mM BME pH 8.0	8M urea 100mM NaH <sub>2</sub> PO <sub>4</sub> 10mM Tris HCl 100mM NaCl*** pH 8.0
Wash	50 mM Na <sub>2</sub> HPO <sub>4</sub> 0.5 M NaCl pH 8.0	8M Urea 20mM Na <sub>2</sub> HPO <sub>4</sub> 0.5 M NaCl pH 7.0	50mM NaH <sub>2</sub> PO <sub>4</sub> 10mM Tris HCl 300mM NaCl 10mM BME pH 8.0	8 M urea 100mM NaH <sub>2</sub> PO <sub>4</sub> 10mM Tris HCl 100 mM NaCl*** pH 8.0
Elution 1*	20mM NaH <sub>2</sub> PO <sub>4</sub> 0.5 M NaCl pH 5.0	8M Urea 20mM NaH <sub>2</sub> PO <sub>4</sub> 0.5 M NaCl pH 5.0	50mM NaH <sub>2</sub> PO <sub>4</sub> 10mM Tris HCl 300mM NaCl 10mM BME 250mM imidazole pH 8.0	8 M urea 100mM NaH <sub>2</sub> PO <sub>4</sub> 10 mM Tris HCl 100 mM NaCl*** pH 4.0
Elution 2*	20mM Na <sub>2</sub> HPO <sub>4</sub> 0.5M NaCl 100mM imidazole pH 8.0	8M Urea 20mM Na <sub>2</sub> HPO <sub>4</sub> 0.5M NaCl 100mM imidazole pH 8.0	N/A	8 M urea 100mM NaH <sub>2</sub> PO <sub>4</sub> 10 mM Tris HCl 100 mM NaCl*** 200 mM imidazole pH 8.0

Table 3.1. Buffers used for rLBP purification.

\*. Elution buffers 1 and 2 were used interchangeably.

\*\*. CHAPS was added in some purifications to decrease aggregation of rLBP

\*\*\*. 500 mM NaCl was used in some purifications. See the Results section.

10 mM  $\beta$ -mercaptoethanol can be added to all buffers to decrease aggregation of rLBP

### Purification of shed LBP

Cells (DG44CHO modified to overexpress  $\alpha 6\beta 1$  integrin, which leads to overexpression of LBP, or MCF7 or NIH OVCAR-3) were grown in 25 cm<sup>2</sup> flasks until approximately 60% confluent, at which point the medium was replaced and fresh serum-free medium was added. Incubation continued for additional 48 hours. The conditioned

medium was removed and sterile filtered. Conditioned medium was passed 5 times through a laminin-affinity column (laminin-1 immobilized on cyanogen bromide-activated sepharose) (2 mL bed volume, flow rate 2 mL/min). The column was washed with cPBS until absorbance at 280 nm reached the baseline, and captured LBP was eluted either by cPBS supplemented with 1 M NaCl or cPBS pH 2.0. Eluted LBP was dialyzed against ddH<sub>2</sub>O and lyophilized.

#### Site-directed mutagenesis

For site-directed mutagenesis of cysteines within rLBP, two pairs of primers were synthesized, one pair for each cysteine. Primer sequences are shown below (5' → 3'):

C148A-FOR: CGTCAACCTGCCACCATGCTCTG**GCT**AACACAGACTCTCCTCTGCGCTACG

C148A-REV: CGTAGCGCAGAGGAGAGTCTGTGTTA**GCC**CAGAGCAATGGTGGGCAGGTTGACG

C163A-FOR: GCGCTACGTGGACATTGCCATCCCG**GCC**CAACAACAAGGGAGCTCACTCAGTGG

C163A-REV: CCACTGAGTGAGCTCCCTTGTTGTT**GCC**CGGGATGGCAATGTCCACGTAGCGC

Primers are complimentary to the LBP sequence, except for the bases shown in bold and underlined. These bases mismatch with the LBP sequence, leading to mutation of the codons coding for C148 and C163. Primers were PAGE-purified. Each cysteine was mutated separately. For creation of the double mutant, the C163A mutation was introduced into the previously obtained C148A mutant. PCR was performed with pairs of mutagenic primers specific for each cysteine. LBP cDNA cloned into pET15b vector and propagated in a Dam-positive strain of *E. coli* was used as a template. Amplification

reactions were carried out in 50  $\mu$ l volumes with: 1X *Pfu* turbo buffer (Stratagene), 2.5 mM MgSO<sub>4</sub>, 10-50 ng of template DNA, 6.25 pMol of each mutagenic primer, 200  $\mu$ M dNTPs, 2.5 U *Pfu* turbo. PCR parameters were: 5 min at 94°C, followed by 16 cycles of 30 sec at 94°C, 1 min at 55°C, 14 min at 68°C, followed by 1 cycle of 2 min at 4°C. After PCR, 10U of restriction endonuclease DpnI was added to the PCR product and incubated 1 hr to overnight at 37°C. DpnI discriminates between methylated/hemimethylated sites and non-methylated sites and introduces cuts only in methylated sites, thus removing the surviving parental DNA or parental/amplified heteroduplexes and leaving homoduplexes of newly synthesized mutated strands intact. After DpnI digestion, DNA was ethanol precipitated, washed with 70% ethanol, dissolved in 10  $\mu$ L of ddH<sub>2</sub>O and transformed into Top10F' *E. coli* by electroporation. Presence of mutations and the integrity of the LBP coding sequence were verified by sequencing from two external and two internal primers.

#### Laminin binding assays

Ninety-six well microtiter plates (Immulon 4HB, Dynex), were coated rLBPs (0.1 mg/mL in cPBS) for 3 hours at room temperature. Plates were blocked with 5% non-fat dry milk, and exposed to laminin-1 (Sigma) (50  $\mu$ g/mL). The plates were developed using polyclonal rabbit anti-laminin antibodies and goat anti-rabbit IgG conjugated to alkaline phosphatase (Bio Rad). Laminin binding was determined by optical density at 425 nm.

## Results

### Expression and purification of rLBP and sLBP

Figure 3.3 shows a time course of expression of wild-type polyhis-tagged rLBP in CD41(DE3) cells. At 7 hours after induction, expressed LBP amounts to about half of the total cellular protein. As was previously reported (94), LBP displays an anomalous electrophoretic mobility on SDS PAGE. While the deduced molecular weight of the protein is 34 kDa with the polyhistidine tag, the expressed protein migrates at apparent molecular weight of 45 kDa. Figure 3.4 demonstrates the results of purification of rLBP. The protein was purified to an apparent >90% homogeneity as evidenced by Coomassie Blue staining. Overloading of the gel reveals additional minor bands in the purified rLBP fraction. Most of them, if not all, are degradation products of the rLBP, as evidenced by a proportionate mobility shift after thrombin cleavage (data not shown). The polyhistidine tag was successfully removed by thrombin cleavage and the protein was re-purified. The time course of thrombin cleavage is shown in figure 3.5. The reactions shown on this figure were run in 200  $\mu$ L, with the concentration of LBP at 0.12 mg/mL. As demonstrated in this figure, nearly 100% cleavage can be achieved in 8 hours. Performing the cleavage in a larger volume, however, required longer incubation times to achieve ~ 90% cleavage (data not shown).

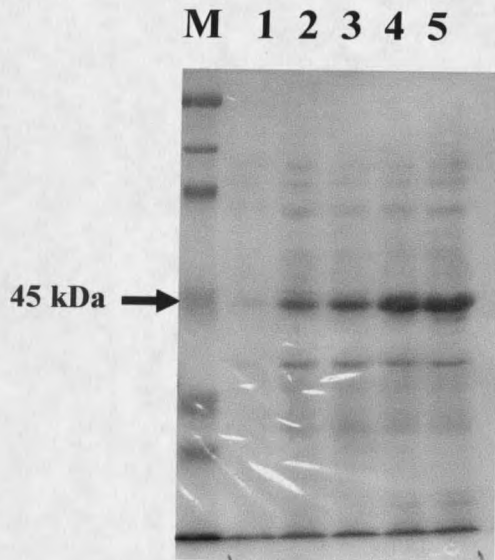


Figure 3.3.  
Time course of expression of rLBP in CD41(DE3). 1 – pre-induction; 2 – 1 hr; 3 – 2 hrs; 4 – 4 hrs; 5 – 7 hrs. post-induction.

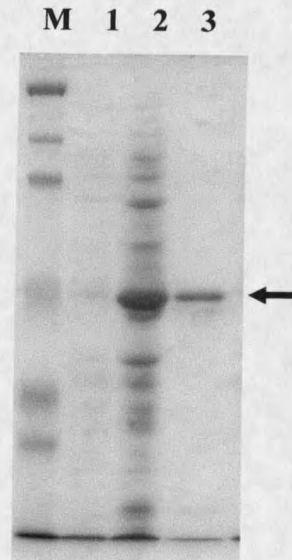


Figure 3.4.  
Purification of rLBP. 1 – lysate non-induced; 2 – lysate induced; 3 – purified rLBP. Position of rLBP is indicated by an arrow.

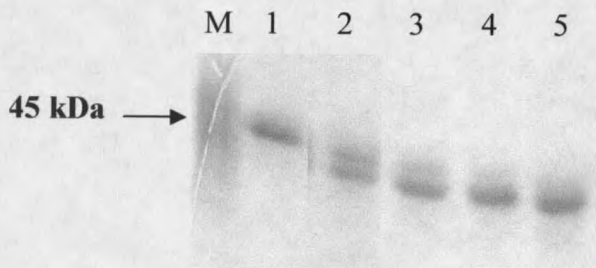


Figure 3.5.  
Removal of the polyhistidine tag from rLBP. 1 – Before thrombin cleavage; 2 – 2 hours; 3 – 4 hours; 4 – 8 hours; 5 – 18 hours.

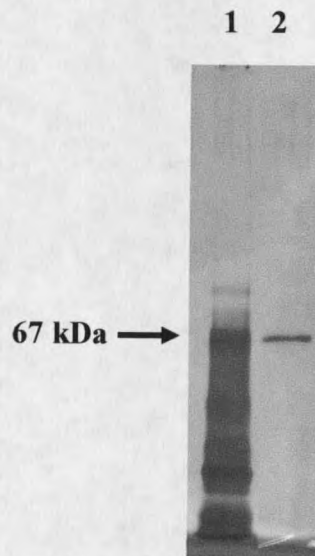


Figure 3.6.  
Affinity-purified sLBP. 1 – low molecular weight markers (overloaded); 2 – purified sLBP





































































































































































































































